

University of Memphis

University of Memphis Digital Commons

Electronic Theses and Dissertations

12-2-2013

Model Bias Analysis Using Statistical Methods with the NGA East Ground Motion Database

Luke Philip Ogweno

Follow this and additional works at: <https://digitalcommons.memphis.edu/etd>

Recommended Citation

Ogweno, Luke Philip, "Model Bias Analysis Using Statistical Methods with the NGA East Ground Motion Database" (2013). *Electronic Theses and Dissertations*. 826.

<https://digitalcommons.memphis.edu/etd/826>

This Thesis is brought to you for free and open access by University of Memphis Digital Commons. It has been accepted for inclusion in Electronic Theses and Dissertations by an authorized administrator of University of Memphis Digital Commons. For more information, please contact khhgerty@memphis.edu.

**MODEL BIAS ANALYSIS USING STATISTICAL METHODS WITH THE
NGA EAST GROUND MOTION DATABASE**

by

Luke Philip Ogweno

A Thesis

**Submitted in Partial Fulfillment of the
Requirements for the Degree of
Master of Science**

Major: Earth Sciences

The University of Memphis

December 2013

Acknowledgement

I would like to register my appreciation to Dr. C. Cramer for his persistence and patience with me during the entire time I joined CERl and started working on a totally new field. Further thanks to my committee members Dr. M. Withers and Dr. C. Powell for their guidance and insightful suggestions to make this thesis a success. Thanks to Dr. J. Kaklamanos for his suggestions to improve on the residual analysis during the 2013 annual SSA meeting in Utah Salt Lake City.

Many thanks to my colleagues (students) for their contributions in various ways. I would also like to thank Dr. Céline Beauval for sharing with me her code for log likelihood. Special thanks to Adewale Amosu and Cecilia Nyamwandha for their time whenever I was stuck with my codes. Finally thanks to CERl for the financial support.

May God bless you all.

Abstract

Ogweno, Luke Philip. MS. The University of Memphis. December, 2013. Model Bias Analysis Using Statistical Methods with the NGA East Ground Motion Database. Major Professor: Chris H. Cramer.

The Next Generation Attenuation (NGA) East project has an updated database for Central and Eastern North America (CENA) ground motions. I analyzed the performance of ground motion prediction equations (GMPEs) used in the United States Geological Survey (USGS) National Seismic Hazard Mapping Project (NSHMP) and other potential GMPEs used in the CENA through bias analysis, model inadequacies check using statistical tests and finally ranking the GMPEs using log likelihood (LLH), and the Euclidean Distance Based Ranking (EDR) technique.

From bias analysis, Atkinson and Boore (2011) (model A08p), Atkinson and Boore (2011) (model AB06p), and Atkinson and Boore (2006) (model AB06+) with 200 bar stress drop performed better than other GMPEs. EDR results show models A08, AB06p, and AB06+ as the best performing models for combined site classes. Models AB06p, EPRI (2004) cluster2 model (EPRI2), AB06+ and Silva *et al.* (2002) (SD02) matched the data well in rock sites.

Table of Contents

	Page
List of Tables	vi
List of Figures	viii
1. Introduction	1
1.2 Problem statement.....	2
1.3 Objectives	3
1.4 Justification	4
1.5 Significance of the study.....	5
2 Previous Studies	6
3 Methods and approach	11
3.1 Classical Residual (Model bias) in GMPE	11
3.2 Testing normality and model adequacies on GMPEs.....	12
3.3 Log Likelihood (LLH).....	14
3.4 Euclidean-Distance Based Ranking (EDR) method	16
4. Results and Discussions	23
4.1 Data selection	23
4.2 Parameter compatibility	23
4.3 Classical Residual Analysis Method	26
4.4 NGA-East Database statistics	31

4.5	Normality Test.....	33
4.5.1	Skewness	34
4.5.2	Kurtosis.....	37
4.6	Testing the shape of the residual distributions	40
4.6.1	Hypotheses testing	42
4.6.2	The z-test.....	43
4.6.3	The Lilliefors test	44
4.6.4	Kolmogorov-Smirnov test	44
4.6.5	Jarque-Bera (JB) test	46
4.7	Log likelihood (LLH) Ranking Method.....	47
4.8	Euclidean Distance Ranking Method	52
5	Conclusions	59
	References	62
	Appendices	70
	Appendix 1: Comparative rankings of candidate GMPEs as a function of Distance (Classical residual Analysis) for all classes	70
	Appendix 2: Plots of Residual distribution, cumulative and standardized residual plots for rock sites	75
	Appendix 3: Results of LLH	110
	Appendix 4: Results for EDR Methodology.....	112

List of Tables

	Page
Table 1 : Abbreviations for ENA GMPEs as used in this thesis	24
Table 2: Summary of GMPEs Parameters	25
Table 3: Summary Table of all three classes of site conditions.....	26
Table 4: Selected soil class average (rock sites)	28
Table 5: Selected soil class average (soil sites).....	29
Table 6: Selected soil class average (Deep soil sites)	29
Table 7: NGA-Database Summary Statistics for All Sites	32
Table 8: NGA-Database Summary Statistics for Rock Sites	32
Table 9: NGA-Database Summary Statistics for Soils	32
Table 10: NGA-Database Summary Statistics for Deep Soils.....	33
Table 11: Summary table of Skewness results for all sites	35
Table 12: Summary table of Skewness results for rock site.....	35
Table 13: Classification of the GMPEs according to skewness (all sites)	36
Table 14: Summary table of Kurtosis Results (all sites).....	38
Table 15: Classification of the GMPEs according to kurtosis (all sites).....	38
Table 16: Critical Values for the Two-sample Kolmogorov-Smirnov test (2- sided).....	45
Table 17: Summary table for LLH results for all sites and within 100km.....	48
Table 18: Summary table for LLH results for rock sites and within 100km.....	48
Table 19: Summary table for LLH results for soils sites and within 100km	49
Table 20: Summary table for LLH results for deep soils sites and within 100km	49

Table 21: MDE Results Ranking for all sites combined.....	53
Table 22: Kappa Results Ranking for all sites combined	54
Table 23: EDR Results Ranking for all sites combined	54
Table 24: MDE ranking for Rock sites	55
Table 25: Kappa ranking for rock sites	56
Table 26: EDR ranking for rock sites	56
Table 27: Summary Table for LLH results for Soil sites and within 100km	110
Table 28: Summary Table for LLH results for Deep Soil sites and within 100km.....	110
Table 29: Summary Table for MDE results for Soil sites and within 100km	112
Table 30: Summary Table for Kappa results for Soil sites and within 100km ...	112
Table 31: Summary Table for EDR results for Soil sites and within 100km	112
Table 32: Summary Table for MDE results for Deep Soil sites and within 100km.....	113
Table 33: Summary Table for Kappa results for Deep Soil sites and within 100km.....	113
Table 34: Summary Table for EDR results for Deep Soil sites and within 100km.....	114

List of Figures

	Page
Figure 1: NGA-East Ground Motion Database	2
Figure 2: Normal probability plots (a) ideal; (b) heavy-tailed distribution; (c) light-tailed distribution; (d) positive skew; (e) negative skew. (Modified after Montgomery <i>et al.</i> 2003).	13
Figure 3: Model description for the comparison between KL distance and negative average log likelihood. The heavy solid line in the top panel shows the PDF for a lognormal distribution ($\mu = 10, \sigma = 0.5$), which is assumed to act as a reference model f (reality) from which 1000 synthetic observations were generated (shown in histogram). In addition, three-candidate model functions g_1, g_2 and g_3 are superimposed. For each of the samples, logarithms of the PDFs were calculated with respect to the different candidate models. The lower row shows the corresponding histogram. The average log-likelihood values (equation 5) for each model are indicated on top of each panel (Scherbaum <i>et al.</i> , 2009).....	16
Figure 4: Probability distribution definitions given in Equation 8: (a) $\Pr(D < d)$, (b) $\Pr(D < -d)$, (c) $\Pr(D < d)$. (Kale and Akkar, 2012)	18
Figure 5: Probability distribution definitions given in Equation 9: (a) $\Pr(- d_j + dd_2 < D < d_j + dd_2)$, (b) $\Pr(- d_j - dd_2/2 < D < d_j - dd_2/2)$, (c) difference between the probabilities given in (a) and (b); total discrete probability, $\Pr(D < d_j)$, (d) probability density function of $ D $. The	

probabilities of (a) and (b) are equivalent to $\Pr (|D| < |d_j + dd_2|)$ and $\Pr (|D| < |d_j - dd_2|)$, respectively. The gray shaded area in (d) represents the summation of the discrete probabilities in negative and positive sides of the probability density function in (c) [i. e. $\Pr (|D| < |d_j|)$]. D is normally distributed random variable with μ_D and σ^2_D while $|D|$ is a non- negative random variable (Kale and Akkar, 2012). 20

Figure 6: Detailed Standard Normal Distribution	41
Figure 7: Distribution of mean μ when H_0 is true and false	42
Figure 8: Current GMPEs	72
Figure 9: Atkinson Series GMPEs.....	72
Figure 10: Proposed GMPEs	73
Figure 11: EPRI 2004 GMPEs	74
Figure 12: Plot for the Peak Ground Acceleration	79
Figure 13: Plot for the 0.1s spectral Acceleration	84
Figure 14: Plot for the 0.2s spectral Acceleration	89
Figure 15: Plot for the 0.3s spectral Acceleration	94
Figure 16: Plot for the 0.5s spectral Acceleration	99
Figure 17: Plot for the 1.0s spectral Acceleration	104
Figure 18: Plot for the 2.0s spectral Acceleration	109
Figure 19: LLH Values versus Spectral periods calculated for the GMPEs under study	111

1. Introduction

The characterization of earthquake ground motions for engineering applications generally involves the use of empirical models referred to as ground motion prediction equations (GMPEs). GMPEs describe the variation of the median and lognormal standard deviation of particular intensity measures (such as peak acceleration, spectral acceleration, or duration) conditional on magnitude, site-source distance, site condition, and other parameters. A number of GMPEs have been introduced in recent years that are re-defining the state of practice for probabilistic seismic hazard analysis (PSHA) in many earthquake-prone regions worldwide. For example the Next Generation Attenuation (NGA)-East is developing a new ground motion characterization (GMC) model for the Central and Eastern North-American (CENA) region. The GMC model consists in a set of new ground motion prediction equations (GMPEs) for median and standard deviation of ground motions (GMs) and their associated weights in the logic-trees for use in probabilistic seismic hazard analyses (PSHA).

The NGA East project has developed an updated database of Central and Eastern North America (ENA) ground motions (Cramer *et al.*, 2009, 2010, 2012) containing over 11,000 records and covering distance and magnitude ranges of 1-3,500 km and M 2.2-7.6, but mostly less than M 6.0 (Figure 1). This dataset was used to rank GMPEs used in United States Geological Survey (USGS) national seismic hazard mapping project (NSHMP) and other alternative GMPEs at various distances and magnitudes using various statistical methods and procedures.

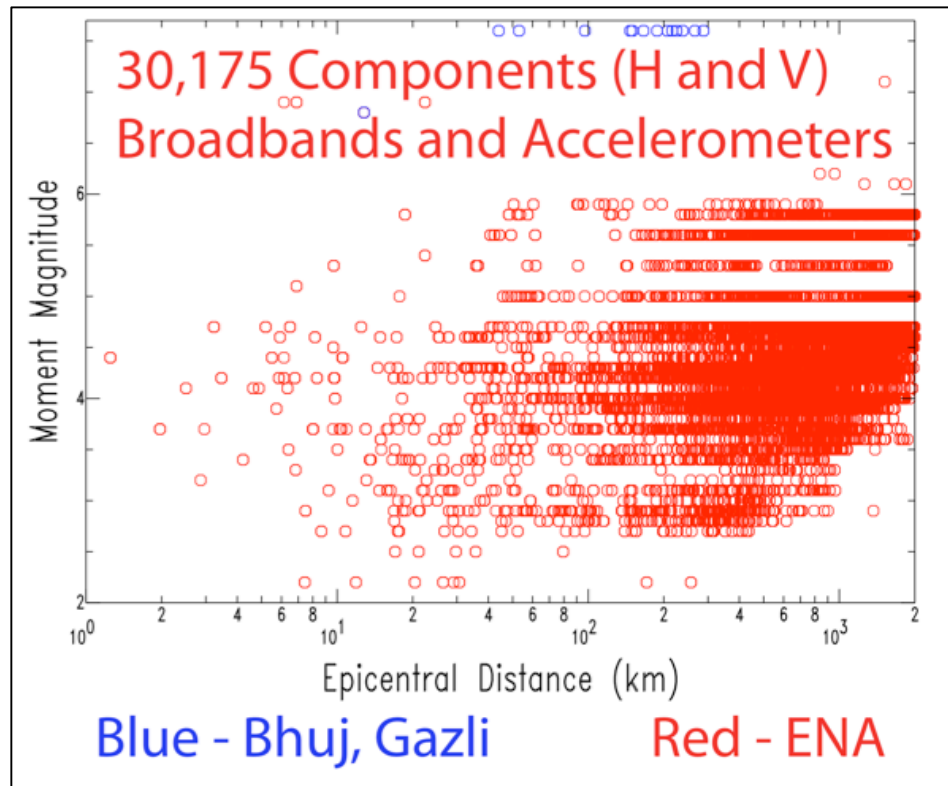


Figure 1: NGA-East Ground Motion Database

1.2 Problem statement

GMPEs are developed for specific tectonic environments using multivariate regression on ground motion databases, and the relationships are updated as more earthquake data are obtained (Kramer, 1996; Abrahamson and Shedlock, 1997). It is important to note that many GMPEs are not purely statistical and that non-statistical information such as nonlinear site response, basin effects, oversaturation, and anelastic attenuation, is often used in the models (Abrahamson *et al.*, 2008). Because of the improvement of seismological

networks, and increasing size of quality of the ground motion database the number of proposed ground motion models has increased significantly in the last decade to reflect the seismological features of the seismic prone regions. Douglas (2011) gives 289 empirical GMPEs for PGA and 188 models for the prediction of elastic response spectral ordinates. The selection of candidate models, especially the assignment of logic tree weights, has become important. Selecting appropriate predictive models to calculate hazard in a site (or a region) of interest has become popular topic in engineering seismology. The ground shaking in the target region must be well reflected by the selected GMPEs as ground motion variability directly affects the computed hazard in the study area. Therefore, there is a need for quick and efficient testing to determine if a model is appropriate for a particular target region and how it performs over a given range of the dataset. In the context of a logic tree with more than a few alternative GMPE model branches, it will therefore be hard if not impossible to keep the judgment of the complete set of candidate models internally consistent and the verdict on a particular model reproducible.

1.3 Objectives

The objectives of this study were threefold, namely:

1. To analyze the performance of CENA GMPEs over the entire magnitude-distance (and other independent variables, e.g. site classification) range using model bias (residual) analysis

2. To check the normality and model inadequacies in various CENA GMPEs, as used in the USGS national seismic hazard-mapping project (NSHMP), using various statistical test parameters
3. To use the Euclidean-Distance Based Ranking (EDR) and log likelihood concepts to rank CENA GMPEs used in the USGS NSHMP under a given set of observed data.

1.4 Justification

The analysis was to provide useful information such as establishing the GMPE logic-tree to the seismic hazard analyst depending on the objective of the hazard project in forecasting either the regional or site-specific hazard.

Euclidean distance was preferred over residual analysis, as it results in non-negative differences between observations and estimations that were easily transformable into an index. The EDR method also accounts for aleatoric variability in ground motion estimations (through standard deviations of GMPEs). It also considers the bias between median estimations and observed ground-motion data (model bias). Other methods such as Log likelihood (LLH) computes the occurrence probability of the observed data point by using the corresponding estimation that is assumed to be log-normally distributed with median and sigma values of the candidate GMPE. The deviation of the mean and the median from zero, and the deviation of the standard deviation from 1, helps to detect non-normally distributed models. A large difference between mean and median is a means to help identify models for which the residual distributions were skewed.

By scaling the data by the model mean and variance, it was possible to evaluate the hypothesis that the mean of the normalized distribution is zero (Scherbaum *et al.*, 2004).

1.5 Significance of the study

Following any modeling procedure, it is a good idea to assess the validity of the resulting model. Residuals and diagnostic statistics allow one to identify patterns that are either poorly fit by the model, or have strong influence upon the estimated parameters, or which have a high leverage. It is helpful to interpret these diagnostics jointly to understand any potential problems with the model. Also, the quantitative decision favoring different candidate models (GMPEs) requires a meaningful measure to distinguish candidate probabilistic models

The selection of a ground motion model, and the determination of the contribution weight to assign to each of them is a fundamental component of any seismic hazard analysis. It has been demonstrated that the uncertainty corresponding to the selection of the attenuation model influences the hazard results more than other aspects of seismicity modeling (Toro 2006). This epistemic uncertainty is often treated with the expert opinion approach through a logic tree framework (Budnitz *et al.*, 1997). The branch weights in a logic tree framework correspond to a degree of belief of experts in different prediction models. Statistical tools can be used to replace the expert opinion, which are often subjective. The results of this study can be used to give weighting in the seismic hazard assessment in the United States.

2 Previous Studies

Douglas and Gehl (2008) proposed a quantitative approach to investigate and separate the variability in earthquake ground motion into that attributable to site effects and that due to source effects. The technique was based on analysis of variance (ANOVA) of residuals of ground motion parameters computed using ground motion models that approximately remove the effects of magnitude, style of faulting, source-to-site distance and simple site classification. They applied this to four sets of observed strong-motion records: two from Italy (Umbria-Marche and Molise), one from the French Antilles and one from Turkey. From their study they concluded that for the data from Italy the observed variance could be attributed to un-modeled site effects whereas those from the French Antilles and Turkey were largely attributable to source effects not modeled by the ground-motion estimation equations they had used. The thesis study shows the need for improved modeling of different source effects within central and eastern northern America (CENA) GMPEs. Bindi *et al.*, (2006), Scassera *et al.*, (2009), and Shoja-Taheri *et al.* (2010) used residual analysis to evaluate GMPEs under different ground motion databases.

Scherbaum *et al.* (2004) show how observed ground motion records can help to guide one in the selection and ranking of appropriate models for a particular target area. They developed a new, likelihood based, goodness-of-fit measure that had the property not only to quantify the model fit but also to measure in some degree how well the underlying statistical models are met. They developed a scheme to rank candidate ground motion models into different

classes (likelihood method (LH)). This scheme was intended to assist the seismic-hazard analyst in judging the appropriateness of ground motion models for a particular target area in a data-driven (magnitude, distance and frequencies), consistent and reproducible way. The LH method calculates the normalized residuals for a set of observed and estimated ground motion data by considering that GMPEs are normally distributed in natural logarithm unit. This method calculates the exceedance probabilities of residuals as likelihood (LH) values. The suitability of candidate GMPEs is identified through the median LH value that is described as LH index, which takes value between 0 and 1.

Scherbaum *et al.* (2009) discuss the challenges of model selection in seismic hazard analysis. They focus on an information-theoretic approach (log-likelihood (LLH)) method that provides a general theoretical foundation to perform quantitative model selection in cases where models can be formulated in terms of PDFs or probability mass functions (PMFs) and the key ingredient, the Kullback-Leibler (KL) distance, can be estimated from the statistical expectation of observations for the models under consideration. This approach does not require any ad hoc assumptions and KL-distance differences between models are a theoretically sound way of quantifying differences in ground-motion models in terms of information. The application of KL distance based model selection to real data using the model generating data set for the Abrahamson and Silva (1997) ground-motion model shows the superior performance of this approach in comparison to earlier attempts at data-driven model selection (e.g., Scherbaum *et al.*, 2004). Kakkamanos and Baise (2011) used the Nash-Sutcliffe model

efficiency coefficient (Nash and Sutcliffe, 1970) to validate the NGA-West GMPEs by making use of a ground motion data set assembled from recent earthquakes recorded in California.

Joshi *et al.* (2012) discuss the applicability of different GMPEs for predicting the values for which it is made and conclude that in order to apply a particular GMPE to any region it needs to be tested against the deviation from normality and model inadequacies. They used cumulative probability plots and random residual plots to check the presence of fat tail and model inadequacies in the GMPE given by BO97, Boore and Atkinson (2008) referred to as BA08, Abrahamson and Litehiser (1989) referred to as AL89 and Joyner and Boore (1981) referred to as JB81. They observed that as long as the data set is similar to the one used for generating the GMPE the normality and model inadequacies are satisfied but when the data are different than that used for generation of the GMPE, deviation is observed in the cumulative probability plot.

Beauval *et al.* (2012a) carried out a study to systematically test global and local models against the same regional datasets ($M \geq 6$), and obtained a hierarchy of their fit to the data. They apply various techniques to various subduction regions and conclude that though the Scherbaum *et al.* (2009) LLH method proved to be efficient in providing one number quantifying the overall fit, additional analysis on the between-event and within-event variability were mandatory, to control if the median prediction per event and/or variability within an event was within the scatter predicted by the model.

In another study, Beauval *et al.* (2012b) use the LLH method of Scherbaum *et al.* (2009) to analyze and quantify the consistency between several GMPEs and three different datasets. Using weak motions recorded in France (191 recordings with source-site distances up to 300 km, $3.8 \leq M_w \leq 4.5$) and a Japanese dataset they confirm that a dataset of ~ 190 observations is large enough to obtain stable LLH estimates. They observe no significant regional variation of ground motions and that magnitude scaling could be the predominant factor in control of ground-motion amplitudes. Using larger magnitudes (5-7) from the Japanese dataset, the ranking of the models is partially modified as an indication of magnitude scaling for some of the models. This showed that extrapolating testing results obtained from low magnitude to higher magnitude ranges is not straightforward.

Mousavi *et al.* (2012) used likelihood method (LH) and an information theory method (LLH) to evaluate candidate ground motion models for the Zagros region of Iran. There was good agreement between the two methods and one of the significant results they obtained was that the regional ground motion models (corresponding to Europe and Middle East data sets) showed more consistency with observed data than the models developed using the NGA models. The testing used in their study did not include data from earthquakes with $M_w > 6.5$ and $R < 50$ km due to a paucity of data.

Kale and Akkar (2012) developed a new novel procedure for selecting and ranking candidate GMPEs for seismic hazard analysis. The methodology makes use of the Euclidean distance concept and modifies it for the objective of proper

ranking of candidate GMPEs under a given empirical ground motion data set.

The method considers the ground motion uncertainty (i.e., the standard deviation term of the ground motion model) and the bias between the observed data and the median estimations of candidate GMPEs.

3 Methods and approach

The most common methodology for assessing the performance of predictive models is still the classical residual analysis. It determines the existence of bias by means of mean residual as well as the slope of the straight lines fitted to different residual components (i.e. between events and within events or total residuals as a function of estimator parameters such as magnitude and source to site distance). The methods employed in this study included the classical residual analysis which formed the basic step for other steps such as, testing normality and model adequacies through construction of a cumulative probability plot of the residuals, log likelihood analysis to rank the GMPEs using the procedure proposed by Scherbaum *et al.*, (2009), and the Euclidean distance based ranking method (EDR) as proposed by Kale and Akkar (2012). The residuals for the GMPEs under study were computed first by running the Fortran codes of the GMPEs models to produce simulated model outputs then obtain the residuals. Detailed descriptions of these methods used are discussed below.

3.1 Classical Residual (Model bias) in GMPE

Residuals ($r_{i,j}$) used in this thesis are defined as the differences between the natural logarithm of the calculated and observed strong motion variable parameters:

$$r_{i,j} = \ln\dot{Y}_{i,j} - \ln Y_{i,j} \quad (1)$$

Here, $\ln Y_{i,j}$ is the value of the j^{th} record of the i^{th} event, and $\ln \hat{Y}_{i,j}$ is the median value from the k^{th} GMPE. The mean of residuals for the i^{th} event with N_i records is defined as

$$\eta_i = \frac{1}{N_i} \sum_{j=1}^{N_i} r_{ij} \quad (2)$$

The between-event and within-event residuals are defined, respectively by equation 3 and 4:

$$r_{i,j}^{(between)} = r_{i,j} - \eta_i \quad (3)$$

$$r_i^{within} = \eta_i - \frac{1}{N_e} \sum_{i=1}^{N_e} \eta_i \quad (4)$$

where N_e is the total number of events, η_i as the mean of residuals for the i^{th} event with N_i records. Negative residuals indicate under-prediction while positive residuals indicate over-prediction.

Once the total, within-event and between-event residuals were obtained for each respective GMPE, a plot of residual values versus source to site distance and magnitudes were plotted. A summary table of the mean residual values of the GMPEs for less or equal to 100km is also presented.

3.2 Testing normality and model adequacies on GMPEs

A normality test for the GMPEs residuals was performed by constructing cumulative probability plots of the residuals versus observed peak ground acceleration (PGA) and other spectral acceleration periods (SAs). A straight line indicates normal distribution whereas a sharp upward and downward curve at both ends indicates that the tail of the distribution is too heavy to be considered

as a normal distribution. Flattening at the extreme end is a typical pattern for a distribution with a thinner tail. GMPEs showing patterns associated with positive and negative skew are shown in Figure 2(d) and 2(e), respectively.

The first step in this process is the calculation of random residuals. The random residual is defined as the difference of the logarithm of actual and predicted values. The random residuals are arranged in an increasing order and are plotted against cumulative probability in order to make a cumulative probability plot.

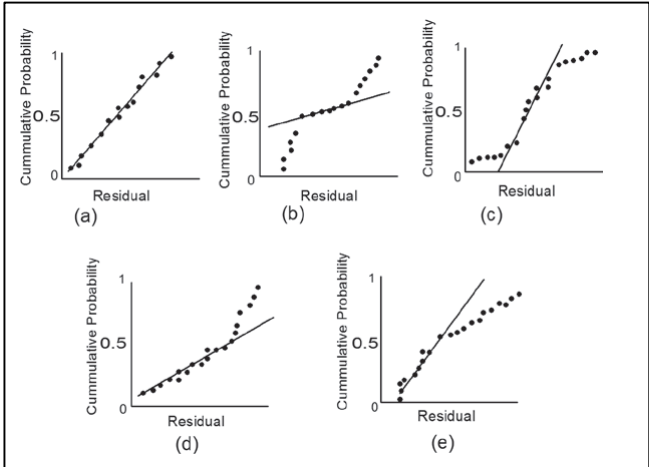


Figure 2: Normal probability plots (a) ideal; (b) heavy-tailed distribution; (c) light-tailed distribution; (d) positive skew; (e) negative skew. (Modified after Montgomery *et al.* 2003).

A substantial departure from a straight line is an indication that the distribution is not normal. A departure from normality is potentially serious as the t or F statistics and confidence and prediction interval depends on the normality

assumption (Montgomery *et al.*, 2003). The plot of random residual versus actual value checks the model inadequacies in the GMPE. If the plot of random residuals versus predicted parameter shows the data points within a horizontal band then there are no obvious model defects. The model inadequacies are shown by deviation in these plots.

3.3 Log Likelihood (LLH)

Ranking of GMPEs followed the recent method proposed in Scherbaum *et al.*, (2009). The LLH method following its predecessor (i.e., LH method; Scherbaum *et al.*, 2004) is sensitive to data size (Delavaud *et al.*, 2009) and it might become biased for GMPE rankings done by using a small number of data.

This method provides a ranking criterion based on information theory (Details of the method can be found in the paper by Scherbaum *et al.*, 2009). The quantitative decision favoring different candidate models requires a meaningful measure to distinguish candidate probabilistic models. Within an information theory framework, this measure is given by Kullback-Leibler distance (Delavaud *et al.*, 2009). The Kullback-Leibler distance between two models $f(x)$ and $g(x)$ is presented as

$$D(f(x), g(x)) = E_{f(x)}(\log_2(f(x))) - E_{f(x)}(\log_2(g(x))) \quad (5)$$

where $E_{f(x)}$ is the expected value taken with respect to $f(x)$. This distance quantitatively represents the amount of information loss if the model $f(x)$ is substituted by model $g(x)$. The distance between the two models is defined by probability density functions $f(x)$ and $g(x)$. The function $f(x)$ represent the

distribution of an observed data point in the ground motion data set. The distribution of the estimated data point is described by $g(x)$ and is assumed as lognormal with the median and standard deviation of the considered GMPE. For model comparisons (e.g., $g(x_1)$ and $g(x_2)$), only their relative Kullback-Leibler distance, $D(f(x), g(x_1)) - D(f(x), g(x_2))$ is taken into account. As a result, the expectation of the unknown model $f(x)$ drops out as a constant. The GMPEs were ranked according to a criterion noted in LLH, which gives the log likelihood of a model given a set of data (i.e. how likely a model has generated the data). LLH is then defined as the negative average log-likelihood of the model g given the sample set x of N observations:

$$LLH = -\frac{1}{N} \sum_{i=1}^N \log_2(g(x_i)) \quad (6)$$

where N is the number of observations x_i , and g the probability density function (PDF) predicted by the GMPE (normal distribution, with standard deviation the total sigma of the model). The ranking of models according to their fit to the data is then straightforward. A small LLH indicates that the candidate model is close to the model that generated the data, while a large LLH corresponds to a model that is less likely to have generated the data. It should be emphasized again that the purpose of this scheme is to provide a data-driven selection and ranking of ground-motion models for seismic-hazard assessment.

Figure 3a shows a case in which a synthetic residual model matches the data exactly in terms of both mean and variance. Figure 3b through 3d show some properties of the distribution of LLH values with different model medians and variances.

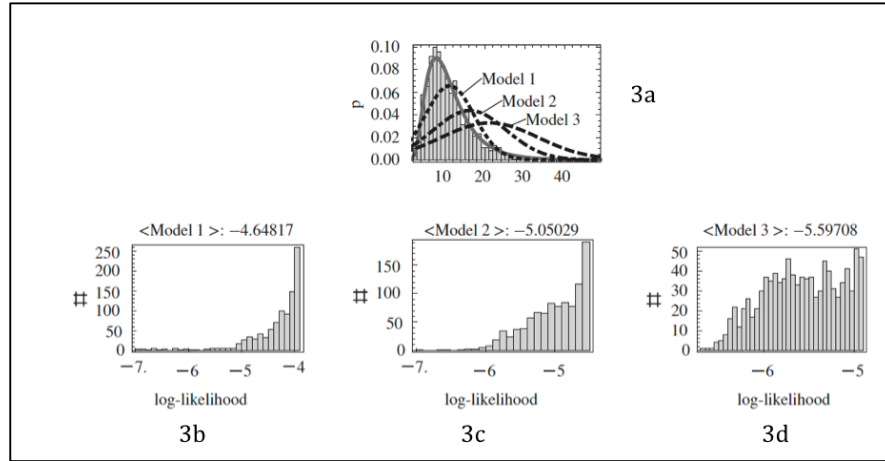


Figure 3: Model description for the comparison between KL distance and negative average log likelihood. The heavy solid line in the top panel shows the PDF for a lognormal distribution ($\mu = 10, \sigma = 0.5$), which is assumed to act as a reference model f (reality) from which 1000 synthetic observations were generated (shown in histogram). In addition, three-candidate model functions g_1, g_2 and g_3 are superimposed. For each of the samples, logarithms of the PDFs were calculated with respect to the different candidate models. The lower row shows the corresponding histogram. The average log-likelihood values (equation 5) for each model are indicated on top of each panel (Scherbaum *et al.*, 2009)

3.4 Euclidean-Distance Based Ranking (EDR) method

The Euclidean distance (DE) is a statistical index where the square root of the sum of squares of the differences between N data pairs (p_i, q_i) is calculated. The parameters p_i and q_i in Equation 7 designate the observed and estimated ground motion data

$$DE^2 = \sum_{i=1}^N (p_i - q_i)^2 \quad (7)$$

Euclidean distance results in non-negative differences between observations and estimations that can be easily transformed into an index. In the

EDR methodology, the estimated ground-motion intensity for a single data point (that consists of a certain magnitude, distance, style-of-faulting and site class) is assumed to take a set of values that are computed from a predetermined range of standard deviation of the considered GMPE. The differences between the observed point and the range of estimations for that single point result in a probability distribution.

The method assumes that the natural logarithm of the predictive model (GMPE) as well as the Euclidean distances computed for each data point is normally distributed. Let D in *Equation 8* denote the difference between the natural logarithms of an observed (a) and estimated (Y) data point. In this expression, a is a scalar quantity (single observation) whereas Y , the estimator for a predictive model, is a Gaussian random variable with mean, μ_Y , and variance, σ_Y^2 . From the basic principles of the summation of random variables, D can be proven to be normally distributed (Devore, 2004) with parameters given in *Equations 9*.

$$D = a - Y \quad (8)$$

$$\mu_D = a - \mu_Y \quad (9a)$$

$$\sigma_D^2 = \sigma_Y^2 \quad (9b)$$

For each single point, the squares of D values contributing to DE are non-negative. To establish an analogy between D and DE , the probability distribution of the absolute values of D [*i. e.*, $Pr(|D|)$] is considered. *Equation 10* is for the probability of $|D|$ being less than a certain value d [*i. e.* $Pr(|D| < d)$], which is

actually the difference between $Pr(D < d)$ and $Pr(D < -d)$ as shown in Figure 4.

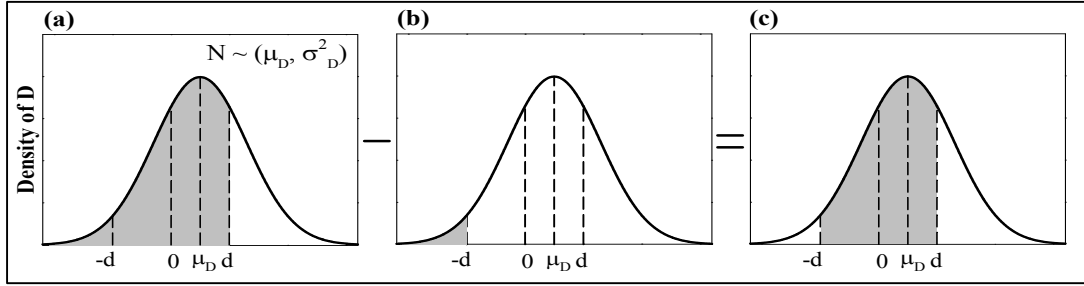


Figure 4: Probability distribution definitions given in Equation 8: (a) $Pr(D < d)$, (b) $Pr(D < -d)$, (c) $Pr(|D| < d)$. (Kale and Akkar, 2012)

The parameter Φ denotes normal cumulative distribution function in Equation 9. This equation is used to derive the probability distribution of $|D|$.

$$Pr(|D| < d) = Pr(D < d) - Pr(D < -d) = \Phi\left(\frac{d-\mu_D}{\sigma_D}\right) - \Phi\left(\frac{-d-\mu_D}{\sigma_D}\right) \quad (10)$$

For discrete values of D , which are denoted by d_j , the occurrence probability of d_j [i. e., $Pr(d_j)$] is described within an infinitesimal bandwidth dd around d_j [i. e., $Pr(d_j - dd/2 < D < d_j + dd/2)$]. Since the method considers the occurrence probabilities of d_j via analogy made between DE and D , it is modified as $Pr(|D| < |d_j|)$. Such a relationship can be derived by Equation 10 resulting in the form of Equation 11. Figure 5 describes the meaning of each term in Equation 11.

$$Pr(|D| < d_j) = Pr\left(|d_j - \frac{dd}{2}| < |D| < |d_j + \frac{dd}{2}|\right) \quad (11)$$

The total occurrence probability for a set of $|d_j|$ values is called Modified Euclidean Distance (MDE). MDE can be considered as a probability-based average that is used as an index to account for the effect of sigma while testing the performance of GMPEs under a given ground-motion dataset.

The discrete Modified Euclidean Distance (MDE_d) is defined by *Equation 12* when $|D|$ is described in discrete points. In this equation, n is the number of discrete points that depend on the bandwidth of dd (Figures 5c and 5d) and the maximum value of $|d|$ (i. e., $|d|_{max}$). If $|D|$ is assumed to be continuous, the integral expression given in *Equation 13* is used to calculate the continuous Modified Euclidean Distance (MDE_c).

$$MDE_d = \sum_{j=1}^n |d_j| Pr(|D| < |d_j|) \quad (12)$$

$$MDE_c = \int_0^{|d|_{max}} d \frac{1}{\sqrt{2\pi}\sigma_D} \cdot \exp\left(\frac{-(d-\mu_D)^2}{2\sigma_D^2}\right) \cdot dd + \int_0^{|d|_{max}} d \frac{1}{\sqrt{2\pi}\sigma_D} \cdot \exp\left(\frac{-(-d-\mu_D)^2}{2\sigma_D^2}\right) \cdot dd \quad (13)$$

For practical applications of EDR method it is suggested by Kale and Akkar (2012) that $|d|_{max}$ value should be selected in accordance with the following relationship:

$$|d|_{max} = \max(|\mu_D \pm x \cdot \sigma_D|) \quad (14)$$

In *Equation 14*, x denotes the multiplier of sigma and $|d|_{max}$ depends on the value of this parameter. If x is selected as 3, then the procedure approximately covers 99.7% of the differences between the observed and estimations of a candidate ground-motion model provided that the normality assumption holds for the considered variables in the methodology. The

distribution of D is asymmetric about zero unless there is a one-to-one match between the observed data point and the corresponding median estimation. On the other hand the $|d_j|$ pairs (*i. e.*, $|d_j|$ and $-|d_j|$) are always symmetric about zero as illustrated in Figure 5c.

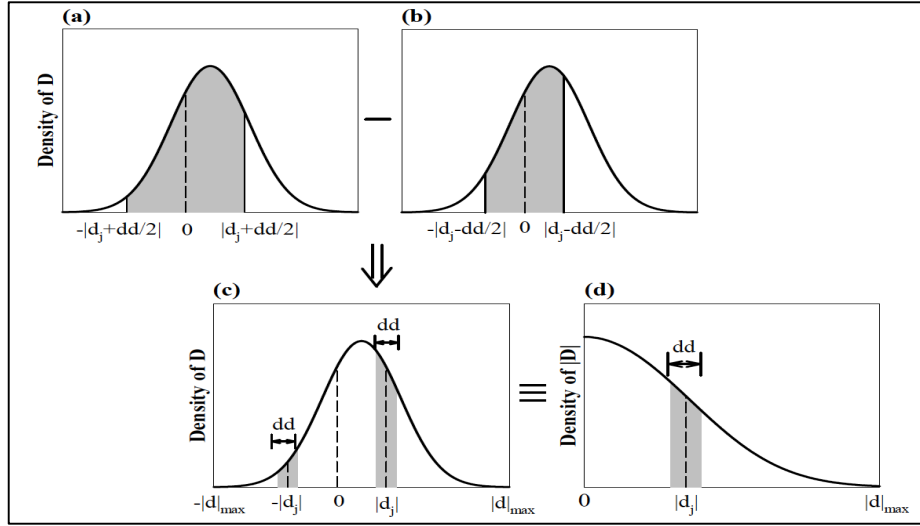


Figure 5: Probability distribution definitions given in Equation 9: (a) $Pr(-|d_j + dd/2| < D < |d_j + dd/2|)$, (b) $Pr(-|d_j - dd/2| < D < |d_j - dd/2|)$, (c) difference between the probabilities given in (a) and (b); total discrete probability, $Pr(|D| < |d_j|)$, (d) probability density function of $|D|$. The probabilities of (a) and (b) are equivalent to $Pr(|D| < |d_j + dd/2|)$ and $Pr(|D| < |d_j - dd/2|)$, respectively. The gray shaded area in (d) represents the summation of the discrete probabilities in negative and positive sides of the probability density function in (c) [*i. e.* $Pr(|D| < |d_j|)$]. D is normally distributed random variable with μ_D and σ^2_D while $|D|$ is a non-negative random variable (Kale and Akkar, 2012).

The MDE values are computed by considering the probability distribution of D either as discrete (MDE_d) or continuous (MDE_c). The values of $x = 3$ and

bandwidth of $dd = 0.1$ will be considered to be sufficient for reliable calculation of MDE while testing the performance of a candidate GMPE.

A significant trend between the observed data and corresponding median estimations can then be interpreted as the biased representation of the ground-motion data by the candidate predictive model. The κ parameter (*Equation 15a*) can be used to measure the level of bias between the observed and estimated data. Note that, unlike MDE , κ parameter is computed using the entire ground-motion database. This parameter is the ratio of original ($DE_{original}$) and corrected ($DE_{corrected}$) Euclidean distances discussed below, which are given in *Equations 15b and 15c*. It should be noted that the squared Euclidean distances in *Equations 15b and 15c* are equivalent to the sums of the squared residuals.

$$\kappa = \frac{DE_{original}}{DE_{corrected}} \quad (15a)$$

$$DE^2_{original} = \sum_{i=1}^N (a_i - Y_i)^2 \quad (15b)$$

$$DE^2_{corrected} = \sum_{i=1}^N (a_i - Y_{c,i})^2 \quad (15c)$$

where a_i and Y_i are the natural logarithms of the i^{th} observed and estimated data respectively. N denote the total number of data in the assembled ground motion database. The parameter $Y_{c,i}$ stands for the corrected estimation of the i^{th} data after modifying Y_i with the straight line fitted on the logarithms of the estimated and observed data. The calculation of $Y_{c,i}$ is given by *Equation 16*.

$$Y_{c,i} = Y_i - (Y_{fit,i} - a_i) \quad (16)$$

where $Y_{fit,i}$ is the predicted value from the regression of Y_i on a_i . The optimum value of k is 1 and occurs when estimated values are very close to the corresponding observation.

The calculations are presented for a single data point while describing MDE and were repeated for the entire ground-motion database, as the EDR index must represent the overall probability of the differences between the estimated and observed data. This probability was then modified by κ to penalize the considered predictive model according to the level of bias detected between the median estimations and overall trend in empirical data. To eliminate the dependency of EDR results on data size, the compound effect of k and MDE was normalized by the total data number, N in the ground motion dataset.

The mathematical expression of EDR is given by *Equation 17*. Note that the EDR index is the square root of the expression given in *Equation 17*. A smaller EDR value implies better representation of the ground-motion dataset by the predictive model.

$$EDR^2 = \kappa \frac{1}{N} \sum_{i=1}^N MDE_i^2 \quad (17)$$

These methods were repeated for various candidate GMPEs and tested at 7 different discrete spectral periods ranging from $T=0.0s$ (PGA) to $T=2.0s$, (i.e., PGA, 0.1s, 0.2s, 0.3s, 0.5s, 1.0s and 2.0s). It is important to note that the values studied here are not peak ground accelerations (PGAs) nor spectral accelerations (SAs), but the residuals between predicted and measured logarithmically transformed accelerations.

4. Results and Discussions

4.1 Data selection

The NGA-East database is a huge file consisting of over 91 earthquakes and over 700 recording 3-component broadband stations. The data for analysis were selected by avoiding the higher attenuating Gulf Coast. The Gulf Coast was assumed to lie below $35.0^{\circ}N$. Also Texas (*west of* $100^{\circ}W$) Gulf earthquakes were avoided plus bad data stations were not included in the analysis. The stations were characterized into three different soil classes as either rock sites (less than 5 m of soil or estimated V_s30 greater than 600 m/s) or soil sites (5m – 100m of soil or estimated V_s30 between 360 and 600 m/s) or as deep soil sites (greater than 100 m or estimated V_s30 less than 360 m/s). Several earthquakes occurring in tectonic settings similar to those in the CEUS were also included (e.g., Nahanni, Gazli, and the Bhuj earthquakes).

The GMPEs were tested against the NGA database dataset. Although most GMPEs have been developed for maximum distances varying from 100 km to 1,000 km, distances as far as 3,000 km were taken into account though from the results of residual analysis at distances greater than 1,000 km, the GMPEs begins to be unstable in their prediction of the ground motion equation.

4.2 Parameter compatibility

All GMPEs considered in this study as presented in *Table 1* use the moment magnitude scale to characterize earthquake size. The distance measure is different from one model to the other as shown in *Table 2*. Some models use

the Joyner and Boore (1981) distance measure (rjb) (which is measured horizontally on the surface) while others are based on the rupture distance (closest distance to the rupture plane). Others use the hypocentral distance. Each model was used with its native distance measure.

Table 1: Abbreviations for ENA GMPEs as used in this thesis

#	Abbreviation	GMPE	TYPE
1	A08	Atkinson, 2008	Hybrid
2	A08p	Atkinson and Boore, 2011 adjustment to A08	Hybrid
3	AB95	Atkinson and Boore, 1995	Double corner frequency
4	AB06	Atkinson and Boore, 2006 (140 bar stress drop)	Dynamic Corner
5	AB06+	Atkinson and Boore, 2006 w/ 200 bar stress drop	Dynamic Corner
6	AB06p	Atkinson and Boore, 2011 adjustment to AB06	Dynamic Corner
7	C03	Campbell, 2003	Hybrid
8	EPRI1	EPRI, 2004 cluster 1 model	Spectral Single Corner
9	EPRI2	EPRI, 2004 cluster 2 model	Spectral Double Corner
10	EPRI3	EPRI, 2004 cluster 3 model	Hybrid
11	EPRI4	EPRI, 2004 cluster 4 model	Finite source model
12	F96	Frankel <i>et al.</i> , 1996	Single Corner
13	PZT11	Pezeshk <i>et al.</i> , 2011	Hybrid
14	S01	Somerville <i>et al.</i> , 2001	Full waveform Simulation
15	SC02	Silva <i>et al.</i> , 2002 single corner, constant stress drop w/saturation	Single Corner-Constant stress drop
16	SD02	Silva <i>et al.</i> , 2002 double corner w/saturation	Double corner w/saturation
17	SV02	Silva <i>et al.</i> , 2002 single corner, variable stress drop	Single corner, variable stress drop
18	T02	Toro <i>et al.</i> , 1997, 2002 update	Single Corner
19	TP05	Tavakoli and Pezeshk, 2005	Hybrid

Table 2: Summary of GMPEs Parameters

#	GMPE	Description	Distance	Magnitude	M-Range	Period (T) s	R-Range	Year	Site Parameters	Grouping	Comments
1	AB95	Atkinson and Boore 1995	Closest distance from the recording site to the ruptured area	M_w	3.5-8.0	0.03 - 5, +PGA, PGV	10-100	1995	V_{s30} a parameter		Double corner frequency
2	AB06	Atkinson and Boore 2006	Closest distance from the recording site to the ruptured area	M_w	3.5-8.0	0.03 - 5, +PGA, PGV	1-1000	2006	V_{s30} a parameter	Current USGS NSHMP (2008)	140 bar stress drop
3	AB06+	Atkinson and Boore 2006	Closest distance from the recording site to the ruptured area	M_w	3.5-8.0	0.03 - 5, +PGA, PGV	1-1000	2006	V_{s30} a parameter	Current USGS NSHMP (2008)	200 bar stress drop. Atkinson and Boore BSSA 2006, A CEUS relation
4	AB06p	Atkinson and Boore 2006	Closest distance from the recording site to the ruptured area	M_w	3.5-8.0	0.03 - 5, +PGA, PGV	1-1000	2006	V_{s30} a parameter	Proposed USGS NSHMP (2014)	No 200 bar, only magnitude dependent stress drop
5	A08	Atkinson 2008	Joyner-Boore Dist.	M_w	4.3-7.6	0.03 - 5, +PGA, PGV	0-200	2008	V_{s30} a parameter	Current USGS NSHMP (2008)	Modified from getBooreNGA07m.f
6	A08p	Atkinson 2009	Joyner-Boore Dist.	M_w	5.0-8.0	0.03 - 5, +PGA, PGV	0-200	2009	V_{s30} a parameter	Current USGS NSHMP (2008)	Modified by from getLAKOBENA.f
7	C03	Campbell et al., 2003	Closest distance from the recording site to the ruptured area	M_w	5.0-8.2	0.01 - 4	0-1000	2003	V_{s30} = 2800 m/s	Current USGS NSHMP (2008)	Hybrid empirical model
8	F96	Frankel et al., 1996	Closest distance from the recording site to the ruptured area	M_w	4.4 to 8.2	0.2, 0.3, 1.0, + PGA	10-1000	1996	V_{s30} = 760 m/s	Current USGS NSHMP (2008)/Proposed USGS NSHMP (2014)	Single corner frequency
9	S01	Somerville et al., 2001	Joyner-Boore Dist.	M_w	6.0-7.5	0 - 4	≤500	2001	V_{s30} = 2830 m/s	Current USGS NSHMP (2008)/Proposed USGS NSHMP (2014)	Finite source model
10	SC02	Silva et al., 2002	Joyner-Boore Dist.	M_w	4.5 - 8.5	0.01 - 10, +PGA, PGV	1 - 400	2002	Hard Rock	Proposed USGS NSHMP (2014)	Single corner frequency, saturated σ
11	SD02	Silva et al., 2002	Joyner-Boore Dist.	M_w	4.5 - 8.5	0.01 - 10, +PGA, PGV	1 - 400	2002	Hard Rock	Proposed USGS NSHMP (2014)	Single corner frequency variable $\Delta\sigma$
12	SV02	Silva et al., 2002	Joyner-Boore Dist.	M_w	4.5 - 8.5	0.01 - 10, +PGA, PGV	1 - 400	2002	Hard Rock	Current USGS NSHMP (2008)	Single corner frequency
13	T02	Toro et al., 1997	Joyner-Boore Dist.	M_w	5.0-8.0	0.03 - 2, +PGA	1-1000	1997	V_{s30} = 1830 m/s	Current USGS NSHMP (2008)/Proposed USGS NSHMP (2014)	Hybrid empirical model
14	TP05	Tavakoli & Pezeshk 2005	Closest distance from the recording site to the ruptured area	M_w	5.0-8.2	0.00 - 4	0-1000	2005	Class A, V_{s30} = 2000 m/s	Current USGS NSHMP (2008)/Proposed USGS NSHMP (2014)	Hybrid empirical model
15	PZT11	Modified Pezeshk, Tavakoli and Zandieh 2011	Closest distance from the recording site to the ruptured area	M_w	5.0-8.2	0.00 - 4	0-1000	2012	Class A, V_{s30} = 2000 m/s	Proposed USGS NSHMP (2014)	Hybrid empirical model
16	EPR1	EPR1 2004	Joyner-Boore Dist.	M_w	5.0-8.5	0.25-100	1-1000	2004		EPR1, 2004 cluster 1 model	Spectral single corner
17	EPR2	EPR2 2004	Joyner-Boore Dist.	M_w	5.0-8.5	0.25-100	1-1000	2004		EPR1, 2004 cluster 2 model	Spectral Double corner
18	EPR3	EPR3 2004	Closest distance from the recording site to the ruptured area	M_w	5.0-8.5	0.25-100	1-1000	2004		EPR1, 2004 cluster 3 model	Hybrid empirical model
19	EPR4	EPR4 2004	Joyner-Boore Dist.	M_w	6.0-7.5	0.25-100	≤500	2004		EPR1, 2004 cluster 4 model	Finite source model

4.3 Classical Residual Analysis Method

This is the more classical residual analysis technique employed in every other GMPE bias analysis. The residual is the difference between the prediction and the observation in terms of the logarithm. Table 3 displays the results of classical residual analysis for combined soil sites namely rock, soil and deep soil sites. The highlighted colors represent red for best category of GMPE, green for second best and blue for third best category of GMPEs within each spectral period studied.

Table 3: Summary Table of all three classes of site conditions

GMPE	PGA(869)	0.1s(755)	0.2s(854)	0.3s(844)	0.5s(827)	1.0s(752)	2.0s(506)	Factor	Rank
A08p	0.180(0.035)	0.092(0.035)	0.165(0.032)	0.082(0.033)	0.105(0.034)	-0.120(0.034)	-0.277(0.040)	0.146	1
AB06p	-0.096(0.034)	-0.036(0.035)	0.005(0.033)	-0.067(0.033)	-0.140(0.031)	-0.313(0.032)	-0.417(0.038)	0.154	2
AB06+	-0.162(0.033)	-0.104(0.035)	-0.043(0.032)	-0.103(0.033)	-0.166(0.031)	-0.334(0.032)	-0.438(0.038)	0.193	3
A08	0.345(0.036)	0.241(0.035)	0.317(0.035)	0.281(0.036)	0.224(0.038)	0.029(0.034)	-0.214(0.038)	0.236	4
EPRI4	0.139(0.034)	0.108(0.036)	0.408(0.037)	0.421(0.038)	0.388(0.037)	0.197(0.034)	0.033(0.036)	0.242	5
AB06	-0.241(0.033)	-0.182(0.035)	-0.100(0.033)	-0.148(0.033)	-0.200(0.031)	-0.364(0.032)	-0.466(0.038)	0.243	6
EPRI2	0.336(0.033)	0.263(0.035)	0.278(0.034)	0.295(0.037)	0.289(0.037)	0.196(0.036)	0.105(0.039)	0.252	7
AB95	0.379(0.035)	0.359(0.038)	0.381(0.035)	0.360(0.036)	0.266(0.034)	0.080(0.032)	-0.086(0.037)	0.273	8
EPRI1	0.311(0.032)	0.266(0.035)	0.372(0.035)	0.431(0.037)	0.427(0.035)	0.174(0.031)	0.001(0.038)	0.283	9
TP05	0.120(0.038)	0.132(0.038)	0.477(0.035)	0.599(0.036)	0.184(0.031)	0.224(0.031)	0.320(0.037)	0.294	10
S01	0.232(0.037)	0.218(0.038)	0.534(0.037)	0.497(0.037)	0.420(0.035)	0.265(0.034)	0.085(0.036)	0.322	11
PZT11	-0.634(0.036)	-0.480(0.039)	-0.138(0.038)	0.142(0.040)	0.174(0.041)	0.309(0.040)	0.400(0.045)	0.325	12
SC02	0.424(0.032)	0.129(0.035)	0.547(0.035)	0.555(0.037)	0.496(0.034)	0.227(0.031)	0.011(0.038)	0.341	13
SD02	0.518(0.032)	0.222(0.036)	0.537(0.034)	0.488(0.036)	0.391(0.035)	0.199(0.034)	0.032(0.036)	0.341	14
F96	0.428(0.036)	0.450(0.038)	0.517(0.035)	0.506(0.035)	0.374(0.032)	0.151(0.031)	0.026(0.036)	0.35	15
SV02	0.628(0.035)	0.323(0.037)	0.658(0.034)	0.608(0.035)	0.482(0.032)	0.178(0.031)	-0.018(0.040)	0.414	16
EPRI3	0.522(0.036)	0.458(0.038)	0.476(0.036)	0.492(0.037)	0.471(0.035)	0.344(0.033)	0.349(0.037)	0.445	17
C03	0.577(0.037)	0.599(0.041)	0.690(0.037)	0.720(0.038)	0.561(0.035)	0.401(0.032)	0.299(0.037)	0.55	18
T02	0.654(0.037)	0.676(0.041)	0.913(0.041)	0.839(0.040)	0.747(0.036)	0.608(0.033)	0.251(0.036)	0.67	19

Legend: Mean residuals for distance ≤ 100 km for seven periods. Factor is average of the absolute value of the seven mean residuals. Numbers in parentheses in the header are numbers of observations at each period whereas in the table are standard deviation. Factor is the absolute average of the seven periods considered. Legend: **Red=1**, **Green = 2** and **Blue = 3**. Note: Positive value indicates over-prediction whereas a negative value indicates under-prediction by the model.

From *Table 3* it can be noted that the classical residual analysis results indicate that A08p is the best performing GMPE model overall followed by AB06p and AB06+ (200 bar). When you consider individual periods, there is varied response from the GMPEs. This implies that the model bias are period dependent with newer GMPEs showing better predictions at shorter periods and older GMPEs showing better predictions at longer periods i.e. 1.0s and 2.0s respectively. At shorter periods, AB06p performs better overall. In general, newer GMPEs tend to predict lower ground motion levels than older GMPEs. This can be attributed to geometrical spreading used in the GMPE; newer GMPEs use $R^{-1.3}$ while older GMPEs use $R^{-1.0}$.

Table 4 summarizes the same results but for rock site only. From these results it is still noted that A08p is still matching the observed ground motion better than the other GMPEs followed by AB95 and A08. The results also indicate that the GMPE performances are varied across the period. A08p though is performing better overall but at long periods it does not match the observed ground motion well, i.e., it under predicts the observed ground motion. EPRI1 performs well in matching the predicted ground motion to observed ground motion at 2.0 seconds.

Table 4: Selected soil class average (rock sites)

GMPE	PGA(421)	0.1s(411)	0.2s(416)	0.3s(410)	0.5s(403)	1.0s(345)	2.0s(175)	Factor	Rank
A08p	-0.108(0.036)	-0.039(0.040)	0.122(0.045)	0.056(0.045)	0.125(0.052)	-0.160(0.052)	-0.421(0.067)	0.147	1
AB95	0.138(0.041)	0.187(0.044)	0.263(0.050)	0.291(0.052)	0.240(0.052)	0.057(0.052)	-0.164(0.064)	0.192	2
A08	0.051(0.040)	0.122(0.042)	0.270(0.052)	0.246(0.055)	0.233(0.062)	-0.032(0.057)	-0.412(0.064)	0.195	3
TP05	-0.237(0.038)	-0.096(0.038)	0.386(0.050)	0.436(0.049)	0.120(0.042)	0.180(0.047)	0.261(0.066)	0.245	4
F96	0.150(0.041)	0.285(0.045)	0.411(0.050)	0.437(0.049)	0.328(0.045)	0.097(0.048)	-0.012(0.062)	0.246	5
AB06p	-0.322(0.038)	-0.167(0.039)	-0.102(0.043)	-0.155(0.042)	-0.170(0.041)	-0.380(0.047)	-0.477(0.067)	0.253	6
S01	-0.056(0.043)	0.069(0.047)	0.482(0.058)	0.489(0.058)	0.456(0.056)	0.314(0.057)	0.090(0.067)	0.279	7
AB06+	-0.385(0.038)	-0.230(0.039)	-0.143(0.043)	-0.185(0.042)	-0.194(0.041)	-0.401(0.047)	-0.495(0.067)	0.291	8
EPRI2	0.175(0.041)	0.224(0.045)	0.334(0.051)	0.404(0.053)	0.432(0.055)	0.332(0.060)	0.165(0.072)	0.295	9
EPRI4	-0.056(0.043)	0.069(0.047)	0.482(0.058)	0.538(0.059)	0.529(0.057)	0.314(0.057)	0.090(0.067)	0.297	10
EPRI1	0.138(0.040)	0.235(0.045)	0.438(0.052)	0.543(0.054)	0.553(0.051)	0.232(0.048)	0.007(0.070)	0.307	11
SD02	0.451(0.032)	0.188(0.038)	0.516(0.037)	0.473(0.039)	0.385(0.039)	0.204(0.038)	0.015(0.038)	0.319	12
SC02	0.356(0.032)	0.093(0.037)	0.528(0.038)	0.542(0.040)	0.487(0.038)	0.211(0.034)	-0.030(0.040)	0.321	13
AB06	-0.460(0.038)	-0.305(0.039)	-0.196(0.043)	-0.225(0.043)	-0.229(0.042)	-0.432(0.047)	-0.524(0.067)	0.339	14
SV02	0.367(0.040)	0.214(0.046)	0.592(0.051)	0.587(0.051)	0.485(0.046)	0.146(0.047)	-0.063(0.076)	0.351	15
PZT11	-0.901(0.042)	-0.628(0.048)	-0.178(0.059)	0.052(0.062)	0.246(0.065)	0.409(0.068)	0.437(0.089)	0.407	16
EPRI3	0.311(0.045)	0.409(0.050)	0.509(0.054)	0.572(0.055)	0.575(0.054)	0.409(0.053)	0.357(0.066)	0.449	17
C03	0.301(0.044)	0.456(0.051)	0.621(0.057)	0.706(0.059)	0.570(0.054)	0.398(0.052)	0.254(0.065)	0.472	18
T02	0.417(0.049)	0.567(0.055)	0.895(0.066)	0.850(0.063)	0.780(0.058)	0.623(0.054)	0.202(0.065)	0.619	19

Legend: Red=1, Green = 2 and Blue = 3. Note: Positive value indicates over-prediction whereas a negative value indicates under-prediction by the model.

From *Table 4* the results indicate that there is mixed response from the GMPEs across the periods studied. The classical residual analysis for rock sites indicates that A08 over-predicts the ground motions slightly but at 0.2s to 0.5s it under-predicts. PZT11 performs well at 0.3s. The best mean residual values lie between -0.03 and 0.2.

Table 5 and Table 6 summarize the results for soil site and deep soil site, respectively. The results indicate that AB06, AB06+ and AB06p perform well in matching the observation for the soil sites. For the deep soil sites EPRI4, EPRI2, and A08 matches the observations well compared to the other GMPEs. The result across all the periods has a mixed performance from the GMPEs. Note that these results highlight the need to test GMPEs as a function of spectral periods (frequencies). Mixing the periods as given by the results in the factor

column would produce a ranking that does not reflect correctly the goodness-of-fit of the models to the data.

Table 5: Selected soil class average (soil sites)

GMPE	PGA(190)	0.1s(169)	0.2s(183)	0.3s(178)	0.5s(169)	1.0s(157)	2.0s(125)	Factor	Rank
AB06	0.063(0.086)	0.057(0.089)	0.139(0.084)	0.111(0.090)	0.007(0.080)	-0.148(0.080)	-0.296(0.093)	0.117	1
AB06+	0.146(0.086)	0.140(0.089)	0.203(0.084)	0.163(0.090)	0.044(0.080)	-0.117(0.079)	-0.268(0.092)	0.154	2
AB06p	0.211(0.088)	0.210(0.090)	0.255(0.085)	0.204(0.090)	0.071(0.080)	-0.100(0.080)	-0.247(0.093)	0.186	3
A08p	0.536(0.085)	0.321(0.089)	0.341(0.084)	0.273(0.088)	0.236(0.079)	0.011(0.080)	-0.097(0.091)	0.259	4
PZT11	-0.285(0.089)	-0.215(0.093)	0.035(0.089)	0.387(0.096)	0.257(0.093)	0.286(0.098)	0.436(0.110)	0.272	5
SD02	0.677(0.045)	0.254(0.056)	0.480(0.046)	0.385(0.048)	0.259(0.044)	0.093(0.040)	0.002(0.043)	0.307	6
SC02	0.585(0.045)	0.163(0.056)	0.482(0.046)	0.446(0.048)	0.372(0.044)	0.170(0.039)	0.001(0.045)	0.317	7
EP04b	0.561(0.087)	0.389(0.089)	0.352(0.084)	0.346(0.090)	0.303(0.082)	0.152(0.086)	0.132(0.098)	0.319	8
EP04d	0.408(0.082)	0.257(0.088)	0.467(0.085)	0.464(0.089)	0.409(0.081)	0.182(0.079)	0.081(0.092)	0.324	9
A08	0.696(0.082)	0.466(0.086)	0.485(0.082)	0.462(0.087)	0.356(0.084)	0.148(0.085)	-0.025(0.092)	0.377	10
EP04a	0.554(0.085)	0.392(0.090)	0.440(0.085)	0.484(0.090)	0.461(0.079)	0.244(0.077)	0.131(0.088)	0.386	11
AB95	0.701(0.087)	0.664(0.090)	0.643(0.084)	0.609(0.090)	0.470(0.082)	0.217(0.083)	0.059(0.096)	0.480	12
S01	0.590(0.082)	0.498(0.088)	0.712(0.085)	0.659(0.089)	0.542(0.081)	0.309(0.079)	0.160(0.092)	0.496	13
EP04c	0.804(0.086)	0.613(0.092)	0.582(0.084)	0.584(0.089)	0.536(0.082)	0.395(0.083)	0.445(0.095)	0.565	14
TP05	0.558(0.087)	0.501(0.089)	0.708(0.086)	0.927(0.090)	0.426(0.081)	0.406(0.081)	0.478(0.093)	0.572	15
F96	0.786(0.085)	0.752(0.091)	0.770(0.084)	0.760(0.089)	0.609(0.078)	0.351(0.077)	0.180(0.090)	0.601	16
SV02	0.954(0.085)	0.537(0.090)	0.853(0.085)	0.789(0.090)	0.641(0.078)	0.344(0.076)	0.154(0.089)	0.610	17
C03	0.919(0.088)	0.860(0.094)	0.888(0.087)	0.895(0.092)	0.716(0.083)	0.513(0.084)	0.433(0.095)	0.746	18
T02	0.945(0.089)	0.895(0.094)	1.047(0.090)	0.971(0.092)	0.861(0.082)	0.681(0.081)	0.390(0.089)	0.827	19

Legend: Red=1, Green = 2 and Blue = 3. Note: Positive value indicates over-prediction whereas a negative value indicates under-prediction by the model.

Table 6: Selected soil class average (Deep soil sites)

GMPE	PGA(258)	0.1s(175)	0.2s(255)	0.3s(256)	0.5s(255)	1.0s(250)	2.0s(206)	Factor	Rank
EP04d	0.257(0.050)	0.055(0.067)	0.246(0.048)	0.203(0.048)	0.152(0.046)	0.043(0.038)	-0.044(0.041)	0.143	1
EP04b	0.434(0.049)	0.232(0.067)	0.133(0.048)	0.085(0.049)	0.053(0.049)	0.037(0.041)	0.038(0.046)	0.145	2
A08p	0.388(0.048)	0.180(0.070)	0.108(0.048)	-0.008(0.049)	-0.014(0.052)	-0.146(0.050)	-0.263(0.056)	0.158	3
AB06p	0.053(0.050)	0.039(0.074)	0.007(0.051)	-0.109(0.050)	-0.227(0.049)	-0.348(0.043)	-0.465(0.047)	0.178	4
AB06+	-0.022(0.050)	-0.035(0.073)	-0.048(0.051)	-0.151(0.050)	-0.255(0.049)	-0.373(0.043)	-0.489(0.047)	0.196	5
EP04a	0.414(0.047)	0.217(0.066)	0.215(0.048)	0.217(0.048)	0.204(0.047)	0.051(0.040)	-0.082(0.046)	0.200	6
A08	0.568(0.048)	0.300(0.066)	0.272(0.048)	0.211(0.049)	0.124(0.048)	0.038(0.039)	-0.160(0.043)	0.239	7
SD02	0.617(0.048)	0.169(0.067)	0.383(0.047)	0.272(0.048)	0.155(0.047)	0.039(0.040)	-0.048(0.042)	0.240	8
PZT11	-0.450(0.052)	-0.382(0.075)	-0.193(0.053)	0.121(0.052)	0.008(0.051)	0.187(0.043)	0.348(0.048)	0.241	9
AB06	-0.103(0.050)	-0.117(0.073)	-0.109(0.051)	-0.196(0.050)	-0.286(0.049)	-0.400(0.043)	-0.515(0.047)	0.246	10
SC02	0.524(0.047)	0.078(0.067)	0.387(0.048)	0.335(0.048)	0.269(0.047)	0.095(0.041)	-0.079(0.046)	0.252	11
AB95	0.539(0.051)	0.476(0.073)	0.391(0.050)	0.305(0.049)	0.178(0.046)	0.031(0.039)	-0.104(0.044)	0.289	12
S01	0.439(0.050)	0.295(0.067)	0.492(0.048)	0.396(0.048)	0.283(0.046)	0.171(0.038)	0.035(0.041)	0.302	13
TP05	0.387(0.049)	0.318(0.073)	0.466(0.051)	0.638(0.049)	0.130(0.048)	0.176(0.041)	0.277(0.043)	0.342	14
EP04c	0.663(0.055)	0.429(0.077)	0.351(0.052)	0.305(0.050)	0.268(0.047)	0.225(0.038)	0.286(0.042)	0.361	15
F96	0.621(0.050)	0.553(0.073)	0.513(0.050)	0.446(0.049)	0.298(0.047)	0.104(0.041)	-0.030(0.044)	0.367	16
SV02	0.816(0.048)	0.370(0.067)	0.624(0.048)	0.515(0.048)	0.373(0.047)	0.119(0.042)	-0.083(0.049)	0.414	17
C03	0.781(0.052)	0.690(0.076)	0.666(0.052)	0.628(0.051)	0.449(0.048)	0.338(0.039)	0.260(0.043)	0.545	18
T02	0.827(0.051)	0.721(0.069)	0.846(0.050)	0.730(0.049)	0.620(0.047)	0.543(0.038)	0.209(0.044)	0.642	19

Legend: Red=1, Green = 2 and Blue = 3. Note: Positive value indicates over-prediction whereas a negative value indicates under-prediction by the model.

Further results of classical residual analysis are presented in Appendix 1 Figures 8-11. From the results of current GMPEs used in the USGS NSHMP plots in Figure 1 in Appendix 1, it can be noted that they are comparable in the 10-1000 km distance range. At both close in distances and beyond 1000 km range, there is a lot of instability and wide variation in the residual values. In general, most of the GMPEs tend to over-predict the ground motion with exception of S01 that deviates significantly at about 400km for spectral period (0.1s, 0.2s, 0.3s, 0.5s 1.0s, and 2.0s) and at 750 km distance for the peak ground acceleration (pga). A08 also shows great deviation (over-predicting greatly) beyond 1000 km distance. For the PGA spectral period, the GMPEs are very close to each other giving no clear advantage of one GMPE from the other. AB06 and AB06+ tend to under-predict the ground motion for most of the spectral periods studied.

For the proposed GMPEs, there is tendency for most of them to over-predict the ground motion for most of the distance range except beyond 1000 km where they all show a tendency to under predict or change sharply towards under-predicting the ground motion. PZT11 is an exception as it generally under-predicts the ground motion between 10-400 km distance range then over-shoots the prediction for 0.1s spectral period. SC02 under-predicts from ~70km till 1000 km at 0.1s. AB06p and PZT11 have similar trends at 0.2s, closely matching the observed ground motion but generally under-predicts. Ab06p generally under-predicts the ground motions for most of the spectral periods studied.

4.4 NGA-East Database statistics

In order to get a clear picture of the properties of the residual results it is imperative to check the statistical properties of the NGA-East database for the periods under consideration. The test statistics for the combined sites (Table 7), shows that all of the PGA and pseudo spectral periods studied in the NGA-East database for skewness can be said to be positively skewed i.e., the right tail is more pronounced than the left tail. This implies that most of the observed ground motion values are concentrated on the left of the mean, with extreme values to the right. The same pattern is repeated for the rock sites (Table 8) and soil sites (Table 9). The deep soil sites (Table 10) have negative skewness for most of the periods studied except at 2.0s where they have positive skewness, i.e., the data for the deep soil sites are concentrated on the right of the mean, with extreme values to the left. From the kurtosis tests, the result for the observed ground motion at the specified periods (PGA, 0.1s, 0.2s, 0.3s, 0.5s, 1.0s, and 2.0s) shows that for the soil sites the kurtosis is platykurtic, i.e., the data has flatter than normal distribution with wider peaks. This is also repeated for deep soil sites except at 0.1s where the distribution is leptokurtic, i.e., the distribution has a sharper peak and most of the values are concentrated around the mean and have thicker tails with high probability for extreme values. For the rock sites, the distribution is also leptokurtic except at 0.1s where the distribution is platykurtic. For combined site classes, the distribution is platykurtic except for PGA where the distribution can be considered almost as mesokurtic. The *KS*, Lilliefors and Jarque-Bera statistical tests on the NGA-East observed ground motions at the

PGA, 0.1s, 0.2s, 0.3s, 0.5s, 1.0s, and 2.0s shows that these ground motion data are not normally distributed. It can be concluded that the statistics of the database affects the statistics of the residual values and hence the GMPEs statistics.

Table 7: NGA-Database Summary Statistics for All Sites

Period	Mode	Skewness	Kurtosis
PGA	-4.9914	0.4697	3.0056
0.1s	-2.9393	0.3608	2.9197
0.2s	-3.9914	0.3143	2.8542
0.3s	-3.9747	0.2985	2.8158
0.5s	-3.9318	0.3145	2.7861
1.0s	-4.9586	0.3771	2.8253
2.0s	-4.9747	0.3104	2.6201

Table 8: NGA-Database Summary Statistics for Rock Sites

Period	Mode	Skewness	Kurtosis
PGA	-4.9914	0.9671	3.6361
0.1s	-2.9914	0.6689	2.9828
0.2s	-3.9747	0.8616	3.6784
0.3s	-4.9626	0.9262	3.8684
0.5s	-4.9031	0.9830	4.0134
1.0s	-4.9586	0.9597	3.9338
2.0s	-5.7878	0.6565	3.2705

Table 9: NGA-Database Summary Statistics for Soils

Period	Mode	Skewness	Kurtosis
PGA	-3.9830	0.3127	2.9597
0.1s	-3.9914	0.3537	2.9031
0.2s	-3.9706	0.2512	2.8561
0.3s	-3.9872	0.1744	2.8469
0.5s	-3.9914	0.1536	2.7272
1.0s	-4.8827	0.2844	2.8626
2.0s	-3.8697	0.2140	2.3647

Table 10: NGA-Database Summary Statistics for Deep Soils

Period	Mode	Skewness	Kurtosis
PGA	-3.7570	-0.0818	2.8725
0.1s	-2.9393	-0.0744	3.5252
0.2s	-2.7595	-0.3087	2.9662
0.3s	-2.9706	-0.2783	2.8275
0.5s	-2.9586	-0.1039	2.5996
1.0s	-3.9957	-0.0217	2.3371
2.0s	-4.9469	0.1021	2.2643

4.5 Normality Test

In univariate data analysis, one of the most widely used assumptions is the assumption of “normality”. Furthermore, the commonly assumed “normality”, helps us estimate and make inferential comparisons and judgments. However, violation of this assumption might produce misleading inferences and the results of using unreliable inferences are to produce misleading interpretations.

The random residual is usually assumed to be lognormal distributed (Campbell 1981). It is assumed that random residuals behave normally for all

computations related to the ground motion variability. Deviation of this random residual with respect to normality is one of the main causes of the presence of a fat tail in the distribution function. To check this hypothesis, plots of cumulative probability with respect to residuals were plotted as illustrated in the Figures in Appendix 2. A linear trend indicates that the model is adequate for predicting the ground motions in the dataset. It can be noted that in the plot of random residual versus cumulative probability (Figures in Appendix 2) there is a varied response in the tails. This was probed further using skewness and kurtosis test as discussed in the skewness and kurtosis sections respectively.

4.5.1 Skewness

Skewness is a measure of the asymmetry of the data around the sample mean. If skewness is negative, the data are spread out more to the left of the mean than to the right. If skewness is positive, the data are spread out more to the right. The skewness of the normal distribution (or any perfectly symmetric distribution) is zero. The skewness of a distribution is defined as

$$s = \frac{E(x_i - \mu)^3}{\sigma^3} \quad (18)$$

where μ is the mean of x , σ is the standard deviation of x , and $E(t)$ represents the expected value of the quantity t . A negative skew indicates that the distribution is spread out more to the left of the mean value, assuming increasing values on the axis to the right. The mean is smaller than the mode. Distributions with positive skewness have large tails that extend to the right. By skewed left, we mean that the left tail is long relative to the right tail. Similarly, skewed right

means that the right tail is long relative to the left tail. A skewness test was done for the GMPEs under study at the seven spectral periods considered.

Tables 11 – 12 summarize the outcomes of this test.

Table 11: Summary table of Skewness results for all sites

GMPE	PGA	0.1s	0.2s	0.3s	0.5s	1.0s	2.0s	Factor	Rank
A08p	-0.606	-0.503	-0.179	0.049	0.214	0.440	0.556	0.004	1
EPRI 2	-0.338	-0.473	0.091	0.186	0.142	0.086	0.157	0.021	2
C03	0.088	0.049	-0.055	0.039	0.010	0.005	0.080	0.031	3
TP05	0.181	0.041	-0.064	-0.091	0.032	0.146	0.156	0.057	4
EPRI 3	0.068	0.096	0.068	0.101	0.115	0.137	0.177	0.109	5
PZT11	0.013	-0.192	-0.121	-0.212	-0.194	-0.162	-0.016	0.126	6
AB06	0.247	0.038	0.012	0.034	0.059	0.212	0.307	0.130	7
AB06+	0.249	0.039	0.013	0.032	0.057	0.211	0.314	0.131	8
AB06p	0.252	0.060	0.034	0.047	0.069	0.211	0.296	0.139	9
AB95	0.297	0.148	0.138	0.139	0.085	0.162	0.279	0.178	10
T02	-0.151	-0.538	-0.407	-0.193	-0.137	-0.153	0.000	0.226	11
EPRI 1	0.260	0.289	0.129	0.138	0.180	0.265	0.488	0.250	12
SV02	0.296	0.256	0.119	0.195	0.244	0.364	0.378	0.265	13
F96	0.442	0.367	0.208	0.210	0.139	0.234	0.308	0.273	14
SD02	0.320	0.234	0.119	0.237	0.323	0.365	0.356	0.279	15
SC02	0.327	0.230	0.132	0.254	0.312	0.346	0.364	0.280	16
EPRI 4	-0.762	-0.896	-0.579	-0.355	-0.266	-0.262	-0.135	0.465	17
S01	-0.769	-0.864	-0.629	-0.412	-0.300	-0.274	-0.134	0.483	18
A08	2.946	1.453	1.412	1.346	0.689	1.070	0.580	1.357	19

Table 12: Summary table of Skewness results for rock site

GMPE	PGA	0.1s	0.2s	0.3s	0.5s	1.0s	2.0s	Factor	Rank
C03	0.06416	-0.13499	-0.13706	-0.04741	-0.05621	0.03126	0.34525	0.009	1
TP05	0.16059	-0.26432	-0.25998	-0.14083	-0.1567	0.14522	0.41828	0.014	2
AB95	0.20285	-0.06557	-0.18236	-0.22542	-0.23336	-0.0429	0.43076	0.017	3
A08p	-0.62555	-0.3261	-0.17015	-0.09036	0.10051	0.41012	0.56988	0.019	4
SV02	-0.07825	-0.31622	-0.34918	-0.21649	-0.12003	0.24546	0.57775	0.037	5
F96	0.22906	0.01443	-0.11924	-0.18257	-0.23653	0.10854	0.57293	0.055	6
EPRI 1	-0.09403	-0.03082	-0.37404	-0.25847	-0.16896	0.05862	0.40528	0.066	7
AB06+	0.11858	-0.28701	-0.3651	-0.36119	-0.25496	0.05504	0.48404	0.087	8
AB06	0.11925	-0.28503	-0.3662	-0.36598	-0.2606	0.04713	0.46906	0.092	9
AB06p	0.08843	-0.28107	-0.35938	-0.35241	-0.25472	0.0369	0.44635	0.097	10
T02	-0.17709	-0.41022	-0.28803	-0.14246	-0.10809	-0.07367	0.28276	0.131	11
SD02	0.12559	0.11599	-0.01088	0.03859	0.10301	0.22396	0.34109	0.134	12
EPRI 3	0.02893	-0.26764	-0.4703	-0.40653	-0.29539	0.02264	0.42648	0.137	13
SC02	0.13509	0.11439	-0.0067	0.04825	0.09111	0.20726	0.39593	0.141	14
EPRI 2	-0.30967	-0.39888	-0.23724	-0.2014	-0.22229	-0.13713	0.19807	0.187	15
EPRI 4	-0.65511	-0.5722	-0.41706	-0.23836	-0.16165	-0.0949	0.14129	0.285	16
S01	-0.65511	-0.5722	-0.41706	-0.24511	-0.15668	-0.0949	0.14129	0.286	17
PZT11	-0.33123	-0.41938	-0.57725	-0.55077	-0.70484	-0.73249	-0.24024	0.508	18
A08	3.13208	1.14329	1.90842	1.64763	0.72886	1.29681	0.70697	1.509	19

The skewness results were interpreted as: If skewness = 0, the data are perfectly symmetrical. But a skewness of exactly zero is quite unlikely for real-world data, so how can you interpret the skewness number? The rule of thumb suggested by Bulmer (1979) was used to interpret the skewness values, i.e.,

- If skewness is less than -1 or greater than $+1$, the distribution is highly skewed.
- If skewness is between -1 and $-\frac{1}{2}$ or between $+\frac{1}{2}$ and $+1$, the distribution is moderately skewed.
- If skewness is between $-\frac{1}{2}$ and $+\frac{1}{2}$, the distribution is approximately symmetric.

The results of this classification are summarized in *Table 13*.

Table 13: Classification of the GMPEs according to skewness (all sites)

GMPE	PGA	0.1s	0.2s	0.3s	0.5s	1.0s	2.0s
A08	Highly skewed	Highly skewed	Highly skewed	Highly skewed	Moderate	Highly Skewed	Moderate
A08p	Moderate	≈symmetrical	≈symmetrical	≈symmetrical	≈symmetrical	≈symmetrical	Moderate
AB06+	≈symmetrical	≈symmetrical	≈symmetrical	≈symmetrical	≈symmetrical	≈symmetrical	≈symmetrical
AB06	≈symmetrical	≈symmetrical	≈symmetrical	≈symmetrical	≈symmetrical	≈symmetrical	≈symmetrical
AB06p	≈symmetrical	≈symmetrical	≈symmetrical	≈symmetrical	≈symmetrical	≈symmetrical	≈symmetrical
AB95	≈symmetrical	≈symmetrical	≈symmetrical	≈symmetrical	≈symmetrical	≈symmetrical	≈symmetrical
C03	≈symmetrical	≈symmetrical	≈symmetrical	≈symmetrical	≈symmetrical	≈symmetrical	≈symmetrical
EPR 1	≈symmetrical	≈symmetrical	≈symmetrical	≈symmetrical	≈symmetrical	≈symmetrical	≈symmetrical
EPRI 2	≈symmetrical	≈symmetrical	≈symmetrical	≈symmetrical	≈symmetrical	≈symmetrical	≈symmetrical
EPRI 3	≈symmetrical	≈symmetrical	≈symmetrical	≈symmetrical	≈symmetrical	≈symmetrical	≈symmetrical
EPRI 4	Moderate	Moderate	≈symmetrical	≈symmetrical	≈symmetrical	≈symmetrical	≈symmetrical
F96	≈symmetrical	≈symmetrical	≈symmetrical	≈symmetrical	≈symmetrical	≈symmetrical	Moderate
PZT11	≈symmetrical	≈symmetrical	Moderate	Moderate	Moderate	Moderate	≈symmetrical
S01	Moderate	Moderate	≈symmetrical	≈symmetrical	≈symmetrical	≈symmetrical	≈symmetrical
SC02	≈symmetrical	≈symmetrical	≈symmetrical	≈symmetrical	≈symmetrical	≈symmetrical	≈symmetrical
SD02	≈symmetrical	≈symmetrical	≈symmetrical	≈symmetrical	≈symmetrical	≈symmetrical	≈symmetrical
SV02	≈symmetrical	≈symmetrical	≈symmetrical	≈symmetrical	≈symmetrical	≈symmetrical	Moderate
T02	≈symmetrical	≈symmetrical	≈symmetrical	≈symmetrical	≈symmetrical	≈symmetrical	≈symmetrical
TP05	≈symmetrical	≈symmetrical	≈symmetrical	≈symmetrical	≈symmetrical	≈symmetrical	≈symmetrical

From *Table 13*, it can be seen that most of the GMPEs can be considered as symmetrical and A08 shows highly skewed results while a few GMPEs shows moderate skewness. The skewness is also a function of the spectral period, which further highlights the need to rank the GMPEs based on spectral periods rather than overall ranking (mixed spectral periods/frequencies).

4.5.2 Kurtosis

Kurtosis is a measure of how outlier-prone a distribution is. The kurtosis of the normal distribution is 3. Distributions that are more outlier-prone than the normal distribution have kurtosis greater than 3; distributions that are less outlier-prone have kurtosis less than 3. The kurtosis of a distribution is defined as

$$k = \frac{E(x-\mu)^4}{\sigma^4} \quad (19)$$

where μ is the mean of x , σ is the standard deviation of x , and $E(t)$ represents the expected value of the quantity t . A kurtosis test was performed for the GMPEs studied at each of the seven spectral periods. The results of this test are shown in *Table 14* for all sites combined.

Table 14: Summary table of Kurtosis Results (all sites)

GMPE	PGA	0.1s	0.2s	0.3s	0.5s	1.0s	2.0s	Factor	Rank
PZT11	3.153	3.023	3.030	3.102	2.902	2.823	3.017	3.007	1
EPRI 3	3.354	3.155	2.974	2.966	3.072	3.325	3.704	3.221	2
EPRI 1	3.287	3.972	3.051	2.882	2.938	3.170	3.811	3.302	3
SD02	3.518	3.412	3.064	3.181	3.370	3.489	3.803	3.405	4
SC02	3.549	3.424	3.081	3.207	3.352	3.520	3.728	3.409	5
T02	2.947	4.030	3.593	3.374	3.187	3.283	3.719	3.447	6
A08p	3.411	4.235	3.783	3.320	3.135	3.195	3.260	3.477	7
C03	3.388	3.710	3.549	3.366	3.302	3.429	3.642	3.484	8
EPRI 2	3.686	4.640	3.379	3.162	3.118	3.061	3.373	3.489	9
AB95	3.713	3.717	3.533	3.466	3.412	3.465	3.643	3.564	10
SV02	3.604	3.733	3.475	3.470	3.541	3.670	3.702	3.599	11
AB06p	3.799	3.904	3.523	3.415	3.364	3.580	3.757	3.620	12
AB06	3.871	3.939	3.526	3.403	3.389	3.606	3.814	3.650	13
AB06+	3.899	3.952	3.539	3.405	3.379	3.602	3.836	3.659	14
F96	4.108	3.976	3.640	3.567	3.522	3.652	3.725	3.741	15
S01	4.084	5.304	4.267	3.705	3.114	2.960	3.085	3.789	16
EPRI 4	4.113	5.443	4.297	3.721	3.144	2.994	3.124	3.834	17
TP05	4.017	4.601	3.700	3.753	3.680	3.685	3.703	3.877	18
A08	24.963	7.017	14.783	10.257	6.155	8.116	4.886	10.882	19

The results of kurtosis were interpreted using the following classification

- Kurtosis > 3 - Leptokurtic distribution, sharper than a normal distribution, with values concentrated around the mean and thicker tails. This means high probability for extreme values.
- Kurtosis < 3 - Platykurtic distribution, flatter than a normal distribution with a wider peak. The probability for extreme values is less than for a normal distribution, and the values are wider spread around the mean.
- Kurtosis = 3 - Mesokurtic distribution - normal distribution for example.

The results of this classification are summarized in *Table 15* for the rock sites.

Table 15: Classification of the GMPEs according to kurtosis (all sites)

GMPE	PGA	0.1s	0.2s	0.3s	0.5s	1.0s	2.0s
A08	Leptokurtic	Leptokurtic	Leptokurtic	Leptokurtic	Leptokurtic	Leptokurtic	Leptokurtic
A08p	Leptokurtic	Leptokurtic	Leptokurtic	Leptokurtic	Leptokurtic	Leptokurtic	Leptokurtic
AB06+	Leptokurtic	Platykurtic	Leptokurtic	Leptokurtic	Leptokurtic	Leptokurtic	Leptokurtic
AB06	Leptokurtic	Platykurtic	Leptokurtic	Leptokurtic	Leptokurtic	Leptokurtic	Leptokurtic
AB06p	Leptokurtic	Platykurtic	Leptokurtic	Leptokurtic	Leptokurtic	Leptokurtic	Leptokurtic
AB95	Leptokurtic	Platykurtic	Leptokurtic	Leptokurtic	Leptokurtic	Leptokurtic	Leptokurtic
C03	Platykurtic	Platykurtic	Platykurtic	Platykurtic	Platykurtic	Leptokurtic	Leptokurtic
EPR 1	Leptokurtic	Leptokurtic	Leptokurtic	Leptokurtic	Leptokurtic	Leptokurtic	Leptokurtic
EPR 2	Leptokurtic	Leptokurtic	Platykurtic	Leptokurtic	Leptokurtic	Leptokurtic	Leptokurtic
EPRI 3	Platykurtic	Platykurtic	Leptokurtic	Leptokurtic	Leptokurtic	Leptokurtic	Leptokurtic
EPRI 4	Leptokurtic	Leptokurtic	Leptokurtic	Leptokurtic	Leptokurtic	Leptokurtic	Leptokurtic
F96	Leptokurtic	Platykurtic	Platykurtic	Leptokurtic	Leptokurtic	Leptokurtic	Leptokurtic
PZT11	Leptokurtic	Platykurtic	Leptokurtic	Leptokurtic	Leptokurtic	Leptokurtic	Leptokurtic
S01	Leptokurtic	Leptokurtic	Leptokurtic	Leptokurtic	Platykurtic	Platykurtic	Platykurtic
SC02	Leptokurtic	Leptokurtic	Leptokurtic	Leptokurtic	Leptokurtic	Leptokurtic	Leptokurtic
SD02	Leptokurtic	Leptokurtic	Leptokurtic	Leptokurtic	Leptokurtic	Leptokurtic	Leptokurtic
SV02	Leptokurtic	Leptokurtic	Leptokurtic	Leptokurtic	Leptokurtic	Leptokurtic	Leptokurtic
T02	Platykurtic	Leptokurtic	Platykurtic	Platykurtic	Platykurtic	Platykurtic	Leptokurtic
TP05	Leptokurtic	Leptokurtic	Platykurtic	Leptokurtic	Leptokurtic	Leptokurtic	Leptokurtic

Table 15 Indicates that most of the GMPEs are leptokurtic in distribution.

This implies that they have sharper peak than a normal distribution, with values concentrated around the mean and thicker tails. With leptokurtic distribution, the GMPEs distributions are likely to be influenced by extreme values. For those GMPEs having platykurtic distributions i.e., flatter peak than normal distribution with wider peak, the probability for extreme values is less than for a normal distribution, and the values are spread widely around the mean. A08 had higher peakedness distribution and this could have come from an extreme deviation.

Small departures from the normality assumption do not affect the model greatly, but gross non-normality is potentially more serious as the test statistics (e.g., t , F , etc) and confidence and prediction interval depends on the normality

assumption (Montgomery *et al.*, 2003). A heavy tail distribution often generates outliers that pull the least square fit too much in their direction.

4.6 Testing the shape of the residual distributions

Several approaches were used to test the shape of the residual distributions such as the Z score, Kolmogorov-Smirnov (KS), Lilliefors, and Jarque-Bera tests.

The tests were done on the GMPEs to see if they obey the rules of normal distribution that normal data have

- Mean = median = mode, also has symmetry about the center and 50% of the values less than the mean and 50% greater than the mean.

In addition;

- Approximately two thirds of the standardized residuals falling between plus and minus one;
- Approximately 95% of the standardized residuals falling between plus and minus two; and
- Almost all (99.7%) of the standardized residuals falling between plus and minus three;

The Z score was calculated using equation 19 and the results presented in Figures in Appendix 1 for rock sites.

$$z = \frac{x - \mu}{\sigma} \quad (20)$$

where μ is the mean of x , σ is the standard deviation of x and z is the Z-score (standard score). Figure 6 depicts the expected distribution from a normal distributed data.

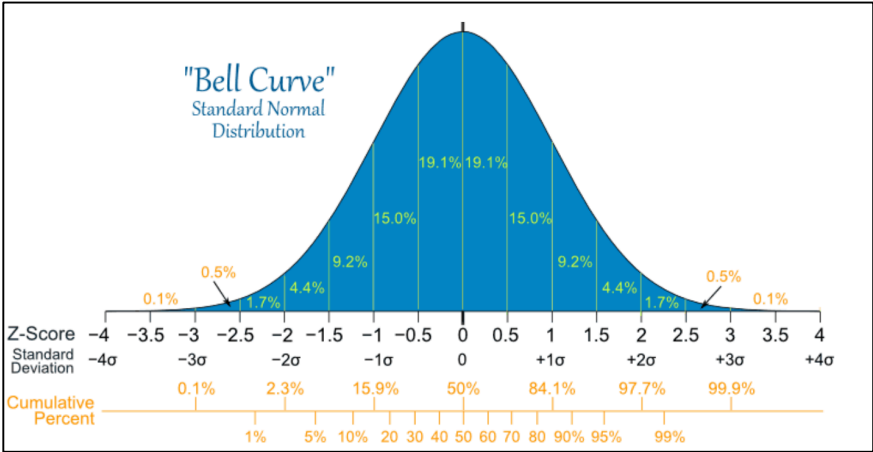


Figure 6: Detailed Standard Normal Distribution

Source: <http://www.mathsisfun.com/data/standard-normal-distribution.html>

Figure 6 shows that 68% cumulative percent are within ± 1 standard deviations, 95% are within 2 standard deviations and 99.7% are within 3 standard deviations. Figure 6 was used to compare the GMPEs residual distributions and to illustrate what standard deviation units are considered normal. The results of this comparison are shown in Figures in Appendix 2 for the rock sites. Comparing the GMPEs with Figure 6, the results indicate that most of the GMPEs closely follow the normal distribution.

4.6.1 Hypotheses testing

The following are the null (H_0) and alternative (H_1) hypotheses used in this distribution:

H_0 : The random residuals come from a population with a normal distribution, with mean μ and standard deviation σ .

H_1 : The data do not represent a sample from the normal distribution with mean μ and standard deviation σ .

The tests are conducted at a $\alpha = 0.05$ level representing the probability of falsely rejecting H_0 . Figure 7 illustrates the hypothesis test procedures.

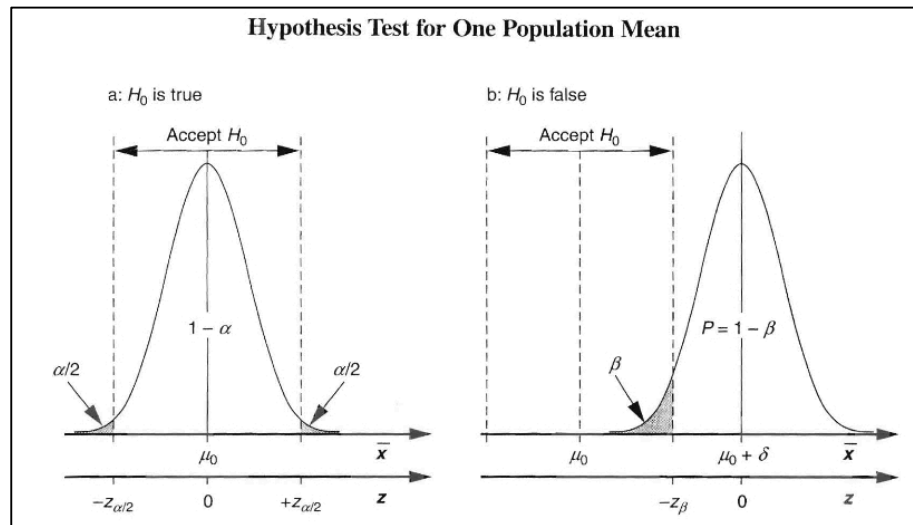


Figure 7: Distribution of mean μ when H_0 is true and false

4.6.2 The z-test

The null hypothesis is that the mean of the normalized residual set is zero. The residuals are assumed to be from a normal distribution of known variance (unit). The p-value indicates the smallest level of significance that would lead to rejection of the null hypothesis with the given data. A small p-value means that the differences between the estimated mean and model mean is significant and thus it is very unlikely that the candidate model produced the observation. On the other hand, a large p-value enhances our confidence in the model (Scherbaum *et al.*, 2004). Figures in Appendix 2 for rock sites include the z-test, and p-value for different GMPEs for residual distribution of seven periods namely (pga (0.0s), 0.1s, 0.2s, 0.3s, 0.5s, 1.0s, and 2.0s).

Figures in Appendix 2 (Rock sites) show the distributions for all the GMPEs. On the left top panel is the histogram fitted with a normal distribution, on the bottom left panel are the parameters tested to show if the distribution is normal for which all of the GMPEs fail the normality test. On the right top panel is the cumulative distribution with a straight-line fit. It indicates that the GMPEs normality is a function of the number of standard deviation units. On the bottom right panel is the normalized residual distribution with z -scores (indication of the number of standard deviation units from the mean). The standardized normal distribution plot indicates that all of the GMPEs have a mean of zero and unit variance.

4.6.3 The Lilliefors test

The Lilliefors test was used to test the null hypothesis that data come from a normally distributed population, when the null hypothesis does not specify the mean and variance of the distribution. Figures in Appendix 2 (Rock sites) shows the parametric test done. The results indicate that the GMPEs residuals are not normally distributed.

4.6.4 Kolmogorov-Smirnov test

The Kolmogorov-Smirnov (K-S) goodness-of-fit test compares a hypothetical or fitted cumulative distribution function (*cdf*) $\check{F}(x)$ with an empirical *cdf* $F_n(x)$ in order to assess fit. The empirical *cdf* $F_n(x)$ is the proportion of the observations $X_1, X_2 \dots X_n$ that are less than or equal to x and is defined as:

$$F_n(x) = \frac{I(x)}{n} \quad (21)$$

where n is the size of the random sample and $I(x)$ is the number of X_i 's less than or equal to (x) . The statistic D_n is the largest vertical distance between $F_n(x)$ and $\check{F}(x)$ for all values of x , i.e.,

$$D_n = \sup_{x \in \mathbb{R}} \{|F_n(x) - \check{F}(x)|\} \quad (22)$$

This was done to check whether or not the residual distribution is significantly different from a zero mean normal distribution with unit variance. The KS test checks the deviations from the model distribution not only in a general sense but also for the most deviant values of the criterion variable.

The hypothesis for the test is presented as

$H_0 :=$ normal distribution, skewness is zero and excess kurtosis is zero

$H_1 :=$ non – normal distribution,

If the test statistic exceeds the $1 - \alpha$ quantile as given by *Table 16* then reject H_0 at the level of significance $\alpha = 0.05$.

Table 16: Critical Values for the Two-sample Kolmogorov-Smirnov test (2-sided)

$n \backslash$ α	0.01	0.05	0.1	0.15	0.2
1	0.995	0.975	0.950	0.925	0.900
10	0.490	0.410	0.368	0.342	0.322
20	0.356	0.294	0.264	0.246	0.231
30	0.290	0.240	0.220	0.200	0.190
50	0.230	0.190	0.170	0.160	0.150
>50	1.63	1.36	1.22	1.14	1.07
	$\frac{1.63}{\sqrt{n}}$	$\frac{1.36}{\sqrt{n}}$	$\frac{1.22}{\sqrt{n}}$	$\frac{1.14}{\sqrt{n}}$	$\frac{1.07}{\sqrt{n}}$

In statistics, the Kolmogorov-Smirnov test (K-S test) is a non-parametric test for the equality of continuous, one-dimensional probability distributions that can be used to compare a sample with a reference probability distribution (one sample K-S test), or to compare two samples (two sample K-S test). The K-S statistic quantifies a distance between the empirical distribution functions of the sample and the cumulative distribution function of the reference distribution, or between the empirical distribution functions of two samples. The null distribution of this statistic is calculated under the null hypothesis that the samples are drawn from the same distribution (in the two sample case) or that the sample is drawn

from the reference distribution (in the one sample case). In each case, the distributions considered under the null hypothesis are continuous distributions but are otherwise unrestricted. Figures in Appendix 2 (Rock sites) show that the GMPEs residual distributions are not normally distributed. This is consistent with results of test statistics obtained from the NGA-East database itself.

4.6.5 Jarque-Bera (JB) test

The equation for Jarque-Bera test is given by

$$JB = n \left[\frac{\text{skewness}^2}{6} + \frac{(\text{kurtosis}-3)^2}{24} \right] \quad (23)$$

The JB statistic has an asymptotic chi-square distribution with two degrees of freedom.

The hypothesis for the test is presented as

$H_0 := \text{normal distribution, skewness is zero and excess kurtosis is zero}$

$H_1 := \text{non - normal distribution,}$

The null hypothesis of normality is rejected if the calculated test statistics exceeds a critical value from the $\chi^2_{(2)}$ distributions. The parameters used in this study were: significance level $\alpha = 0.05$ and critical value = 5.99. The results of this test are presented in Figures in Appendix 2 (Rock sites) and indicate that the GMPEs are not normally distributed.

4.7 Log likelihood (LLH) Ranking Method

The quantitative decision favoring different models requires a meaningful measure to distinguish candidate probabilistic models. Scherbaum *et al.* (2009) provides a ranking criterion based on information theory (see details in the original paper on the theoretical aspects of the method not discussed here). This technique is based on the probability for an observed ground motion to be realized under the hypothesis that a model is true. It provides one value, the negative average log-likelihood (LLH) (Delavaud *et al.*, 2012), which reflects the fit between data and model.

Within an information theory framework, the Kullback-Leibler (*KS*) distance (Delavaud *et al.*, 2009) gives this measure. The *KS* distance between two models f and g is given as

$$D(f, g) = E_f(\log_2(f)) - E_f(\log_2(g)) \quad (24)$$

where E_f is the expected value taken with respect to f . The distance quantitatively represents the amount of information loss if the model f is substituted by model g . Here, for a base 2 logarithm, its unit is bit (binary digit which measures information or entropy, based on logarithmic base 2). For the model comparison, i.e. two models g_1 and g_2 , only their relative *KS* distance $D(f, g_1) - D(f, g_2)$, is taken into account. As a result, the expectation of the unknown model f drops out as a constant. The second expectation, $-E_f(\log_2(g)) = -\int_{-\infty}^{+\infty} f(x) \log_2(g(x_i))$ can be estimated by the average sample log likelihood

$$LLH = -\frac{1}{N} \sum_{i=1}^N \log_2(g(x_i)) \quad (25)$$

with N the number of observations x_i and g the probability density function predicted by the GMPE (normal distribution, with standard deviation and the total sigma of the model). The ranking of the models according to their fit of the NGA-East database is presented in *Tables 17 – 20* for all sites, rock, soil and deep soil sites respectively. A small LLH value indicates that the candidate GMPE is close to the model that has generated the data, while a large LLH value corresponds to a model that is less likely of having generated the data. The final LLH value characterizing the fit between the data and the model is simply the mean of all individual LLH values given in the Factor column.

Table 17: Summary table for LLH results for all sites and within 100km

GMPE	pga	0.1s	0.2s	0.3s	0.5s	1.0s	2.0s	Factor	Rank
EPRI 3	2.767	2.733	2.687	2.626	2.575	2.571	2.499	2.637	1
SD02	2.754	2.715	2.662	2.646	2.603	2.579	2.503	2.637	2
AB95	2.766	2.783	2.706	2.653	2.612	2.537	2.464	2.646	3
AB06p	2.742	2.749	2.680	2.625	2.568	2.614	2.565	2.649	4
AB06	2.752	2.749	2.680	2.625	2.566	2.616	2.570	2.651	5
SC02	2.757	2.715	2.665	2.645	2.603	2.600	2.588	2.653	6
AB06+	2.755	2.748	2.677	2.625	2.572	2.623	2.576	2.654	7
SV02	2.738	2.727	2.687	2.661	2.620	2.592	2.573	2.657	8
F96	2.753	2.779	2.706	2.649	2.597	2.573	2.564	2.660	9
EPRI 1	2.745	2.753	2.670	2.637	2.616	2.596	2.628	2.664	10
EPRI 2	2.950	2.831	2.684	2.631	2.587	2.549	2.457	2.670	11
PZT11	2.747	2.736	2.722	2.765	2.672	2.590	2.471	2.672	12
C03	2.780	2.795	2.793	2.736	2.623	2.575	2.490	2.685	13
TP05	2.789	2.793	2.750	2.899	2.627	2.578	2.506	2.706	14
T02	2.780	2.863	3.016	2.836	2.686	2.614	2.529	2.761	15
EPRI 4	3.292	2.901	3.171	3.192	3.150	3.095	2.746	3.078	16
A08p	4.461	3.068	3.140	2.877	2.658	2.723	2.691	3.088	17
S01	3.327	2.923	3.218	3.234	3.165	3.124	2.761	3.107	18
A08	14.037	3.084	5.625	5.668	3.937	4.430	2.921	5.672	19

Table 18: Summary table for LLH results for rock sites and within 100km

GMPE	pga	0.1s	0.2s	0.3s	0.5s	1.0s	2.0s	Factor	Rank
AB95	2.850	2.830	2.742	2.671	2.642	2.589	2.537	2.694	1
EPRI 3	2.877	2.818	2.763	2.679	2.639	2.605	2.556	2.705	2
F96	2.861	2.826	2.739	2.664	2.623	2.618	2.616	2.707	3
AB06p	2.855	2.820	2.739	2.652	2.623	2.658	2.619	2.709	4
AB06	2.864	2.821	2.738	2.653	2.623	2.660	2.624	2.712	5
SV02	2.852	2.812	2.736	2.687	2.634	2.636	2.624	2.712	6
AB06+	2.866	2.820	2.735	2.649	2.629	2.665	2.629	2.713	7
SD02	2.845	2.813	2.765	2.723	2.686	2.632	2.554	2.717	8
EPRI 1	2.853	2.829	2.741	2.693	2.675	2.639	2.615	2.721	9
EPRI 2	3.016	2.904	2.735	2.667	2.645	2.599	2.514	2.726	10
SC02	2.846	2.813	2.767	2.726	2.680	2.653	2.624	2.730	11
C03	2.870	2.855	2.828	2.763	2.652	2.620	2.560	2.735	12
PZT11	2.860	2.841	2.790	2.793	2.734	2.656	2.534	2.744	13
TP05	2.896	2.850	2.789	2.883	2.650	2.611	2.574	2.751	14
T02	2.871	2.934	3.048	2.867	2.722	2.653	2.596	2.813	15
A08p	4.183	3.099	3.139	2.880	2.706	2.762	2.735	3.072	16
S01	3.316	2.983	3.222	3.227	3.159	3.103	2.727	3.105	17
EPRI 4	3.316	2.983	3.222	3.235	3.185	3.103	2.727	3.110	18
A08	11.879	3.142	5.235	5.300	3.797	4.247	2.940	5.220	19

Table 19: Summary table for LLH results for soils sites and within 100km

GMPE	pga	0.1s	0.2s	0.3s	0.5s	1.0s	2.0s	Factor	Rank
AB06p	2.556	2.503	2.483	2.462	2.370	2.399	2.318	2.442	1
AB06	2.557	2.504	2.481	2.460	2.374	2.400	2.336	2.445	2
AB06+	2.556	2.503	2.482	2.461	2.372	2.399	2.345	2.445	3
EPRI 3	2.598	2.489	2.485	2.449	2.383	2.441	2.361	2.458	4
AB95	2.593	2.542	2.499	2.448	2.397	2.432	2.332	2.463	5
F96	2.581	2.546	2.499	2.461	2.400	2.424	2.338	2.464	6
PZT11	2.550	2.508	2.494	2.540	2.471	2.416	2.377	2.479	7
TP05	2.574	2.552	2.518	2.503	2.435	2.453	2.362	2.485	8
C03	2.606	2.542	2.537	2.482	2.451	2.476	2.351	2.492	9
EPRI 2	2.713	2.640	2.491	2.445	2.401	2.432	2.345	2.495	10
SV02	2.550	2.545	2.507	2.507	2.445	2.485	2.429	2.496	11
EPRI 1	2.537	2.608	2.501	2.489	2.389	2.504	2.590	2.517	12
SC02	2.597	2.585	2.553	2.544	2.491	2.500	2.451	2.532	13
SD02	2.598	2.585	2.551	2.545	2.490	2.505	2.459	2.533	14
T02	2.628	2.684	2.668	2.570	2.510	2.517	2.382	2.566	15
A08p	3.085	2.818	2.656	2.578	2.462	2.550	2.639	2.684	16
S01	2.820	2.712	2.719	2.705	2.760	2.773	2.627	2.731	17
EPRI 4	2.820	2.712	2.719	2.713	2.778	2.773	2.627	2.735	18
A08	5.423	2.932	2.614	2.669	2.467	2.751	2.650	3.072	19

Table 20: Summary table for LLH results for deep soils sites and within 100km

GMPE	pga	0.1s	0.2s	0.3s	0.5s	1.0s	2.0s	Factor	Rank
AB06p	2.628	2.619	2.599	2.526	2.448	2.379	2.304	2.500	1
AB06+	2.628	2.619	2.600	2.526	2.451	2.380	2.304	2.501	2
AB06	2.629	2.620	2.601	2.527	2.454	2.381	2.304	2.502	3
EPRI 1	2.619	2.627	2.590	2.527	2.449	2.374	2.344	2.504	4
PZT11	2.606	2.589	2.592	2.622	2.488	2.360	2.298	2.508	5
SV02	2.625	2.590	2.590	2.538	2.498	2.425	2.345	2.516	6
EPRI 3	2.654	2.612	2.596	2.539	2.466	2.405	2.342	2.516	7
SC02	2.621	2.587	2.588	2.541	2.502	2.429	2.350	2.517	8
SD02	2.622	2.588	2.587	2.539	2.502	2.435	2.367	2.520	9
F96	2.654	2.637	2.623	2.559	2.468	2.399	2.318	2.523	10
AB95	2.664	2.642	2.619	2.556	2.479	2.404	2.324	2.527	11
TP05	2.640	2.643	2.641	2.613	2.489	2.418	2.350	2.542	12
C03	2.659	2.658	2.662	2.589	2.516	2.430	2.346	2.551	13
EPRI 2	2.782	2.745	2.623	2.559	2.479	2.409	2.330	2.561	14
T02	2.663	2.799	2.777	2.655	2.549	2.470	2.355	2.610	15
A08p	3.266	2.910	2.723	2.585	2.481	2.430	2.413	2.687	16
A08	3.622	2.951	2.694	2.751	2.509	2.483	2.317	2.761	17
S01	2.924	2.854	2.859	2.810	2.783	2.770	2.560	2.794	18
EPRI 4	2.924	2.854	2.859	2.816	2.798	2.770	2.560	2.797	19

Information theory model selection gives robust solutions to the problem of determining a meaningful measure of distance (bias) between the unknown model representing reality and the candidate model. This problem is based on the likelihood concept for a set of data observations. The likelihood, which gives the probability of the observed data under the model, enables us to tell how likely a model behaves under a given dataset (Scherbaum *et al.*, 2009).

From *Table 17* it can be noted that the LLH values range roughly between 2.4 and 3.3 except for the A08, which has higher values. The perfect LLH value for normal distribution with $\mu = 0$, and $\sigma = 1$ is between 1.4-1.5. For perfectly GMPE, we expect to have an LLH value close to a normal distribution LLH values. Most of the GMPEs yield stable LLH values across the whole spectral period range considered. The same information is presented in Figures in Appendix 3.

For rock sites (*Table 18*) the results indicate that AB95 is the best performing GMPE overall. The LLH values are stable across the spectral periods and range between 2.5-5.2 with a few exceptions in A08, which yields higher LLH values. The result for the soil sites (*Table 20*) shows that the LLH values range between 2.3-5.4. AB06p is the best GMPEs here followed by AB06 and AB06+ respectively. The LLH value for A08 at peak ground acceleration is consistently higher than the rest. The results for deep soil sites (*Table 20*) indicate that AB06p is the best performing GMPE followed by AB06+ and AB06. The LLH values range between 2.29-3.62 for the deep soil sites.

The LLH technique is a very practical and powerful tool to quantify the fit between predictive equations and observations. For an LLH value of 1.5-1.6, the distribution of the normalized residuals matches well a standard normal distribution, whereas for greater values than ~3-4, the mean, sigma or both values calculated from the residual distribution strongly moves away from the parameters of the standard normal distribution. The fit between the observations and the predictions in several cases tend to vary greatly with spectral period. Finally, it can be noted that the LLH technique favors models with higher sigma (smaller LLH values can be interpreted as the accurate description of aleatory variability posed by the ground motion dataset). Note that the LLH method would only favor a GMPE with smaller sigma if the observed data display a closer distribution to the median estimation of the GMPE in question (Kale and Akkar, 2012).

4.8 Euclidean Distance Ranking Method

The EDR methodology considers separately the ground motion uncertainty (i.e., standard deviation of the ground motion model) and the bias between the observed data and the median estimations of candidate GMPEs (i.e., model bias). Indices computed from the consideration of aleatoric variability and model bias or their combination could be used to rank the GMPEs.

The EDR method assumes that the natural logarithms of the predictive model as well as the Euclidean distances computed for each data point are normally distributed. The Modified Euclidean distance (MDE) is considered as a probability based average that is used as an index to account for the effect of sigma while testing the performance of GMPEs under a given ground motion dataset.

A significant trend between the observed data and the corresponding median estimation can be interpreted as the biased representation of the ground motion data by the candidate predictive model. The measure of bias between the observed and estimated data is calculated by the parameter *kappa* (κ). A higher value of κ indicates dominant bias in the estimation of the considered GMPE. Final ranking is given by the calculated EDR index. The EDR index represents the overall probability of the differences between the estimated and the observed data. A smaller EDR value is an indicator of well representation of the ground motion dataset by the predictive model.

The results of the three indices calculated are presented for all site classes and rock sites in *Tables 21 – 26* and soil and deep soil sites in Appendix 4. The immediate observation from these tables is that given the ground motion database, the performances of GMPEs show differences in terms of addressing the aleatoric variability and model bias. For example A08p, AB06p, AB06+ and AB06 perform better in addressing the aleatoric uncertainty and model bias for the considered ground motion database. These results are consistent with the classical residual analysis for all the sites combined.

Table 21: MDE Results Ranking for all sites combined

GMPE	PGA	0.1s	0.2s	0.3s	0.5s	1.0s	2.0s	Factor	Rankk
A08p	1.300	1.204	1.213	1.187	1.233	1.174	1.298	1.230	1
AB06p	1.246	1.201	1.187	1.195	1.151	1.296	1.428	1.244	2
AB06+	1.270	1.213	1.186	1.205	1.168	1.322	1.461	1.260	3
AB06	1.328	1.258	1.205	1.230	1.196	1.361	1.503	1.297	4
A08	1.492	1.299	1.423	1.420	1.416	1.168	1.191	1.344	5
EPRI 2	1.437	1.359	1.402	1.475	1.461	1.327	1.223	1.384	6
AB95	1.542	1.533	1.539	1.521	1.364	1.166	1.117	1.397	7
EPRI 1	1.387	1.366	1.527	1.639	1.573	1.162	1.173	1.404	8
EPRI 4	1.283	1.263	1.627	1.668	1.578	1.267	1.145	1.404	9
TP05	1.412	1.342	1.675	1.885	1.183	1.254	1.325	1.440	10
S01	1.405	1.351	1.786	1.725	1.562	1.300	1.114	1.463	11
F96	1.630	1.658	1.724	1.696	1.430	1.173	1.078	1.484	12
PZT11	1.926	1.680	1.346	1.415	1.429	1.484	1.503	1.540	13
EPRI 3	1.758	1.669	1.684	1.729	1.655	1.378	1.378	1.607	14
SV02	1.911	1.878	1.945	1.867	1.589	1.185	1.231	1.658	15
C03	1.874	1.926	2.061	2.131	1.784	1.448	1.270	1.785	16
T02	2.009	2.060	2.534	2.372	2.130	1.786	1.223	2.016	17
SD02	4.744	4.001	4.793	5.532	6.637	8.193	9.489	6.198	18
SC02	4.957	4.121	4.766	5.378	6.415	8.224	9.638	6.214	19

Table 22: Kappa Results Ranking for all sites combined

GMPE	PGA	0.1s	0.2s	0.3s	0.5s	1.0s	2.0s	Factor	Rankk
A08p	1.070	1.042	1.107	1.098	1.138	1.063	1.085	1.086	1
AB06p	1.085	1.091	1.084	1.079	1.080	1.126	1.192	1.105	2
AB06+	1.099	1.099	1.087	1.087	1.089	1.136	1.203	1.114	3
AB06	1.134	1.129	1.106	1.108	1.109	1.157	1.224	1.138	4
TP05	1.075	1.084	1.358	1.399	1.095	1.103	1.167	1.183	5
EPRI 2	1.205	1.202	1.250	1.284	1.310	1.279	1.151	1.240	6
EPRI 1	1.281	1.251	1.344	1.397	1.393	1.119	1.006	1.256	7
AB95	1.292	1.293	1.337	1.345	1.309	1.166	1.095	1.262	8
F96	1.359	1.401	1.459	1.429	1.279	1.077	1.031	1.291	9
PZT11	1.358	1.330	1.222	1.247	1.322	1.355	1.346	1.311	10
SV02	1.443	1.433	1.485	1.448	1.342	1.066	1.000	1.317	11
A08	1.339	1.283	1.447	1.420	1.483	1.212	1.129	1.330	12
S01	1.347	1.336	1.622	1.560	1.494	1.321	1.134	1.402	13
EPRI 4	1.367	1.373	1.595	1.566	1.508	1.293	1.123	1.403	14
C03	1.486	1.567	1.658	1.704	1.554	1.340	1.200	1.501	15
EPRI 3	1.626	1.629	1.591	1.590	1.554	1.347	1.280	1.517	16
T02	1.643	1.662	1.934	1.857	1.767	1.545	1.109	1.645	17
SC02	1.866	1.708	1.817	1.891	1.949	2.022	2.113	1.909	18
SD02	1.836	1.676	1.806	1.900	2.005	2.181	2.347	1.964	19

Table 23: EDR Results Ranking for all sites combined

GMPE	PGA	0.1s	0.2s	0.3s	0.5s	1.0s	2.0s	Factor	Rank
A08p	1.391	1.254	1.342	1.304	1.403	1.248	1.408	1.336	1
AB06p	1.352	1.310	1.286	1.289	1.244	1.460	1.702	1.378	2
AB06+	1.395	1.333	1.289	1.309	1.271	1.502	1.757	1.408	3
AB06	1.507	1.420	1.333	1.363	1.327	1.575	1.839	1.480	4
EPRI 2	1.732	1.634	1.752	1.894	1.915	1.698	1.408	1.719	5
TP05	1.517	1.456	2.276	2.636	1.295	1.383	1.547	1.730	6
AB95	1.992	1.982	2.058	2.046	1.786	1.360	1.222	1.778	7
EPRI 1	1.777	1.710	2.053	2.289	2.191	1.301	1.180	1.786	8
A08	1.998	1.667	2.059	2.015	2.100	1.415	1.346	1.800	9
F96	2.216	2.323	2.515	2.424	1.829	1.263	1.112	1.954	10
EPRI 4	1.753	1.734	2.596	2.612	2.378	1.638	1.286	2.000	11
PZT11	2.616	2.233	1.645	1.765	1.889	2.012	2.023	2.026	12
S01	1.893	1.805	2.897	2.692	2.335	1.717	1.263	2.086	13
SV02	2.757	2.692	2.888	2.703	2.132	1.263	1.232	2.238	14
EPRI 3	2.858	2.719	2.680	2.750	2.572	1.856	1.764	2.457	15
C03	2.785	3.017	3.419	3.631	2.771	1.940	1.524	2.727	16
T02	3.302	3.424	4.900	4.404	3.764	2.759	1.357	3.416	17
SC02	9.251	7.036	8.658	10.169	12.504	16.626	20.368	12.087	18
SD02	8.709	6.705	8.654	10.509	13.305	17.871	22.273	12.575	19

For example, when testing results from rock site classes, AB06p, EPRI2, AB06+ perform better in terms of aleatory variability (smaller MDE component in EDR) and model bias, and even overall they still do well. PZT11 performs better overall when you consider the EDR index followed by EPRI1 and SC02 respectively at longer periods (2.0s). Tables 24 – 26 capture the variability in the performance of GMPEs in terms of addressing the aleatoric variability and model bias.

Table 24: MDE ranking for Rock sites

GMPE	PGA	0.1s	0.2s	0.3s	0.5s	1.0s	2.0s	Factor	Rankk
AB06p	0.960	1.021	1.150	1.126	1.298	1.240	1.454	1.178	1
EPRI 2	1.236	1.074	1.117	1.129	1.120	1.399	1.543	1.231	2
AB06+	1.321	1.129	1.142	1.155	1.141	1.431	1.574	1.270	3
TP05	1.136	1.215	1.407	1.454	1.392	1.237	1.161	1.286	4
SD02	1.166	1.066	1.556	1.601	1.092	1.243	1.285	1.287	5
PZT11	1.144	1.330	1.578	1.583	1.363	1.182	1.076	1.322	6
A08p	1.024	1.100	1.429	1.444	1.574	1.287	1.413	1.325	7
AB06	1.439	1.221	1.193	1.203	1.180	1.475	1.619	1.333	8
A08	1.160	1.264	1.491	1.614	1.670	1.552	1.300	1.436	9
EPRI 1	1.103	1.277	1.647	1.815	1.786	1.250	1.230	1.444	10
SV02	1.100	1.170	1.798	1.790	1.702	1.471	1.162	1.456	11
EPRI 4	1.134	1.204	1.811	1.892	1.835	1.479	1.201	1.508	12
T02	1.344	1.569	1.854	1.841	1.602	1.191	1.324	1.532	13
F96	1.358	1.555	1.780	1.887	1.860	1.533	1.410	1.626	14
AB95	1.328	1.647	2.006	2.171	1.858	1.506	1.232	1.678	15
S01	2.305	1.842	1.465	1.487	1.631	1.763	1.700	1.742	16
SC02	1.563	1.873	2.612	2.482	2.272	1.883	1.202	1.984	17
C03	4.797	4.152	4.950	5.728	6.875	8.456	9.463	6.346	18
EPRI 3	5.016	4.264	4.904	5.558	6.679	8.621	9.770	6.402	19

Table 25: Kappa ranking for rock sites

GMPE	PGA	0.1s	0.2s	0.3s	0.5s	1.0s	2.0s	Factor	Rank
AB06p	1.037	1.033	1.133	1.146	1.213	1.114	1.180	1.122	1
EPRI 2	1.178	1.134	1.140	1.153	1.120	1.165	1.213	1.158	2
AB06+	1.221	1.165	1.153	1.166	1.128	1.175	1.222	1.176	3
SD02	1.117	1.100	1.419	1.502	1.108	1.089	1.103	1.206	4
AB06	1.286	1.223	1.190	1.201	1.155	1.198	1.243	1.214	5
A08	1.135	1.216	1.347	1.428	1.475	1.420	1.215	1.319	6
TP05	1.207	1.314	1.436	1.488	1.437	1.230	1.131	1.321	7
PZT11	1.292	1.449	1.569	1.557	1.332	1.069	1.016	1.326	8
EPRI 1	1.225	1.282	1.475	1.582	1.569	1.156	1.000	1.327	9
T02	1.364	1.447	1.555	1.558	1.420	1.058	1.011	1.345	10
A08p	1.291	1.322	1.582	1.596	1.704	1.336	1.261	1.442	11
S01	1.650	1.521	1.323	1.398	1.458	1.490	1.459	1.471	12
SV02	1.392	1.429	1.767	1.736	1.644	1.418	1.148	1.505	13
EPRI 4	1.392	1.429	1.767	1.790	1.714	1.418	1.148	1.523	14
AB95	1.415	1.637	1.789	1.891	1.697	1.368	1.151	1.564	15
F96	1.564	1.710	1.749	1.808	1.742	1.406	1.259	1.605	16
SC02	1.617	1.740	2.091	2.071	1.938	1.583	1.060	1.729	17
EPRI 3	1.823	1.699	1.766	1.820	1.862	1.898	1.846	1.816	18
C03	1.794	1.669	1.755	1.827	1.912	2.053	2.064	1.868	19

Table 26: EDR ranking for rock sites

GMPE	PGA	0.1s	0.2s	0.3s	0.5s	1.0s	2.0s	Factor	Rank
AB06p	0.995	1.055	1.304	1.290	1.574	1.381	1.715	1.330	1
EPRI 2	1.456	1.218	1.274	1.302	1.254	1.630	1.871	1.429	2
AB06+	1.614	1.315	1.317	1.346	1.286	1.681	1.923	1.498	3
SD02	1.303	1.173	2.207	2.405	1.210	1.354	1.418	1.582	4
AB06	1.850	1.493	1.420	1.445	1.362	1.767	2.012	1.621	5
TP05	1.370	1.597	2.020	2.165	2.001	1.521	1.313	1.712	6
PZT11	1.479	1.927	2.476	2.466	1.815	1.263	1.094	1.789	7
A08	1.317	1.537	2.008	2.306	2.462	2.203	1.580	1.916	8
A08p	1.322	1.455	2.261	2.305	2.682	1.720	1.781	1.932	9
EPRI 1	1.351	1.638	2.430	2.872	2.802	1.445	1.230	1.967	10
T02	1.833	2.271	2.884	2.868	2.273	1.260	1.339	2.104	11
SV02	1.531	1.672	3.178	3.108	2.797	2.086	1.335	2.244	12
EPRI 4	1.578	1.721	3.200	3.386	3.145	2.097	1.379	2.358	13
S01	3.803	2.802	1.938	2.080	2.378	2.626	2.479	2.587	14
F96	2.123	2.660	3.114	3.410	3.240	2.156	1.775	2.640	15
AB95	1.879	2.695	3.589	4.106	3.153	2.060	1.419	2.700	16
SC02	2.528	3.260	5.462	5.141	4.404	2.980	1.274	3.579	17
EPRI 3	9.142	7.245	8.659	10.114	12.436	16.362	18.039	11.714	18
C03	8.605	6.932	8.686	10.463	13.145	17.363	19.535	12.104	19

One particular advantage of EDR is that it not only provides an idea on the overall performance of tested predictive models but also informs the analyst about the individual contributions of sigma (i.e., the level of aleatory variability) and bias in median estimations to the overall performance of GMPEs. Accordingly, as indicated before, EDR offers different levels of information to the analyst for considering the aleatory uncertainty, degree of bias between the observed and the median estimations and the combination of these two components.

Kale and Akkar (2012) note that MDE would provide valuable information in site-specific hazard studies if the concern were very long return periods (e.g., $T_R > 2500$ years). Further they suggest that the overall EDR index can be used more favorably to identify the most suitable set of GMPEs for regional

hazard studies because better performance of GMPEs in representing the overall data trend and aleatoric variability may yield more realistic hazard results for return periods that are of interest in regional hazard programs (e.g., $T_R \leq 2500$ years).

5 Conclusions

A08p, AB06p and AB06+ give a better performance over the other GMPEs when I considered the combined site classes. For the rock sites A08p, AB95 and A08 can be considered as better performing GMPEs. For soil sites, AB06, AB06+ and AB06p performs well in matching the predicted to observed ground motion. For deep soil sites, EPRI4, EPRI2 and A08p give better performance overall compared to other GMPEs. The test statistic results for the residual follow similar patterns as those of the database itself, e.g., non-normality and skewed distributions.

The normality test was done using various methods. The results were further probed by kurtosis and skewness analysis. Most of the GMPEs can be considered as having moderate skewness with model A08 showing high skewness. From the kurtosis analysis, most of the GMPEs were classified as being leptokurtic in distribution. This implies that most of the GMPEs are likely to be influenced by extreme values. From the Z score, Kolmogorov-Smirnov (KS), Lilliefors and Jarque-Bera tests, the results indicates that the GMPEs residuals are not normally distributed. In general, from the z-scores, the GMPEs follow closely a normal distribution.

The results from the theoretical information technique (LLH) by Scherbaum *et al.* 2009 gave different results than the classical residual analysis and the EDR method. For all sites combined, the LLH values were within 2.4-3.3, which means that the GMPEs were comparable to each other except the A08 predictive model, which had higher LLH values.

The LLH method favors GMPEs with larger standard deviations as they can predict the outlier observations with higher probabilities. The LLH method indicates a better performing GMPE with larger sigma especially if the observed data are accumulated away from the median estimations. Kale and Akkar (2012) observed the same). This implies that the predictive model with larger sigma would yield larger probability of occurrence indicating that it can capture these outliers better than its alternative. This is why the ranking of the GMPEs using LLH method differs significantly from the other two methods, namely EDR and the classical residual analysis technique

The EDR methodology could be considered as the best method of ranking the GMPEs as it considers separately the ground motion uncertainty and the bias between the observed data and the median estimations of the candidate GMPEs. The EDR methodology accounts for aleatory variability in ground motion estimation (through standard deviations of GMPEs). It also considers the bias between median estimations and observed ground motion data (model bias). The bias between median ground motion estimations and general variation of the observed data is identified by the κ parameter, which makes an analogy to the classical residual analysis concept. The uncertainty in the ground motion variability is addressed by calculating the probability distribution of the difference between the observed data and corresponding estimations for a range of sigma values. This sets this method apart from the LLH method since the LLH method computes the occurrence probability of the observed data point by using the corresponding estimation that is assumed to be log-normally distributed with

median and sigma values of the candidate GMPE. From the EDR results A08, AB06p and AB06+ were considered as the best performing models when you consider combined site classes. For the rock sites, AB06p, EPRI2, AB06+, and SD02 were considered to do better.

Finally it can be concluded that there is no clear dominance of any model over the other for the NGA-East database for a broad range of magnitude and distance intervals. The current GMPEs seem to predict the ground motion better than most of the proposed GMPEs for the 2014 NSHMP maps. In general, newer GMPEs tend to predict lower ground motion levels than older GMPEs. This can be attributed to geometrical spreading used in the GMPE with the newer GMPEs using $R^{-1.3}$ whereas the older GMPEs using $R^{-1.0}$.

References

- Abrahamson N., Atkinson G., Boore D., Bozognia Y., Campbell K., Chiou B., Idriss I. M., Silva W., Youngs R., (2008), Comparisons of the NGA ground-motion relations, *Earthquake Spectra* **24**, p. 45–66.
- Abrahamson, N. A., and K. M. Shedlock (1997). Overview, *Seism. Res. Lett.* **68**, 9–23.
- Abrahamson, N. A., and Litehiser, J.J., (1989). Attenuation of vertical peak acceleration, *Bull. Seism. Soc. Am.*, **79**, p.549-580.
- Abrahamson, N. A., and W. J. Silva, (1997). Empirical response spectral attenuation relations for shallow crustal earthquakes, *Seism. Res. Lett.* **68**, no. **1**, 94–127.
- Atkinson G., and Boore D., (1995). New ground motion relations for eastern North America. *Bull. Seism. Soc. Am.*, **85**, 17-30
- Atkinson G., and Boore D., (2006). Earthquake ground motion prediction equations for eastern North America, *Bull. Seism. Soc. Am.*, **96**, 2181-2205.
- Atkinson G., and Boore D., (2011). Modifications to existing ground motion prediction equations in light of new data. *Bull. Seism. Soc. Am.*, **101**, 1121-1135.
- Atkinson G.M., (2008). Ground motion prediction equations for eastern North America from a referenced empirical approach: implications for epistemic uncertainty, *Bull. Seism. Soc. Am.*, **98**, 1304-1318.

- Beauval, C., F. Cotton, N. Abrahamson, N. Theodoulidis, E. Delavaud, L. Rodriguez, F. Scherbaum and A. Haendel, (2012b). Regional differences in subduction ground motions. *Proceedings of the 15th World Conference on Earthquake Engineering, Lisbon, Portugal, 24-28 September 2012*.
- Beauval, C., H. Tasan, A. Laurendeau, E. Delavaud, F. Cotton, Ph. Guéguen and N. Kühn, (2012a). On the testing of ground-motion prediction equations against small magnitude data. *Bull. Seism. Soc. Am.* **102**, no. 5, 1994-2007.
- Bindi, D., Luzi, L., Pacor, F., Franceschina, G. and Castro, R.R., (2006). Ground-Motion Predictions from Empirical Attenuation Relationships versus Recorded Data: The Case of the 1997–1998 Umbria-Marche, Central Italy, Strong-Motion Data Set. *Bulletin of the Seismological Society of America*, **96**(3), 984-1002.
- Boore D.M., and Atkinson G.M., (2008). Ground Motion prediction equations for the average horizontal component of PGA, PGV and 5% damped PSA at spectral periods between 0.01s and 10.0s, *Earthquake Spectra*, **24**, 1, pp 99-138.
- Budnitz, R. J., Apostolakis, G., Boore, D. M., Cluff, L. S., Coppersmith, K., Cornell, C. A., and Morris, B. J., (1997) "Recommendations for probabilistic seismic hazard analysis, in Guidance on Uncertainty and Use of Experts," *Lawrence Livermore National Laboratory*, Vol. **2**.

- Bulmer, M. G., (1979). Principles of Statistics. New York: Dover, (Originally, 1965)
- Campbell K.W., (1981). Near source attenuation of peak horizontal acceleration, *Bull. Seism. Soc. Am.*, 71, 6, 2,039–2,070.
- Campbell K.W., (2003). Prediction of strong ground motion using the hybrid empirical method and its use in the development of ground motion (attenuation) relations in eastern North America, *Bull. Seism. Soc. Am.*, **93**, 1012–1033.
- Cramer, C.H., J. Kutliroff, and D. Dangkua, (2009), Second year final report on a database of CEUS ground motions, cooperative agreement: 07CRAG0015-Mod1, *Final Report to the USGS, July 22, 2009, CERI*, 12 pp.
- Cramer, C.H., J.R. Kutliroff, and D.T. Dangkua, (2010), A database of eastern North America ground motions for the Next Generation Attenuation East project, Proceedings of the Ninth U.S. National and Tenth Canadian Conference on Earthquake Engineering: Reaching Beyond Borders, *Earthquake Engineering Research Institute and Canadian Association for Earthquake Engineering*, 10 pp.
- Cramer, C.H., J.R. Kutliroff, D.T. Dangkua, and M.N. Al-Noman, (2013), Completing the NGA East ENA/SCR Ground Motion Database, *Final Technical Report to PEER under Sub-agreement 7140*, April 5, 2013, CERI, 18 pp.

- Delavaud, E., F. Cotton, S. Akkar, F. Scherbaum, L. Danciu, C. Beauval, S. Drouet, J. Douglas, R. Basili, M.A. Sandıkkaya, M. Segou, E. Faccioli and N. Theodoulidis, (2012). Toward a Ground-Motion Logic Tree for Probabilistic Seismic Hazard Assessment in Europe. *Journal of Seismology* **16**, 451-473.
- Delavaud, E., Scherbaum, F., Kuehn, N., and Riggelsen, C., (2009). Information-theoretic selection of ground-motion prediction equations for seismic hazard analysis: An applicability study using Californian data. *Bull. Seismol. Soc. Am.*, **99**, no. 6, 3248–3263.
- Devore, J.L., (2004). Probability and Statistics for Engineering and the Sciences. *Thomson Learning Inc., MA*.
- Douglas J, and Gehl P, (2008) Investigating strong ground-motion variability using analysis of variance and two-way-fit plots. *Bull Earthq Eng.* **6**(3): 389–405
- Douglas, J., (2011). Ground-motion prediction equations 1964-2010, *BRGM/RP-59356-FR*, 444 pages, 9 illustrations.
- EPRI (2004). CEUS Ground Motion Project: Final Report, 1009684, *Electric Power Research Institute, Palo Alto, California*
- Frankel, A., C. Mueller, T. Barnhard, D. Perkins, E. Leyendecker, N. Dickman, S.Hanson, and M. Hopper, (1996). *National seismic hazard maps: documentation June 1996, U.S. Geol. Surv.* Open-File Report. 96-532.

<http://earthquake.usgs.gov/hazmaps/publications/hazmapsdoc/Junedoc.pdf> (lastly assessed on 11th October 2013).

Joshi A., Kumar A., Lomnitz C., Castaños H., and Akhtar S., (2012) Applicability of attenuation relations for regional studies. *Geofísica Internacional* (2012) 51-4: 349-363

Joyner, W. B., and D. M. Boore, (1981). Peak horizontal acceleration and velocity from strong motion records including records from the 1979 Imperial Valley, California, earthquake, *Bull. Seismol. Soc. Am.* **71**, no. 6, 2011–2038.

Kaklamanos, J. and L.G. Baise., (2011). Model Validations and Comparisons of the Next Generation Attenuation of Ground Motions (NGA–West) Project. *Bull. Seismol. Soc. Am.* **101**, no. 1, 160-175.

Kale, Ö. and Akkar, S., (2012). A novel procedure for selecting and ranking candidate ground-motion prediction equations (GMPEs) for seismic hazard analysis: Euclidean distance based ranking (EDR) method. *Bulletin of the Seismological Society of America*. Submitted for publication (BSSA-S-12-00153).

Kramer, S., (1996). *Geotechnical Earthquake Engineering*. Prentice- Hall, Upper Saddle River, NJ, USA.

Montgomery D.C., Peck E.A., Vining G.G., (2003), *Introduction to linear regression analysis*, John Wiley and Sons (ASIA) Ptv Ltd, Clementi Loop, Singapore.

- Mousavi, M., A. Ansari, H. Zafarani and A. Azarbakht, (2012). Selection of ground motion prediction models for seismic hazard analysis in the Zagros region, Iran. *J. Earthquake Eng.* **16**, 1184-1207.
- Nash, J.E., and J.V. Sutcliffe, (1970). River flow forecasting through conceptual models: Part I - A discussion of principles. *J. Hydrol.* **10**, 282-290.
- Pezeshk, S., A. Zandieh, and B. Tavakoli, (2011). "Hybrid Empirical Ground Motion Prediction Equations for Eastern North America Using NGA Models and Updated Seismological Parameters". *Bulletin of the Seismological Society of America*, **101**(4), pp. 1859-1870, August 2011, doi: 10.1785/0120100144
- Scasserra, G., Stewart, J.P., Bazzurro, P., Lanzo, G. and Mollaioli, F., (2009). A Comparison of NGA Ground-Motion Prediction Equations to Italian Data, *Bulletin of the Seismological Society of America*, **99**(5), 2961-2978.
- Scherbaum, F., Cotton, F. and Smit, P., (2004). On the Use of Response Spectral-Reference Data for the Selection and Ranking of Ground-Motion Models for Seismic-Hazard Analysis in Regions of Moderate Seismicity: The Case of Rock Motion. *Bulletin of the Seismological Society of America*, **94**(6), 2164-2185.
- Scherbaum, F., Delavaud, E. and Riggelsen, C., (2009). Model selection in seismic hazard analysis: An information-theoretic perspective. *Bulletin of the Seismological Society of America*, **99**(6), 3234-3247.

- Shoja-Taheri, J., Naserieh, S. and Hadi, G., (2010). A Test of the Applicability of NGA Models to the Strong Ground-Motion Data in the Iranian Plateau. *Journal of Earthquake Engineering*, **14**, 278-292.
- Silva, W., N.Gregor, and R. Darragh, (2002). Development of regional hard rock attenuation relations for central and eastern North America, Pacific Engineering and Analysis, El Cerrito, California, 57 pp.
- Silva, W., N.Gregor, and R. Darragh, (2003). Development of regional hard rock attenuation relations for central and eastern North America, Mid-continent and Gulf Coast areas Pacific Engineering and Analysis, El Cerrito, California, 80 pp.
- Somerville, P., N. Collins, N Abrahamson, R. Graves, and C. Saikia, (2001). Ground motion attenuation relations for central and eastern United States, *Final Report to U.S. Geology Survey*.
- Tavakoli, B. and S. Pezeshk, (2005). "Empirical-Stochastic Ground Motion Prediction Equations for Eastern North America". *Bulletin of the Seismological Society of America*, **95**(6), pp. 2283-2296, December 2005, doi: 10.1785/0120050030
- Toro, G. R., (2002). Modification of the Toro *et al.*, (1997) attenuation equations for large magnitudes and short distances. Risk Engineering, Inc, [http://www.ce.memphis.edu/7137/PDFs/attenuations/Toro_2001_\(modification_1997\).pdf](http://www.ce.memphis.edu/7137/PDFs/attenuations/Toro_2001_(modification_1997).pdf) last accessed on 11th October 2013.

Toro, G. R., N. A. Abrahamson, and J.F. Schneider, (1997). A Model of Strong Ground Motions from Earthquakes in Central and Eastern North America: Best Estimates and Uncertainties. *Seismological Research Letters*, v.**68**, no. 1pp 41-57.

Toro, G.R., (2006). "The effects of ground motion uncertainty on seismic hazard results; Examples and approximate results," *Annual Meeting of the Seismological society of America, San Francisco, California.*

Appendices

Appendix 1: Comparative rankings of candidate GMPEs as a function of Distance (Classical residual Analysis) for all classes

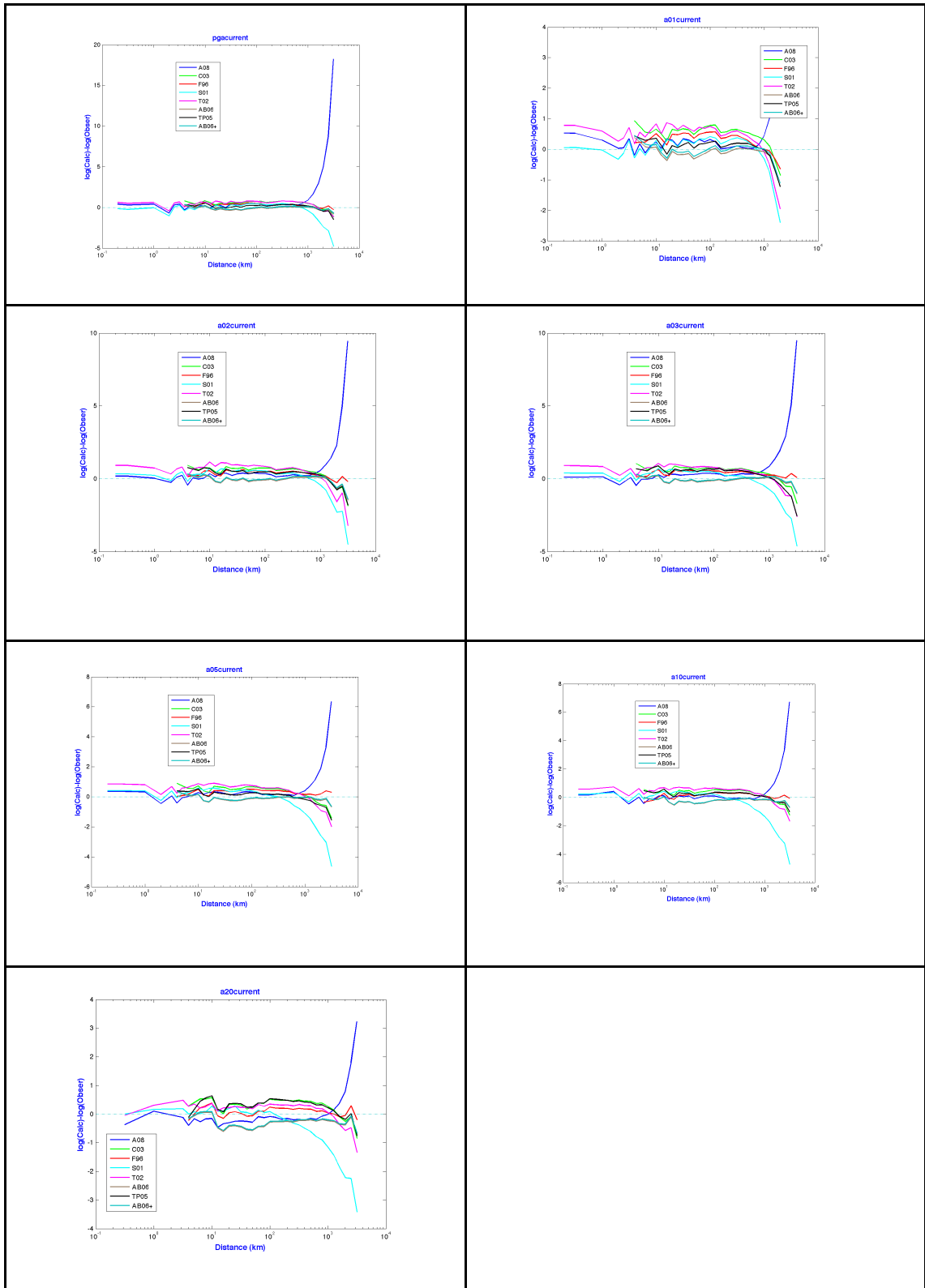


Figure 8: Current GMPEs

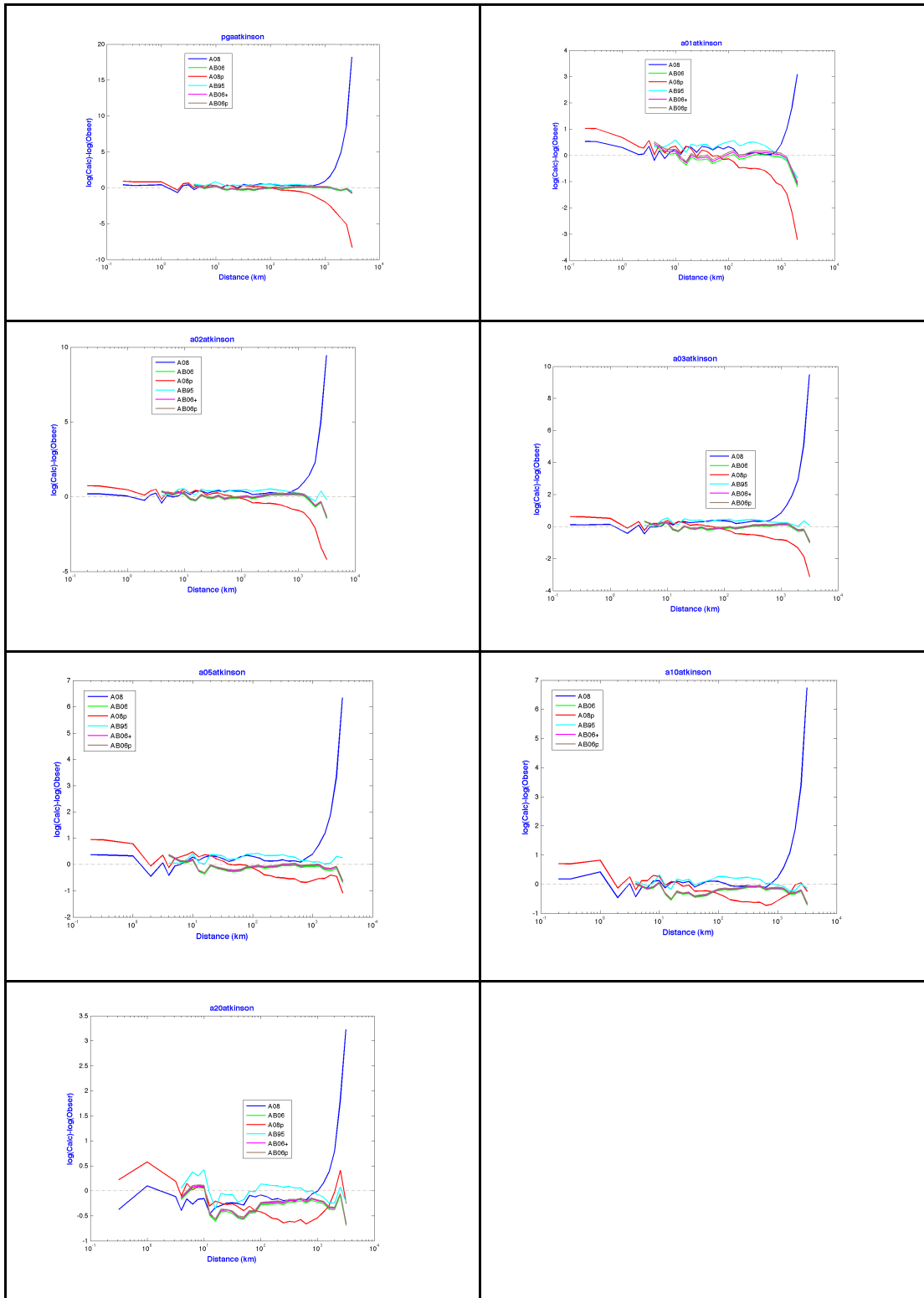


Figure 9: Atkinson Series GMPEs

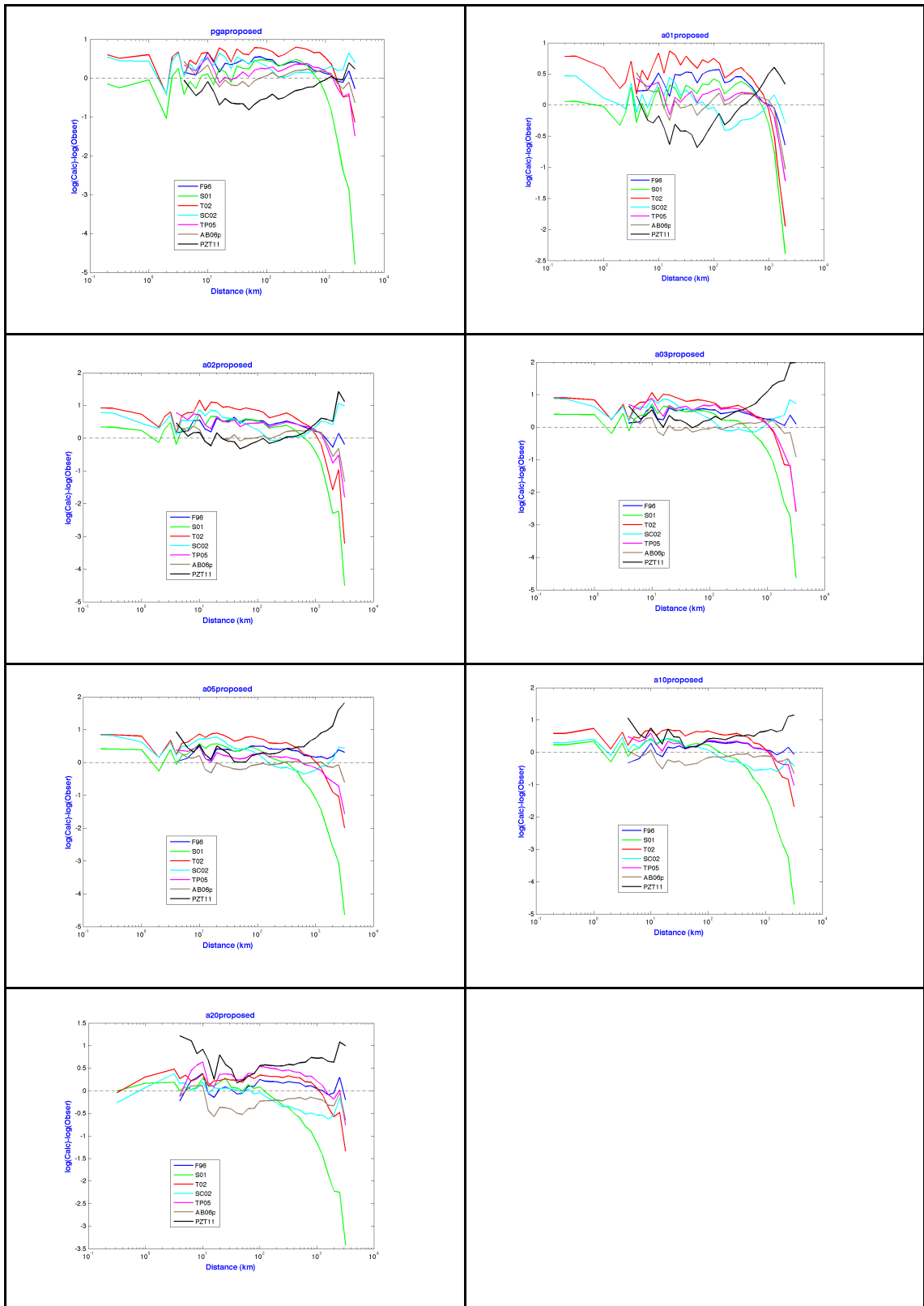


Figure 10: Proposed GMPEs

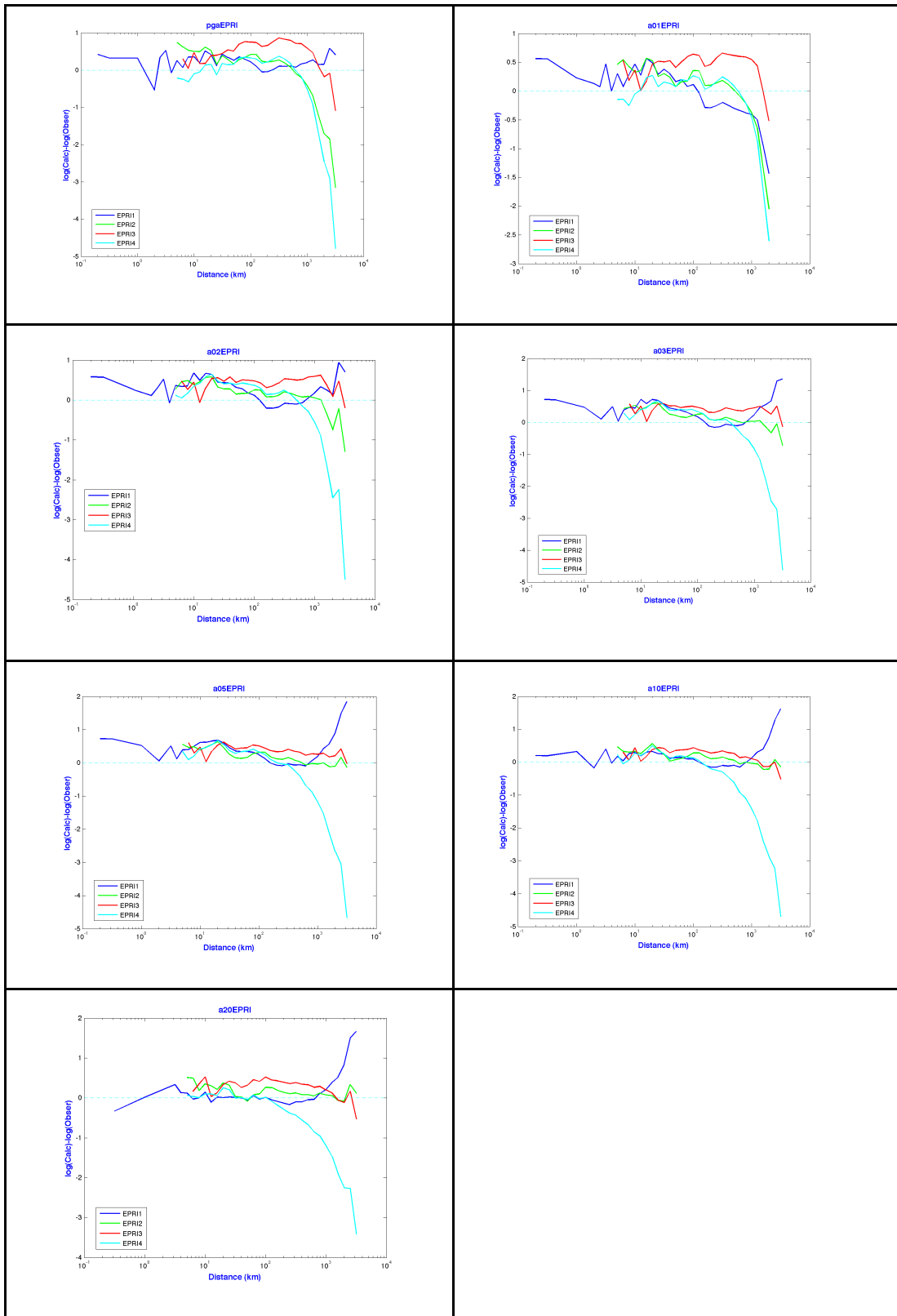
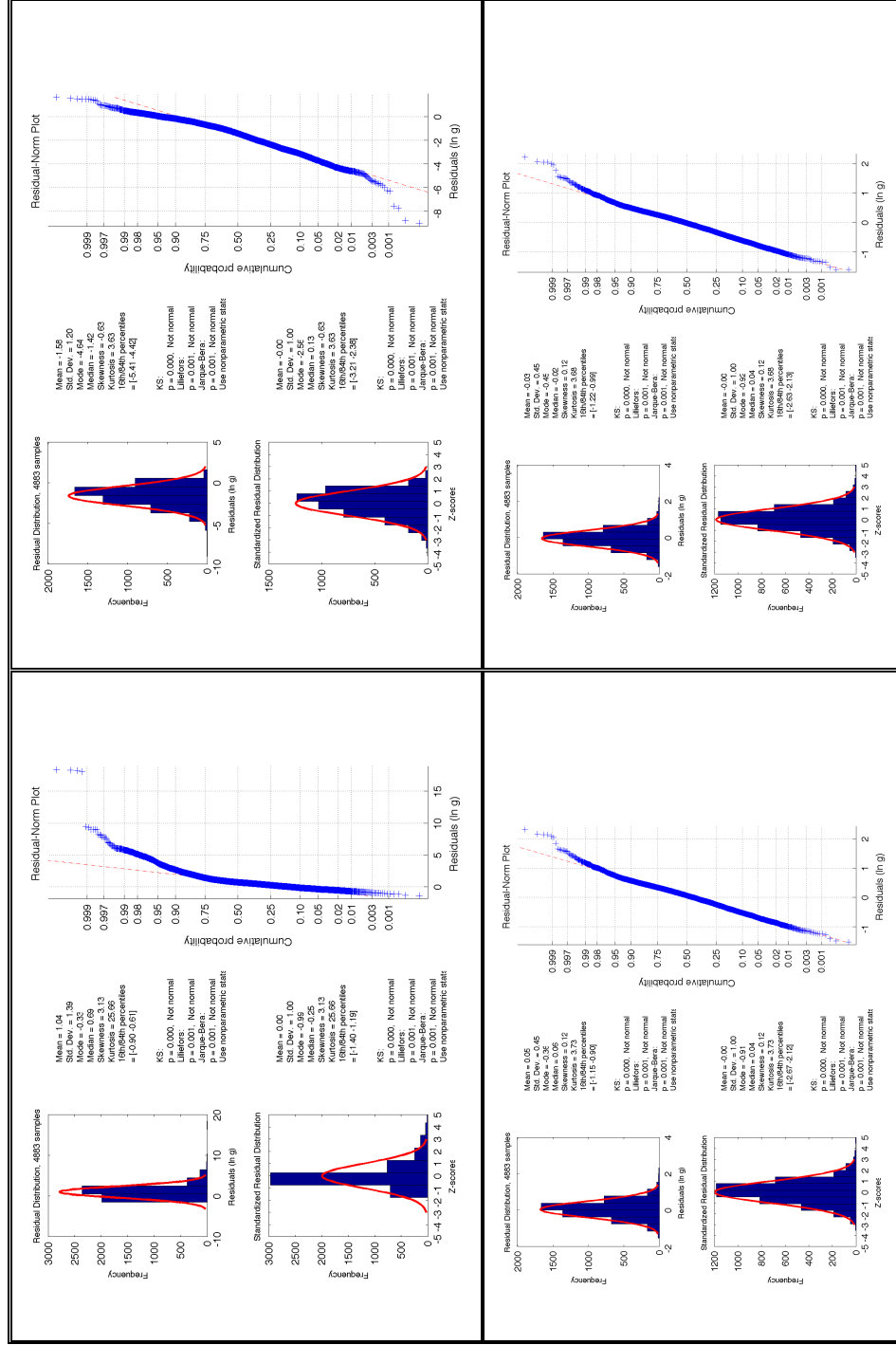
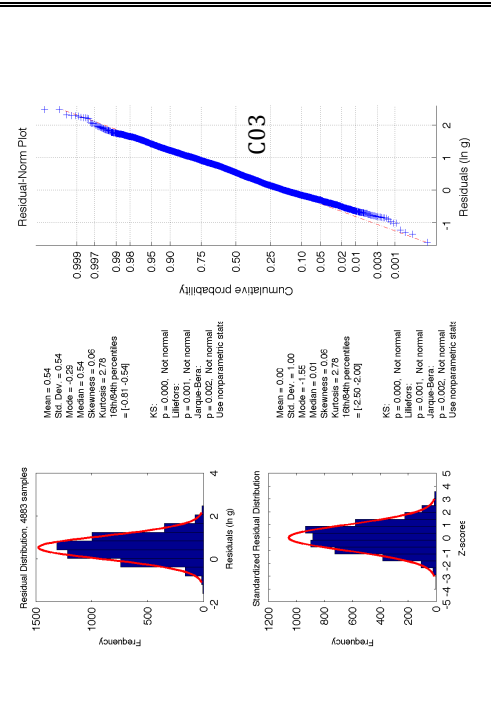
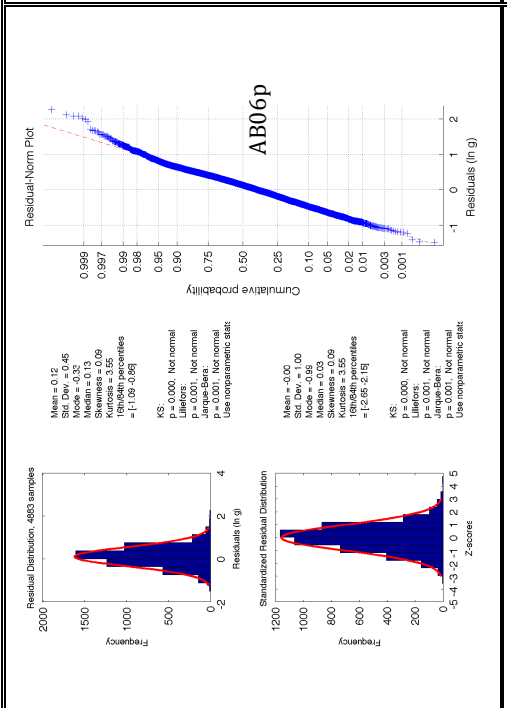
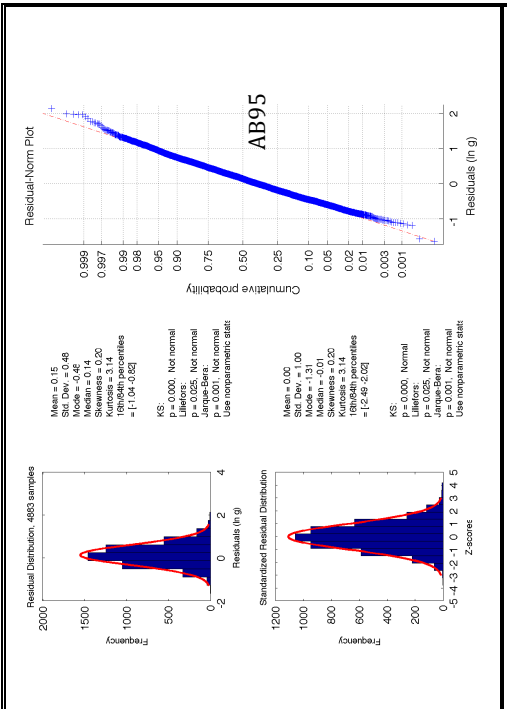
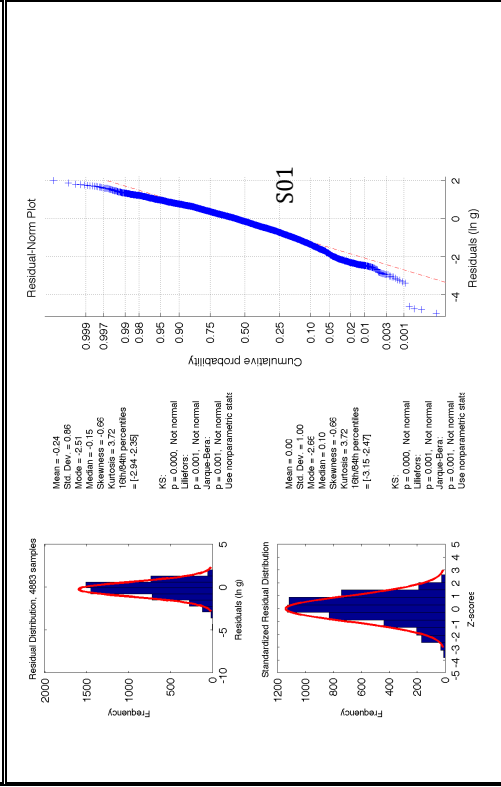
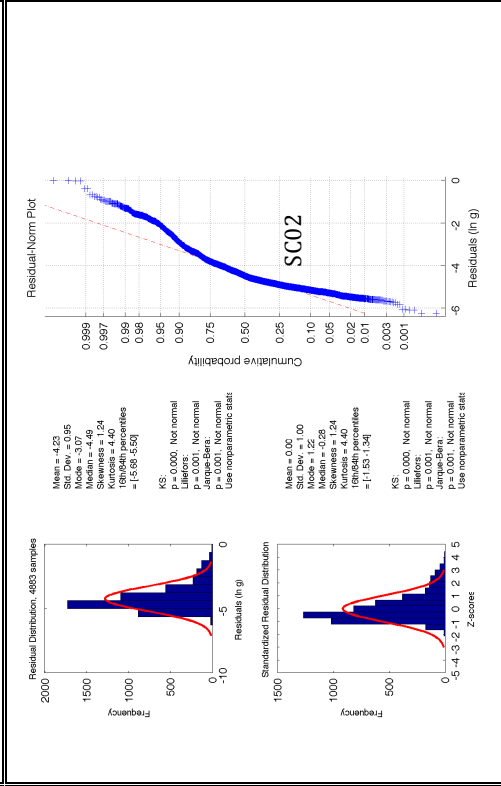
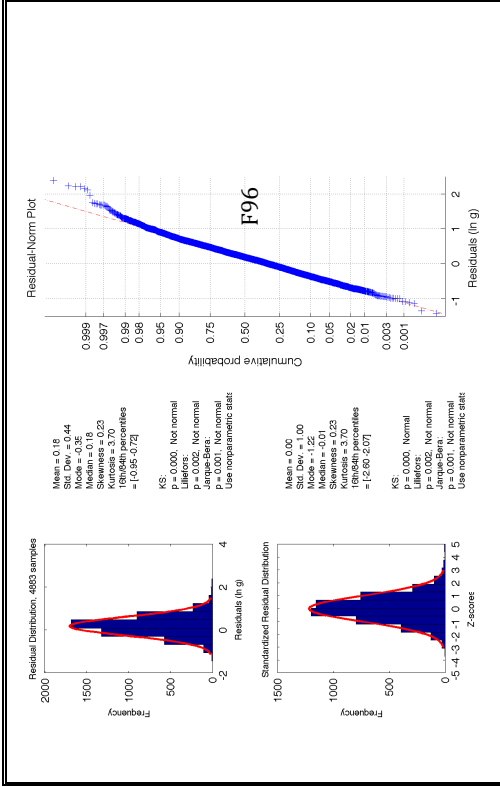
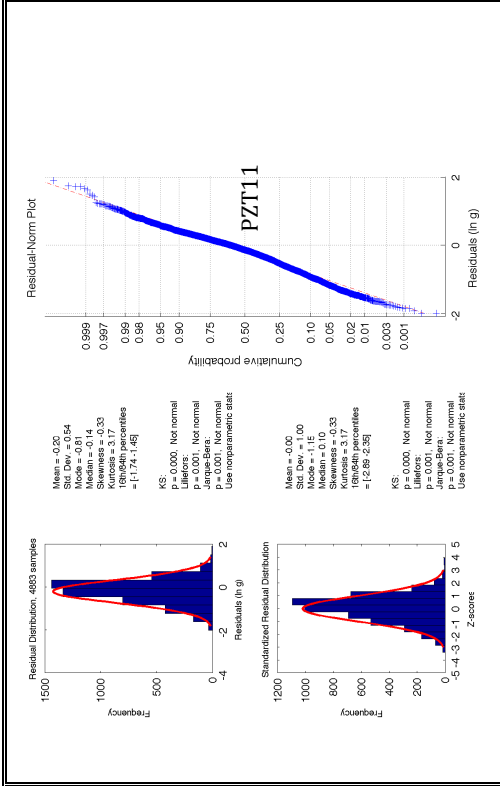


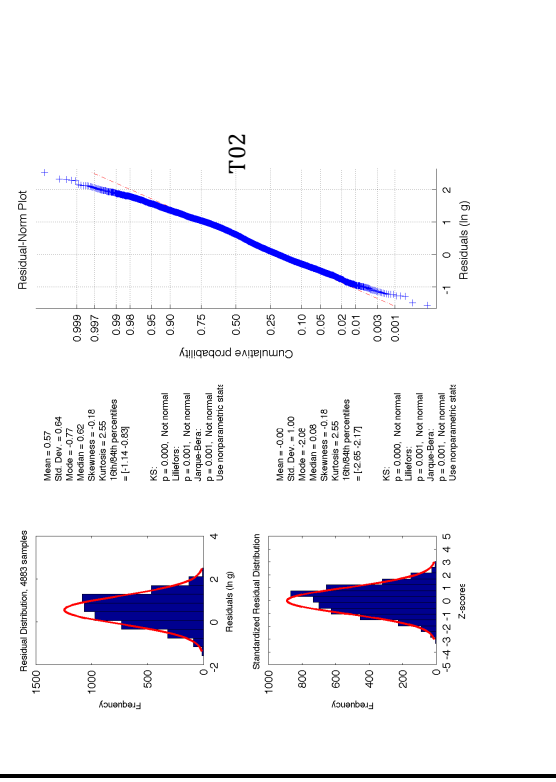
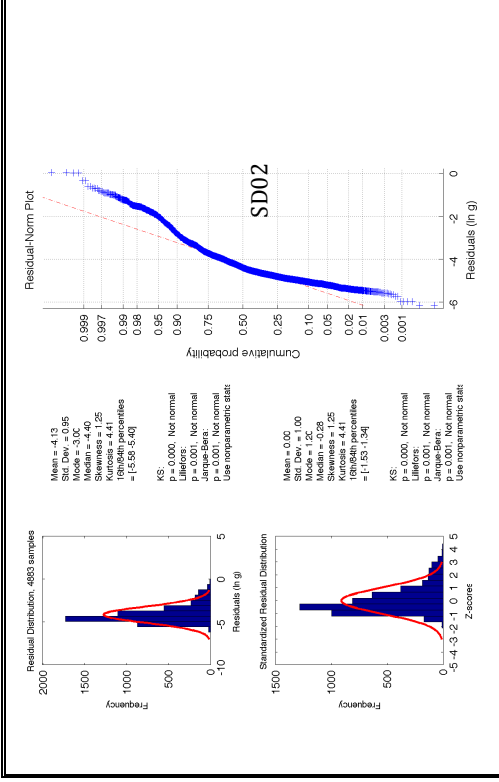
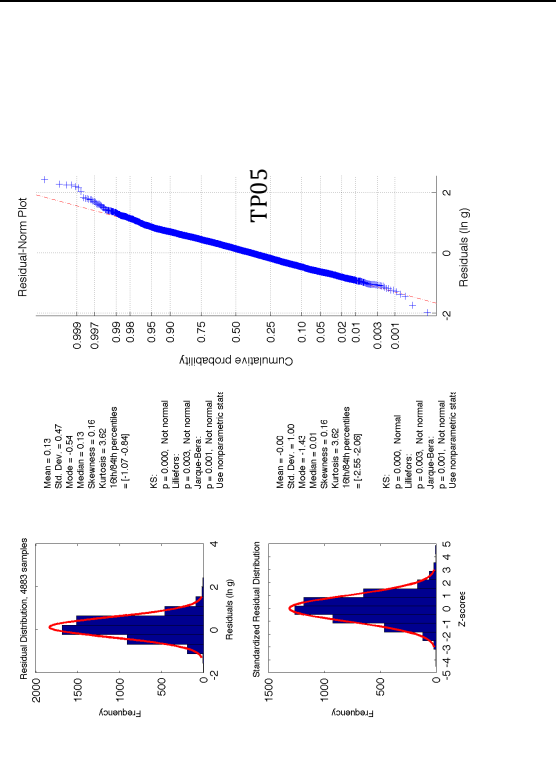
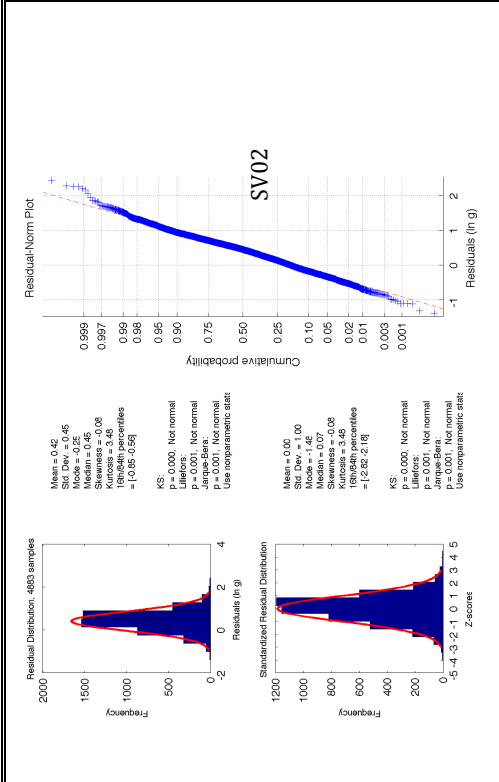
Figure 11: EPRI 2004 GMPEs

Appendix 2: Plots of Residual distribution, cumulative and standardized residual plots for rock sites









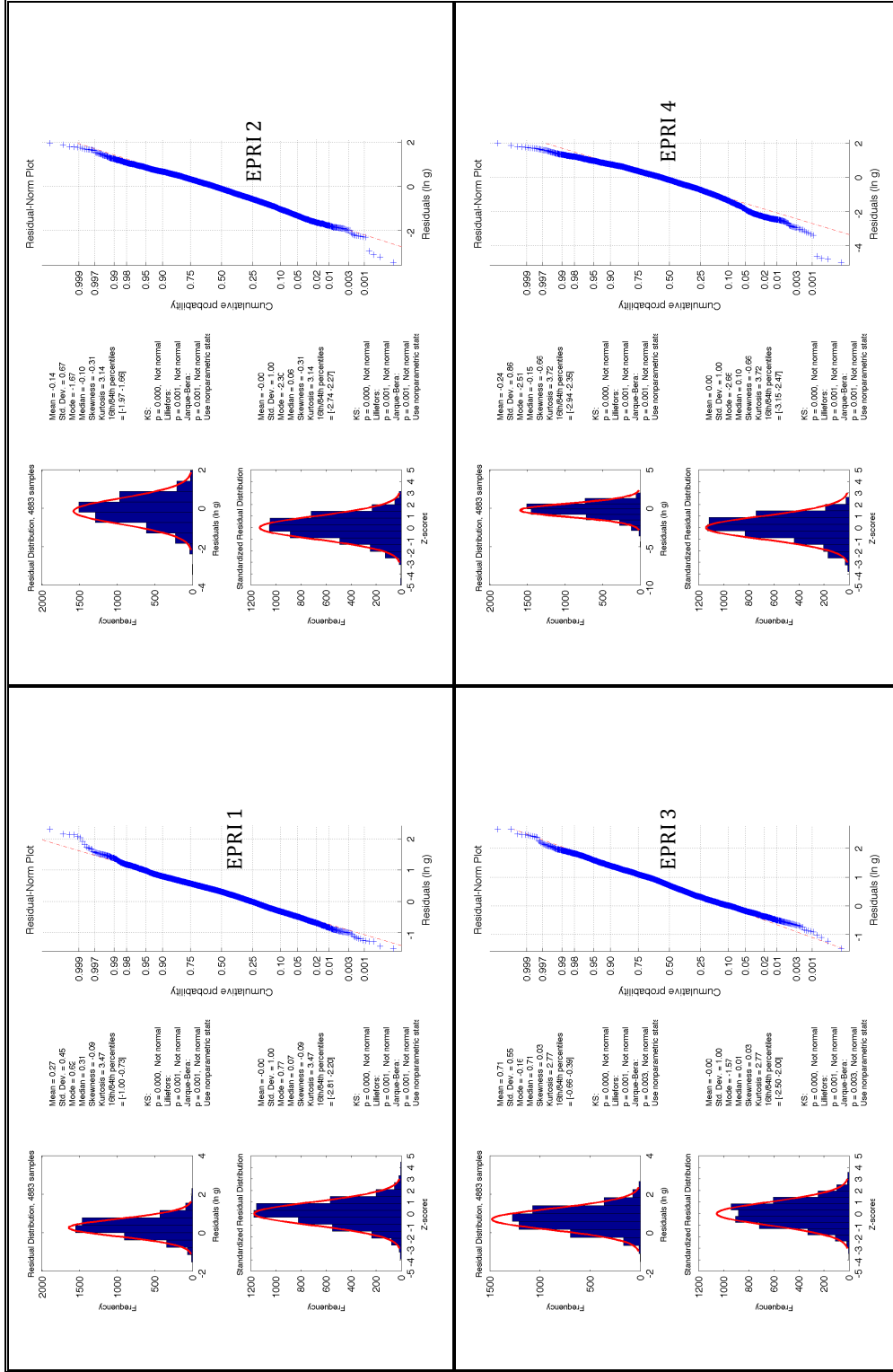
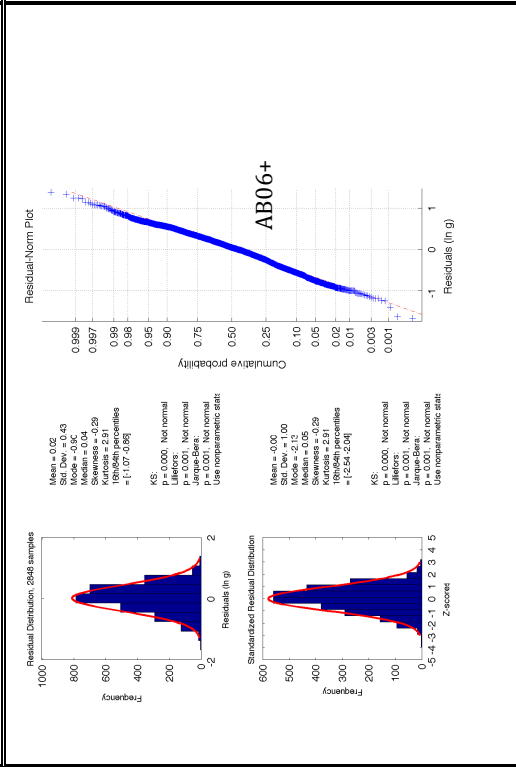
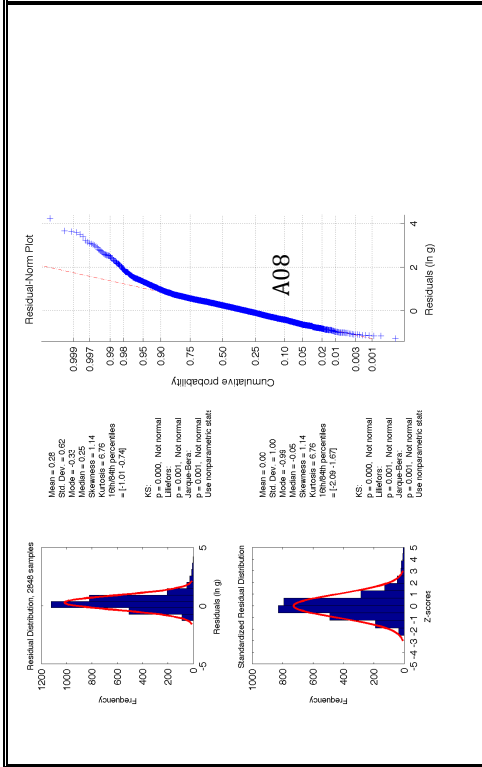
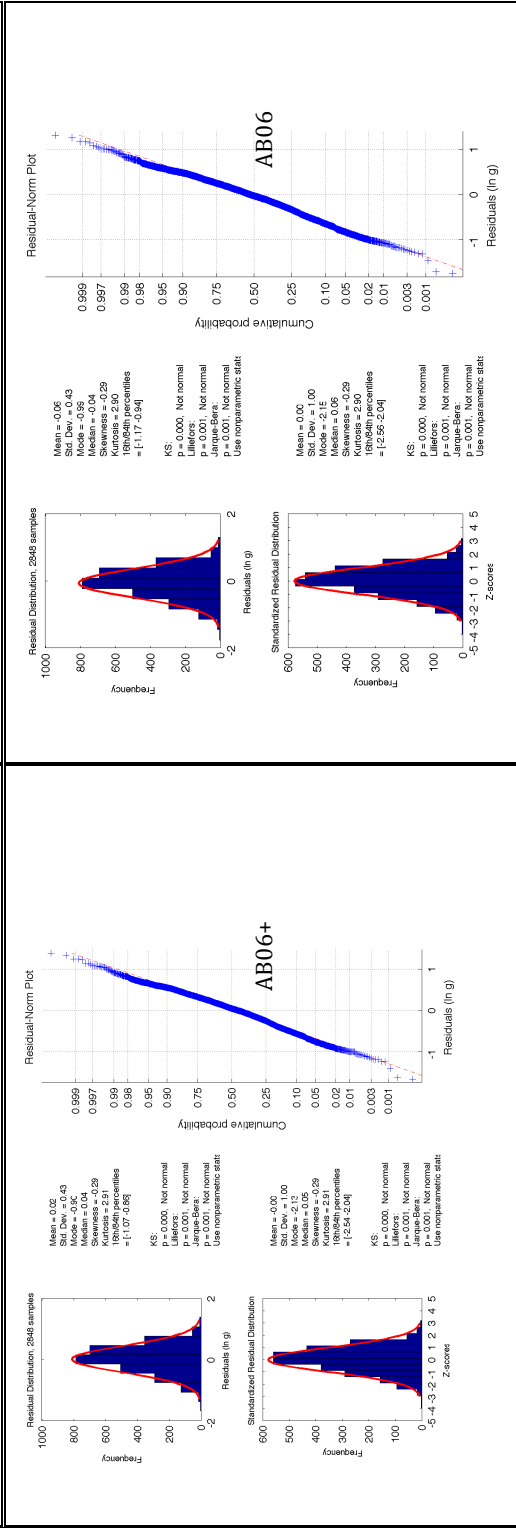
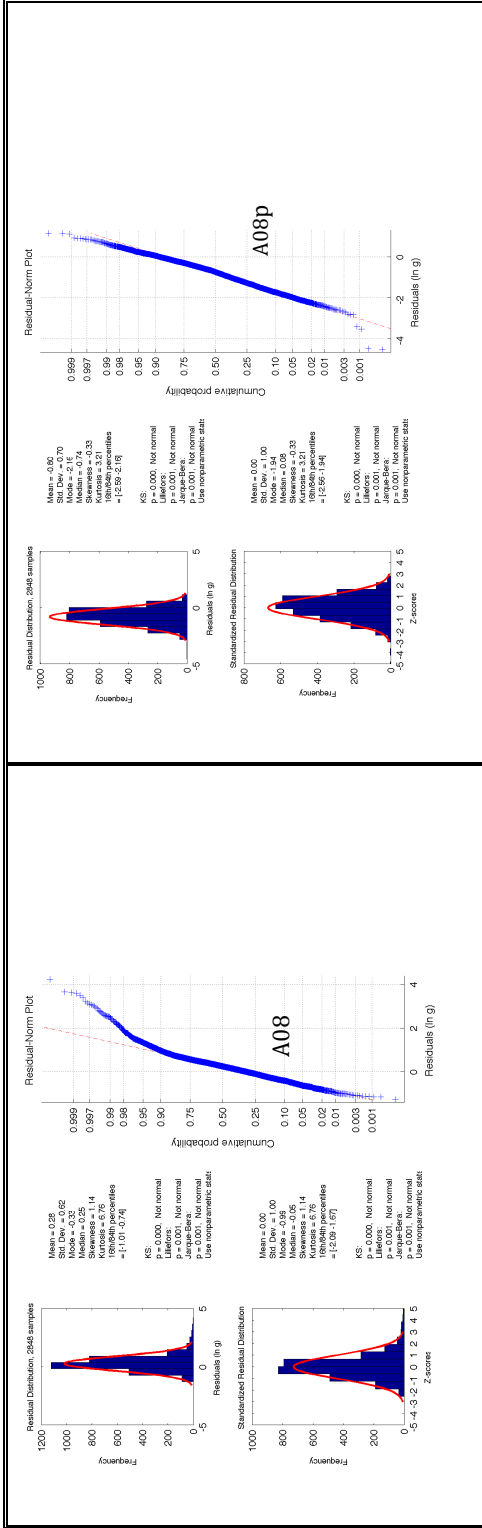
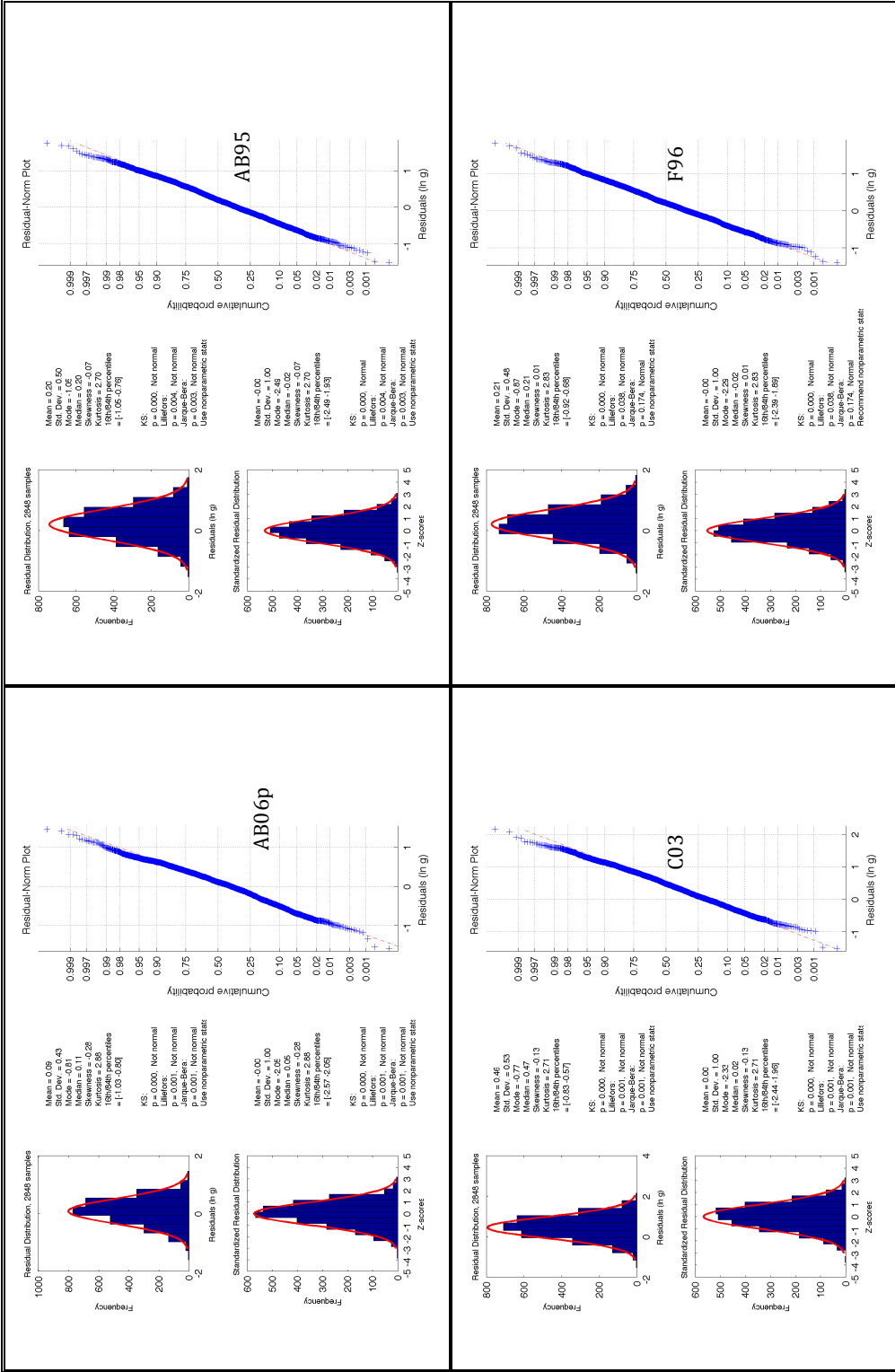
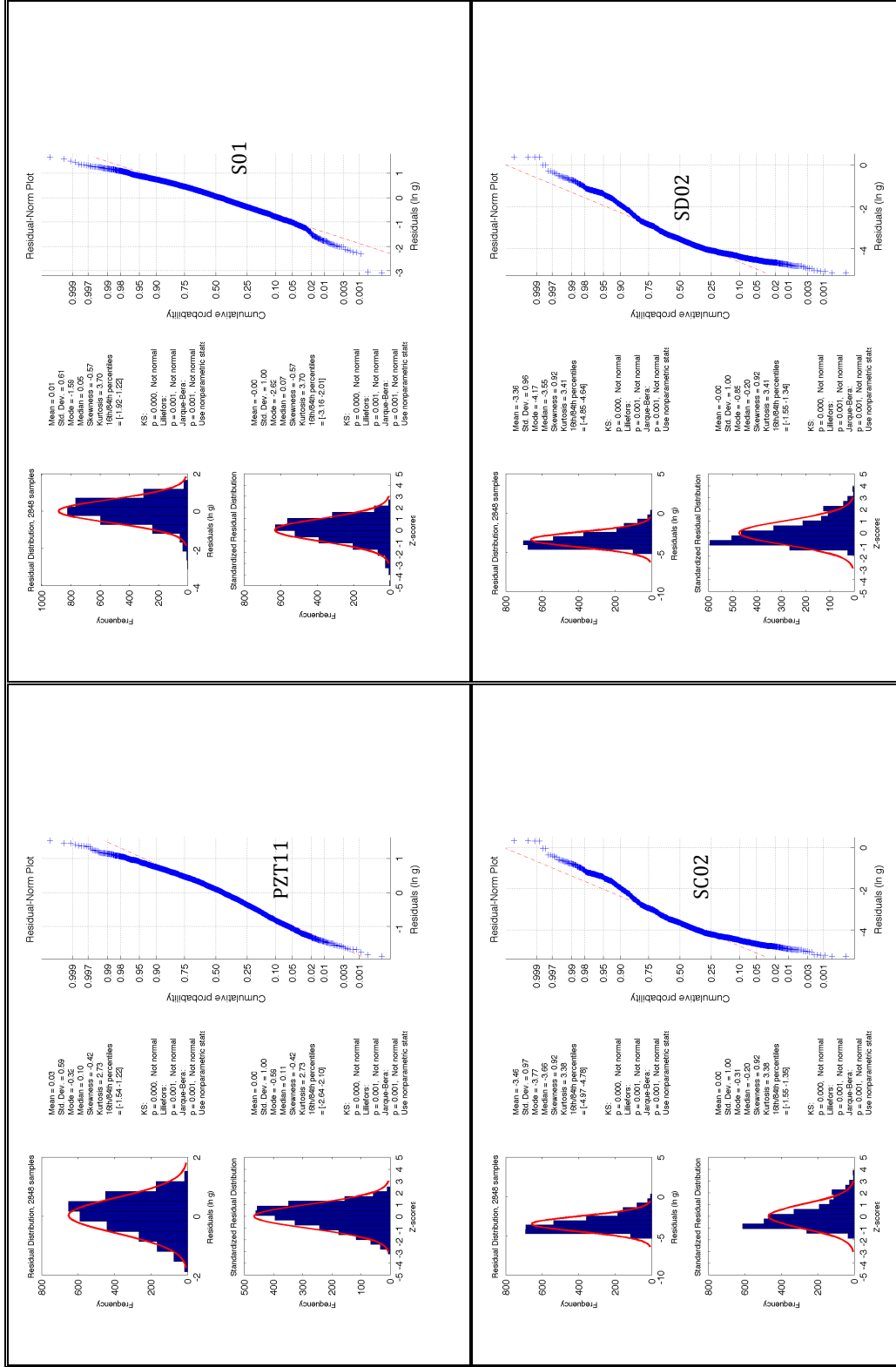
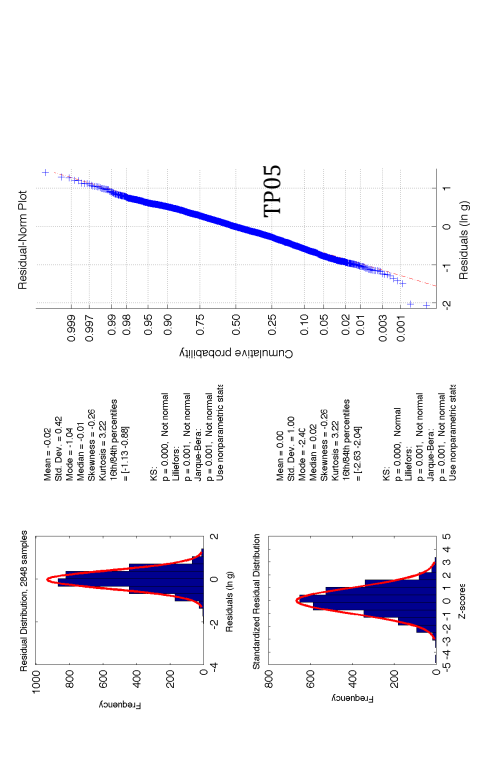
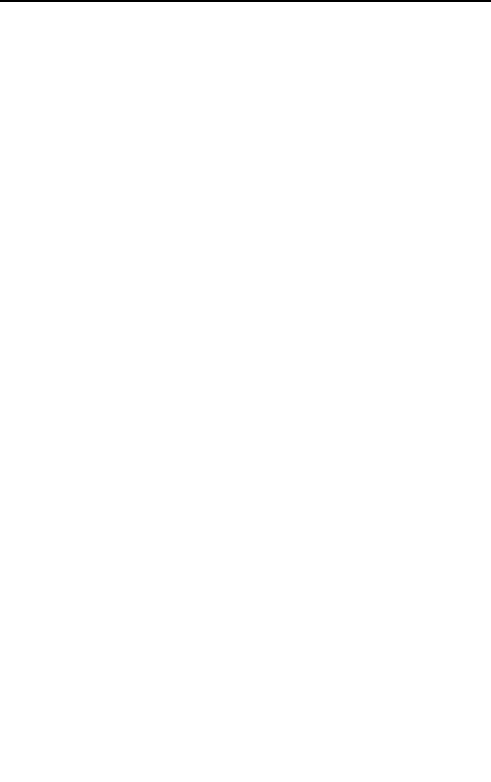
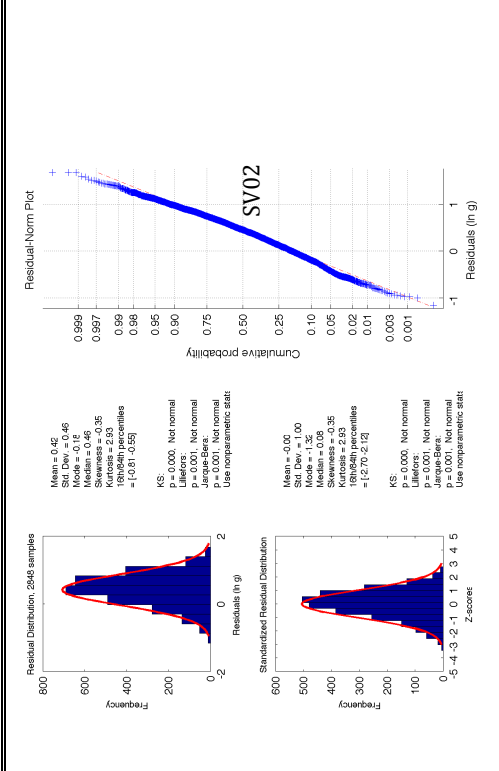
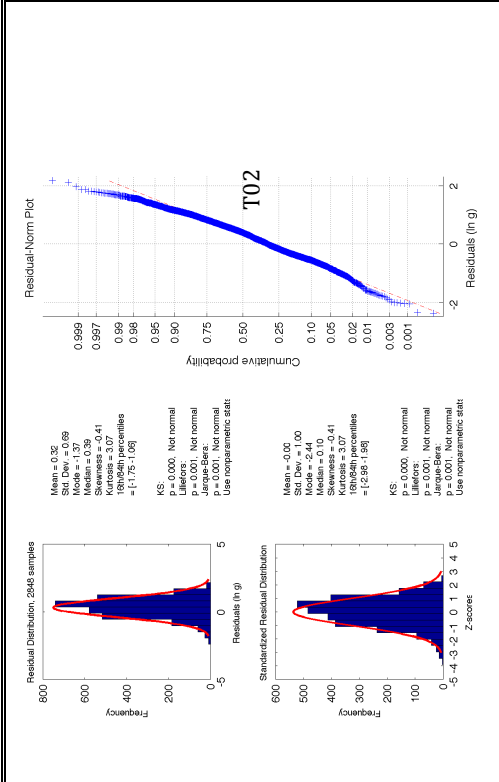


Figure 12: Plot for the Peak Ground Acceleration









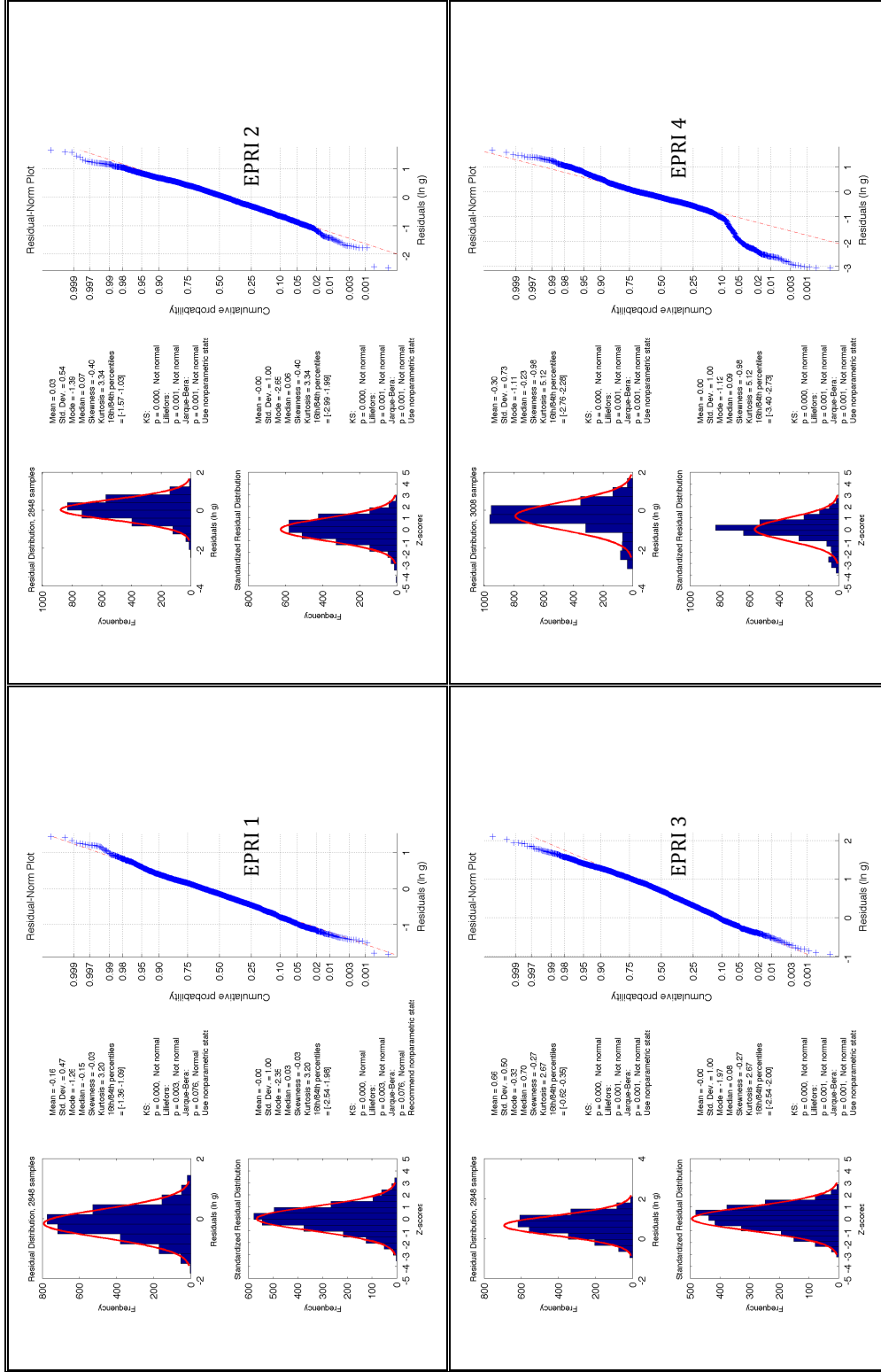
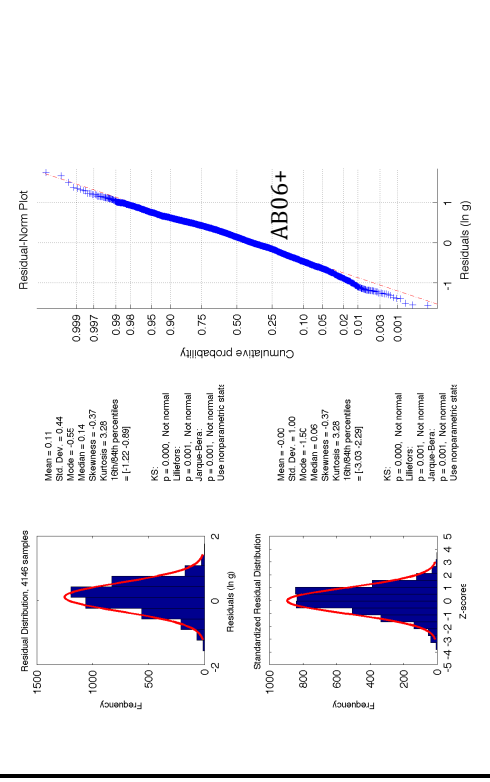
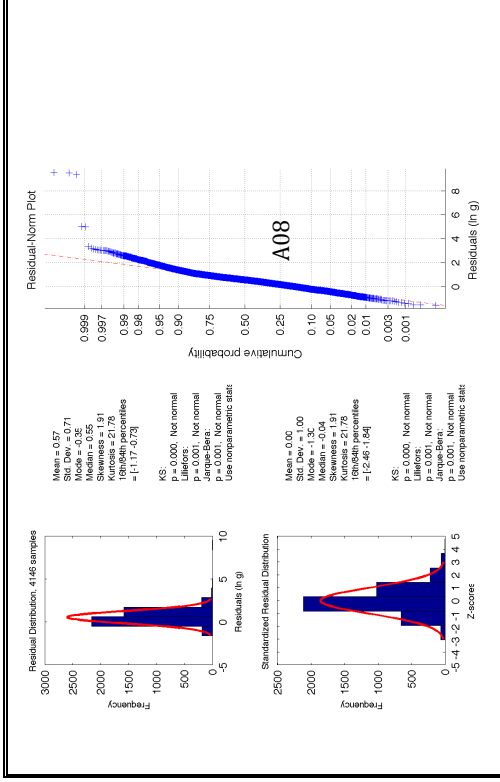
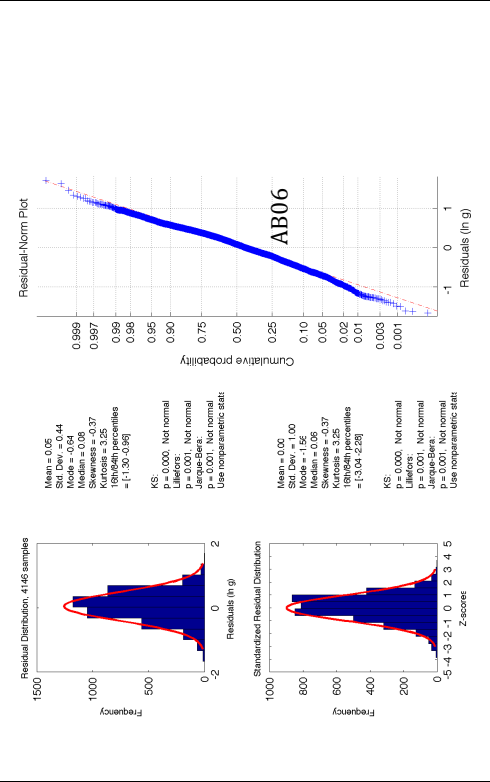
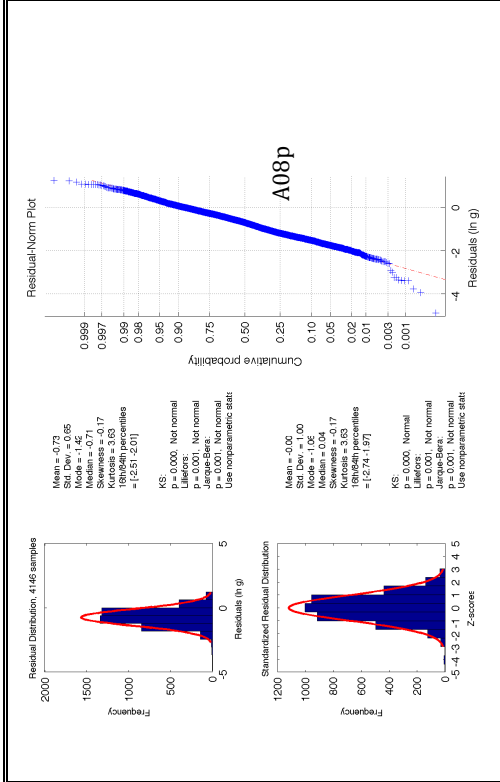
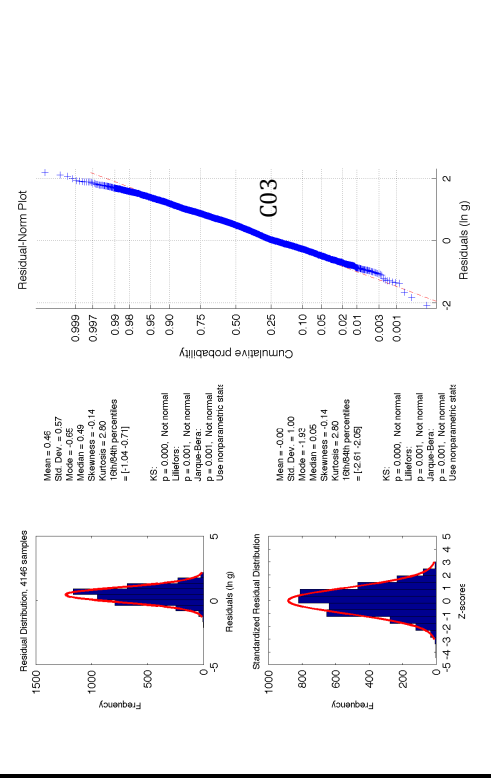
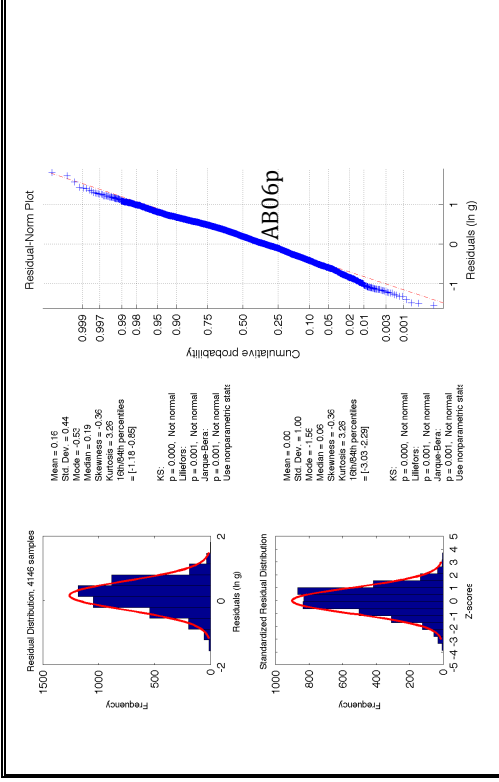
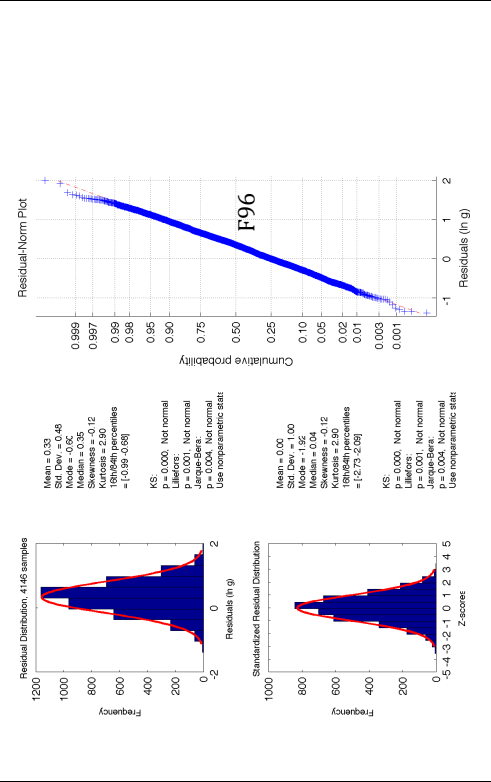
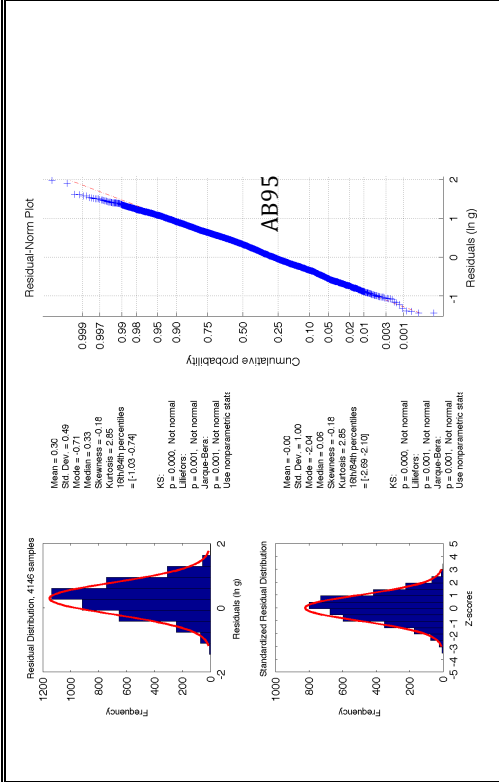
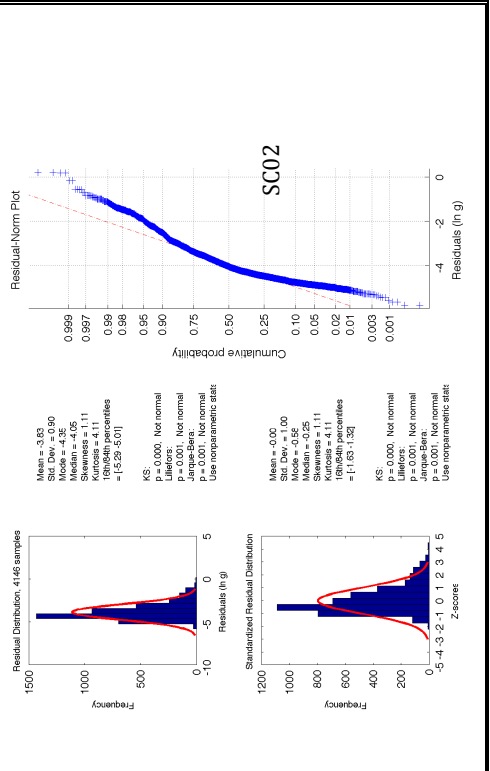
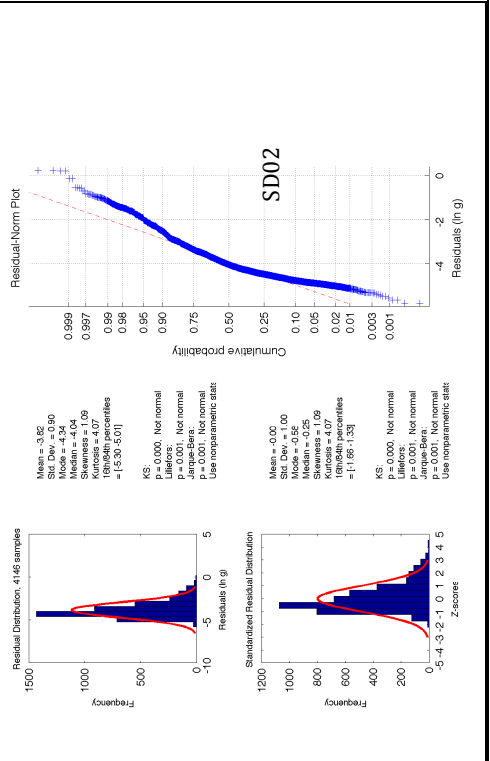
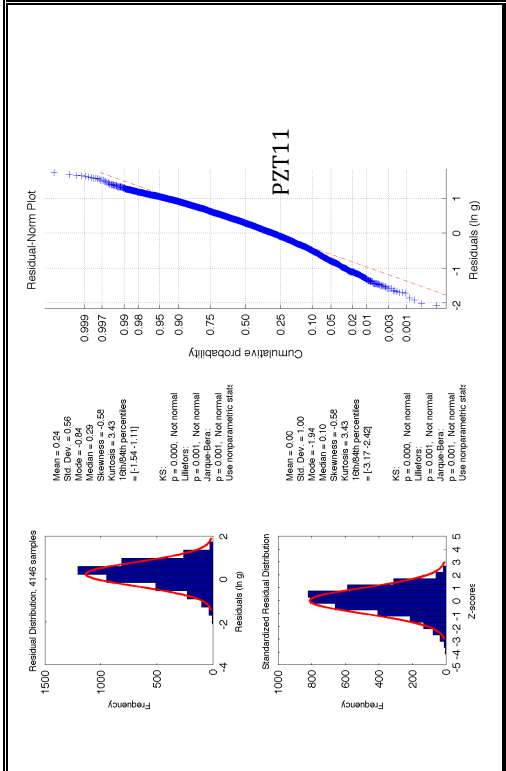
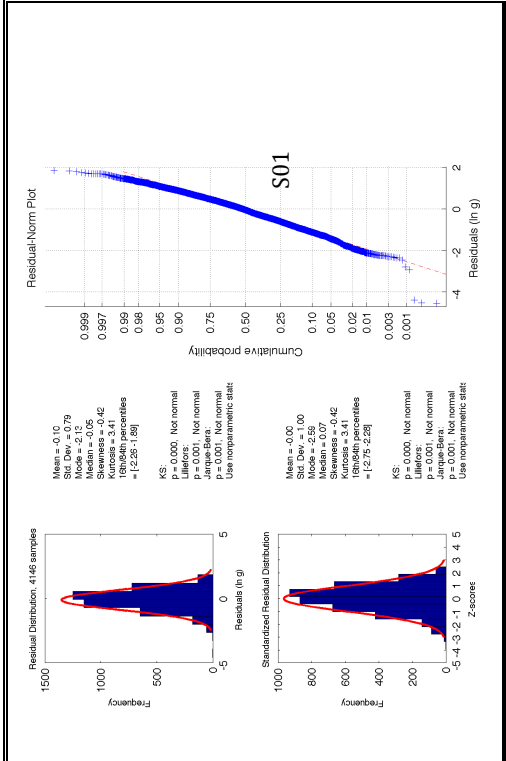
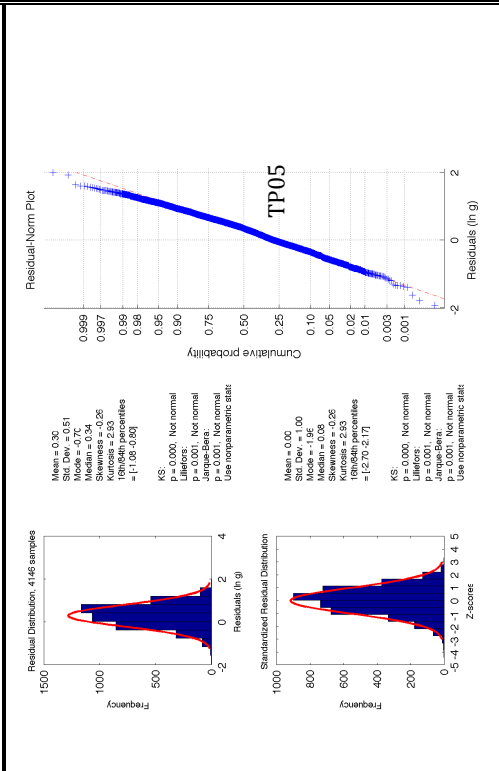
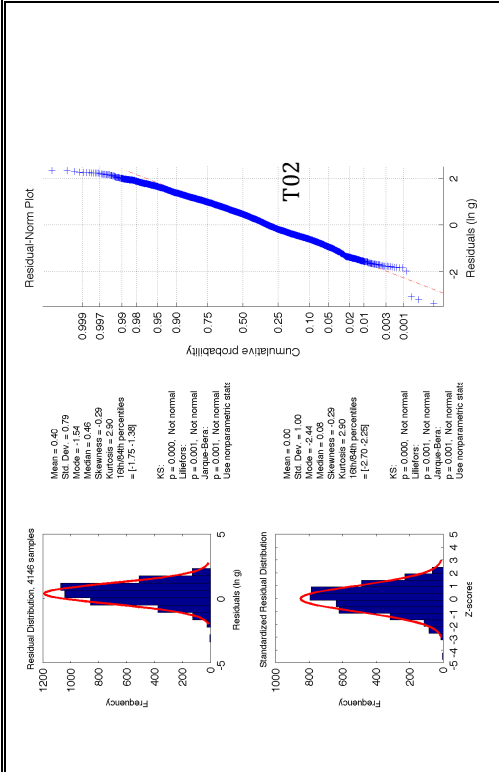
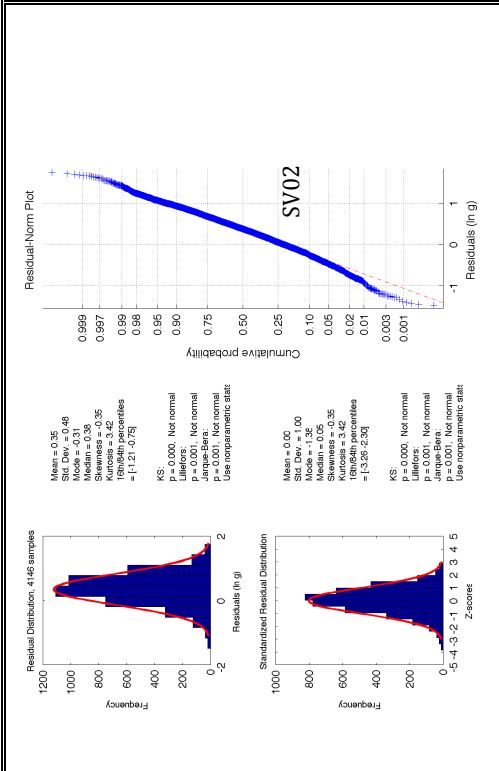


Figure 13: Plot for the 0.1s spectral Acceleration









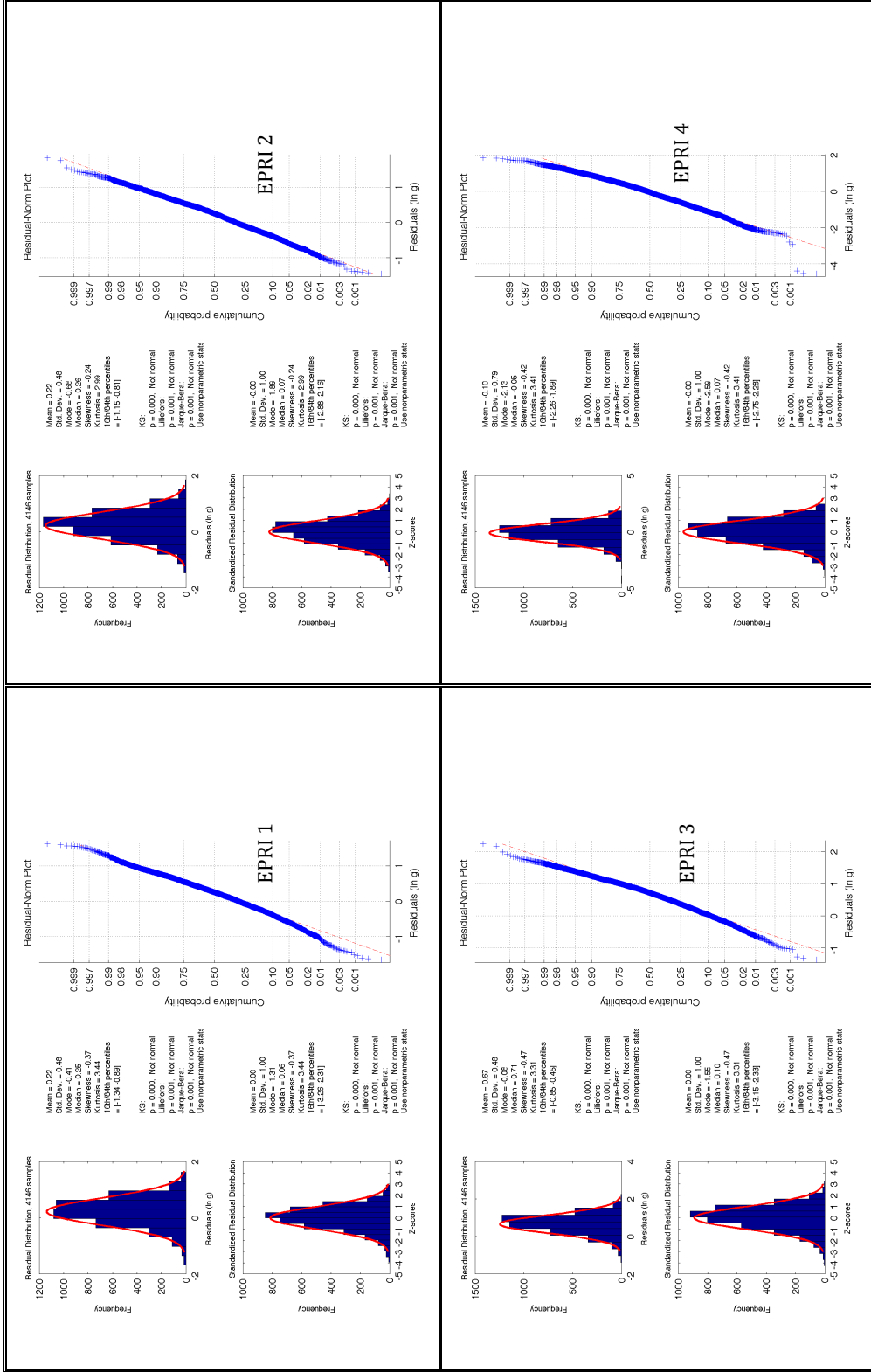
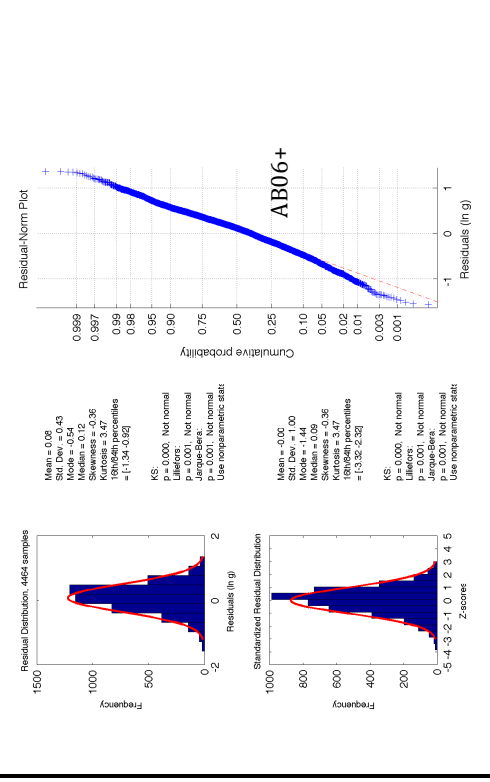
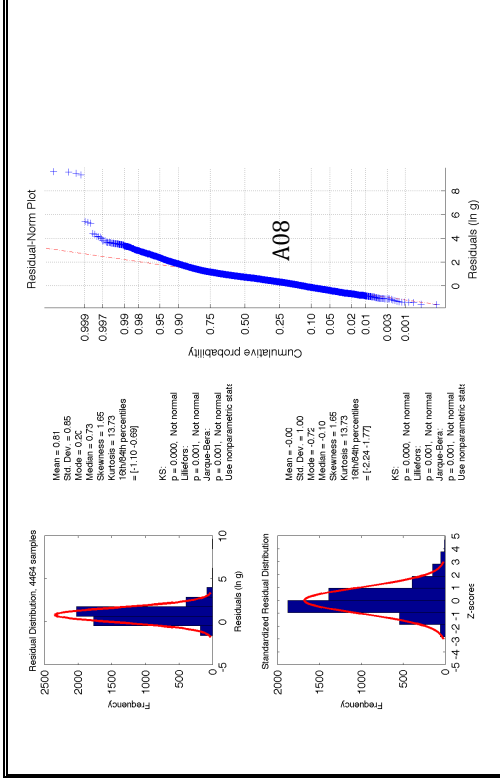
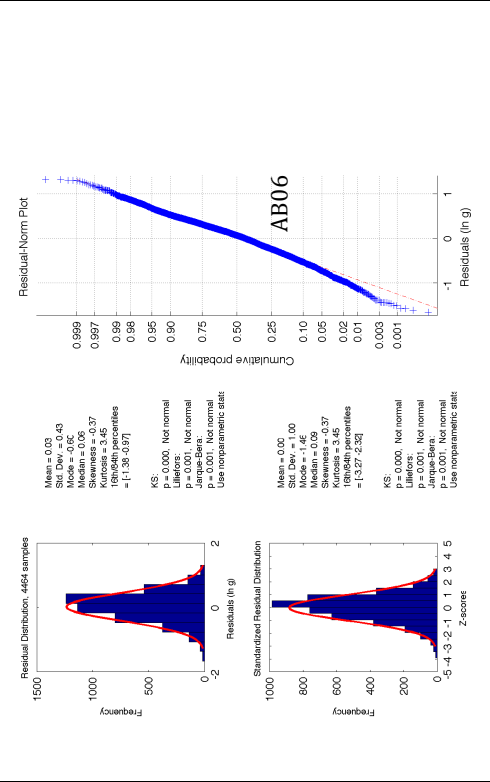
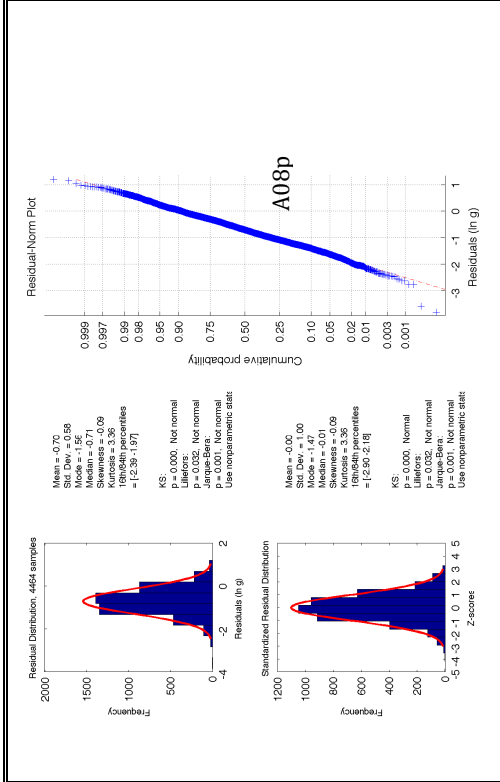
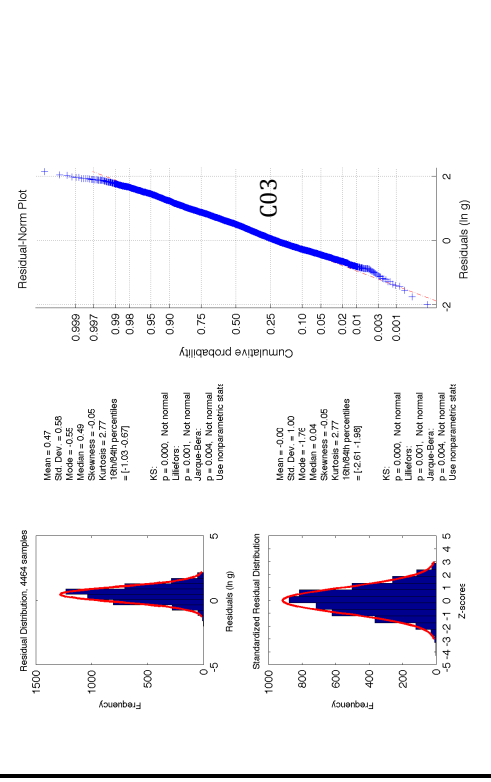
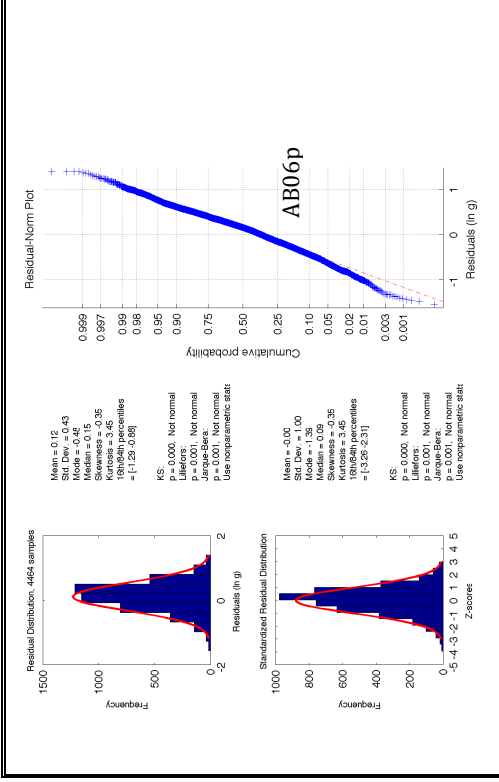
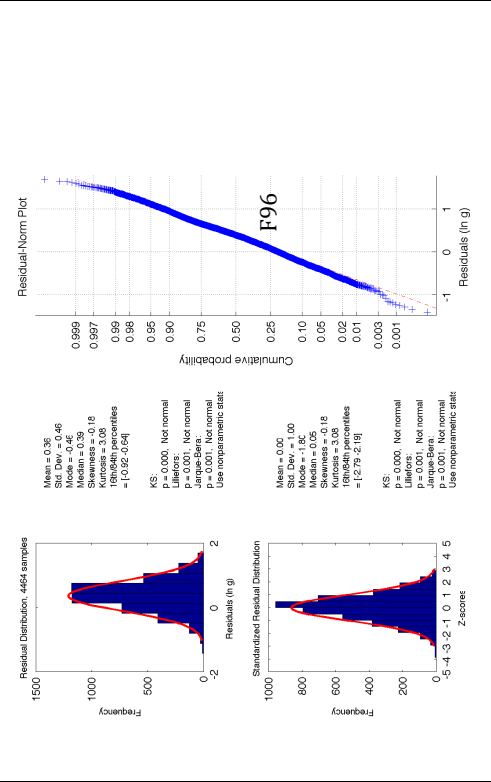
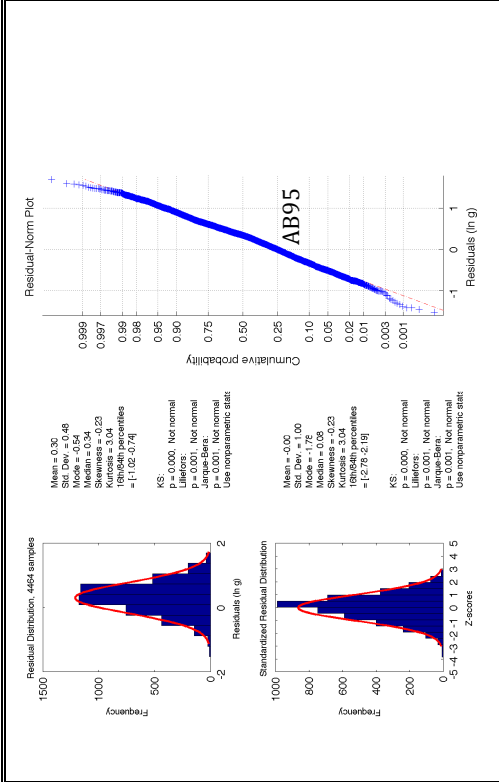
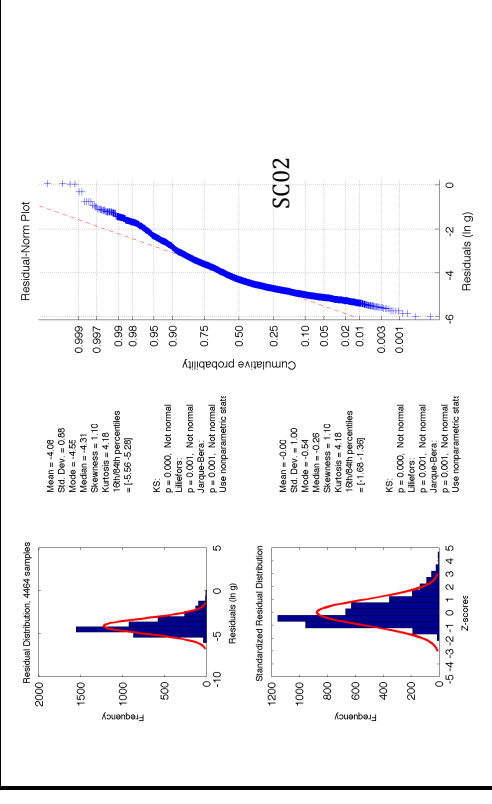
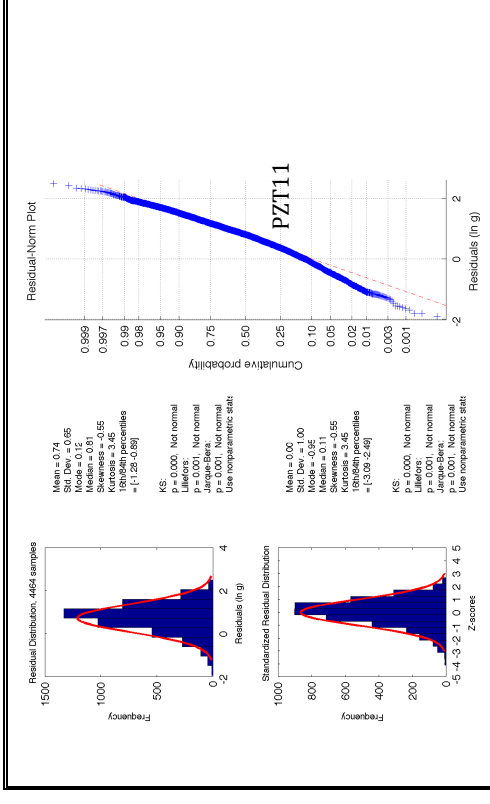
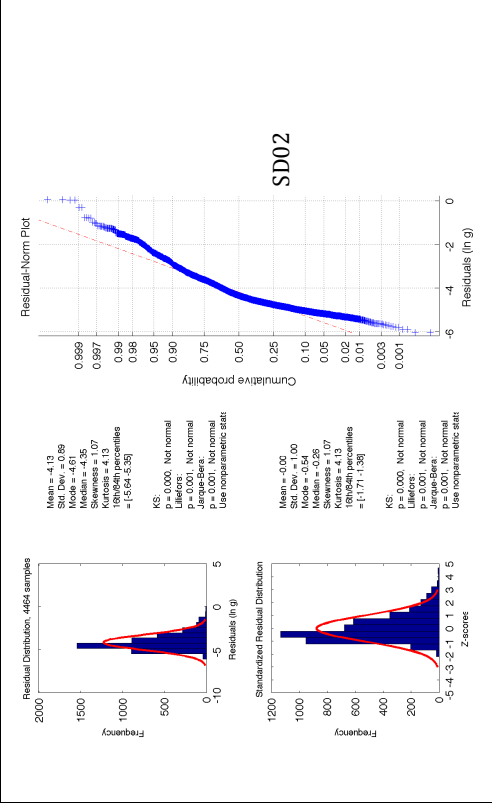
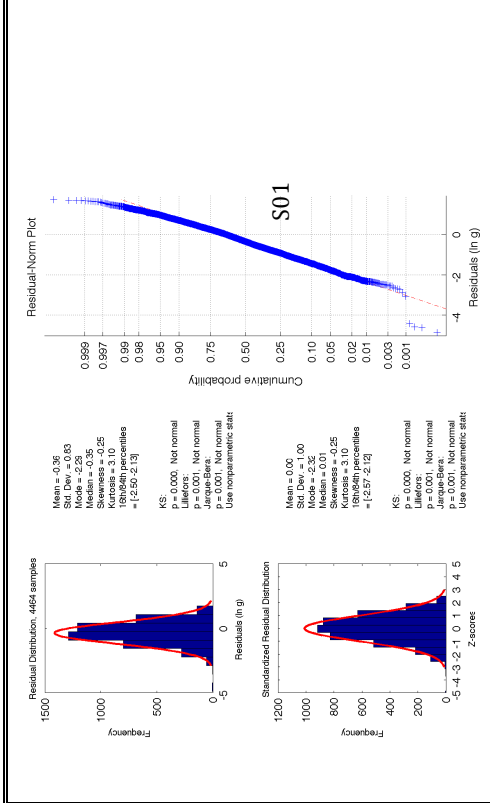
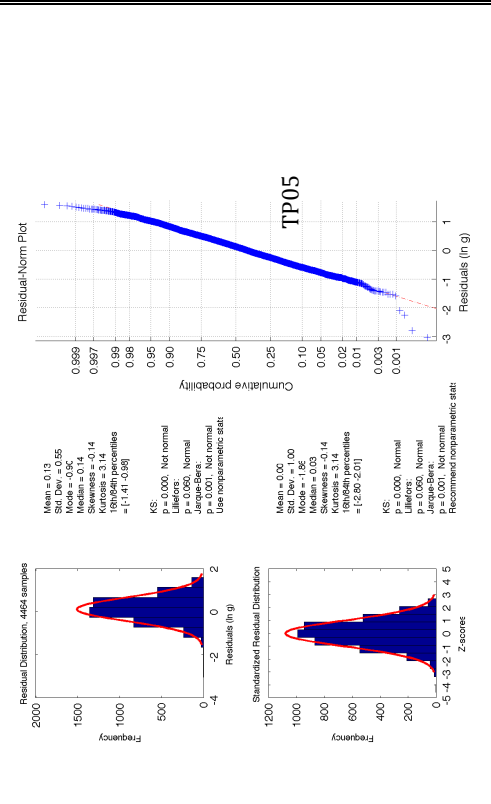
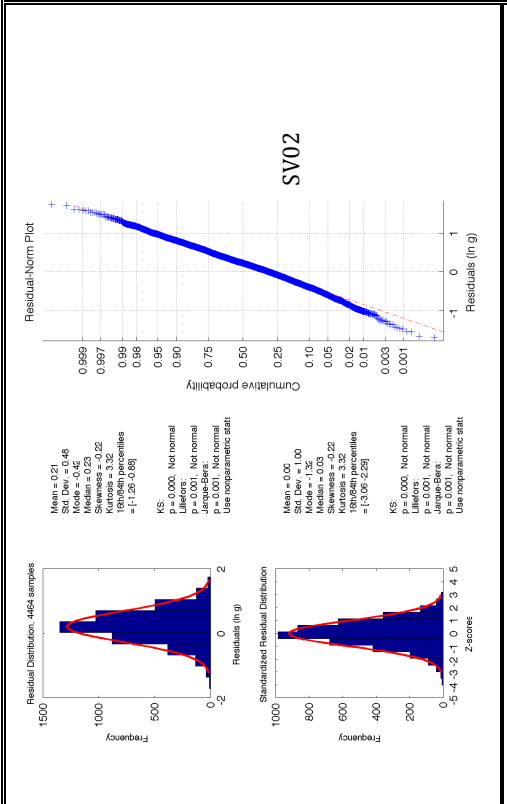
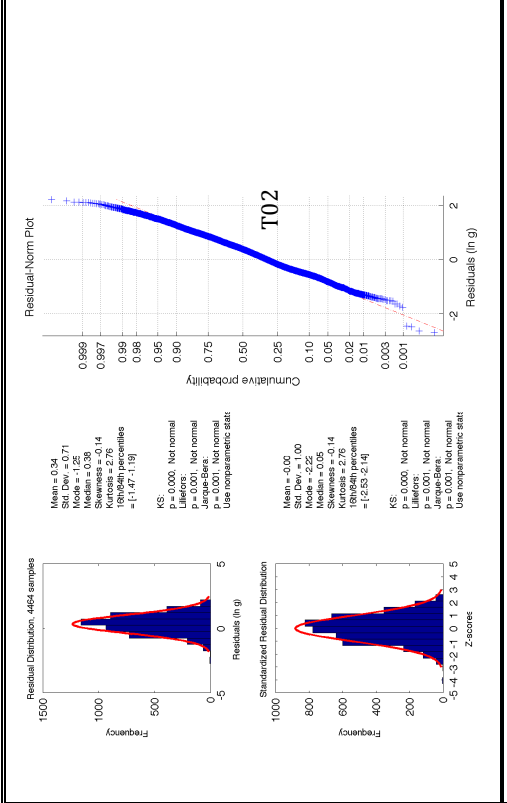


Figure 14: Plot for the 0.2s spectral Acceleration









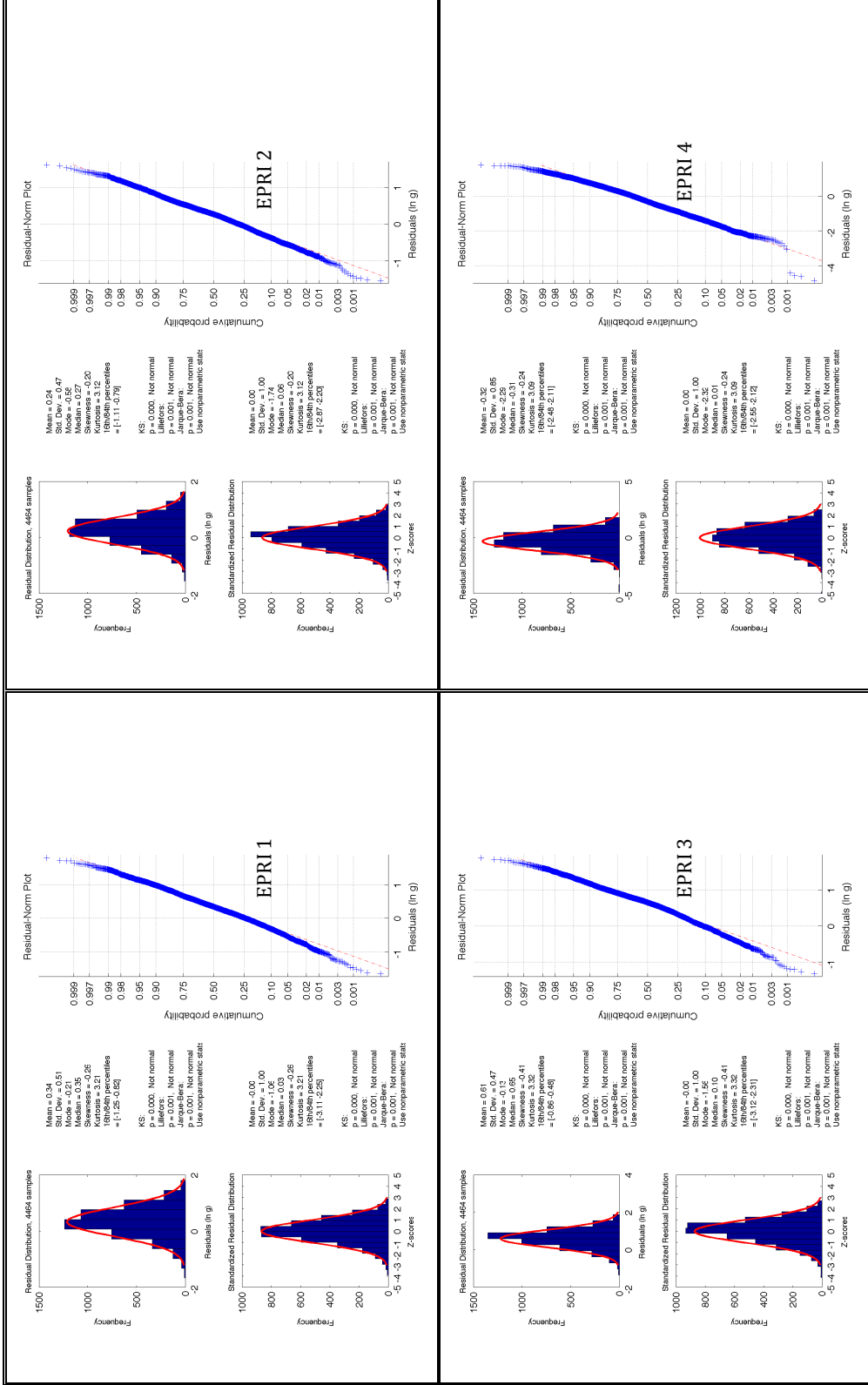
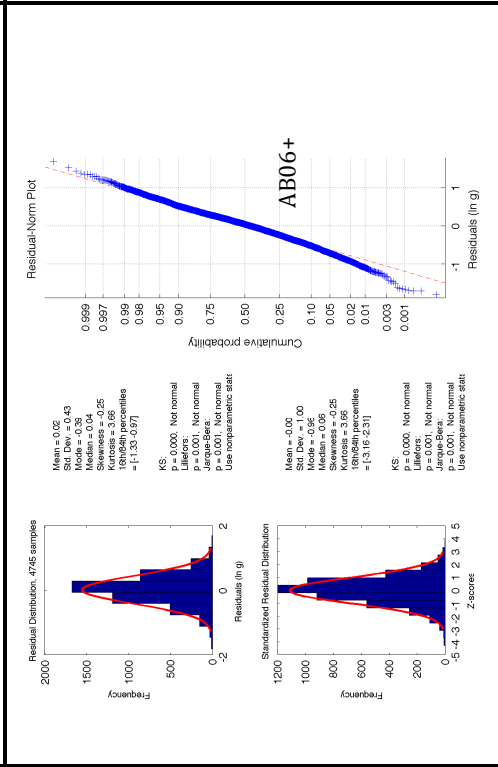
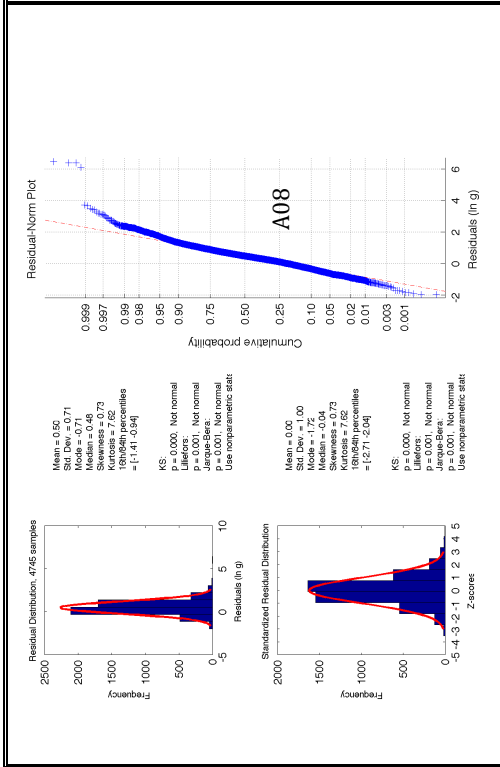
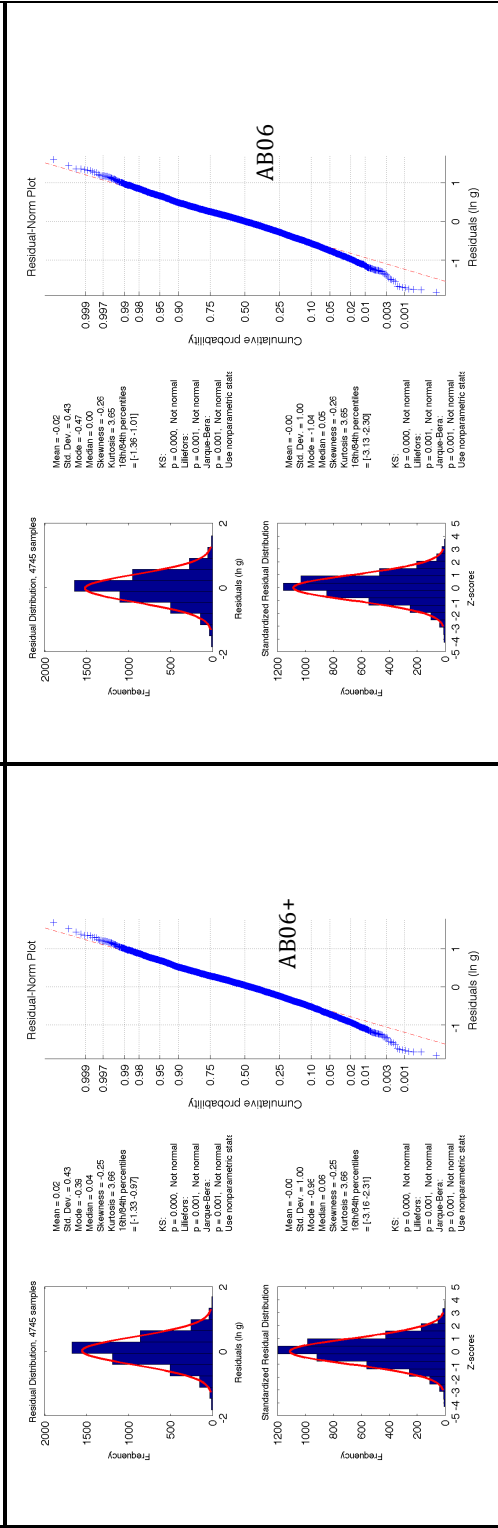
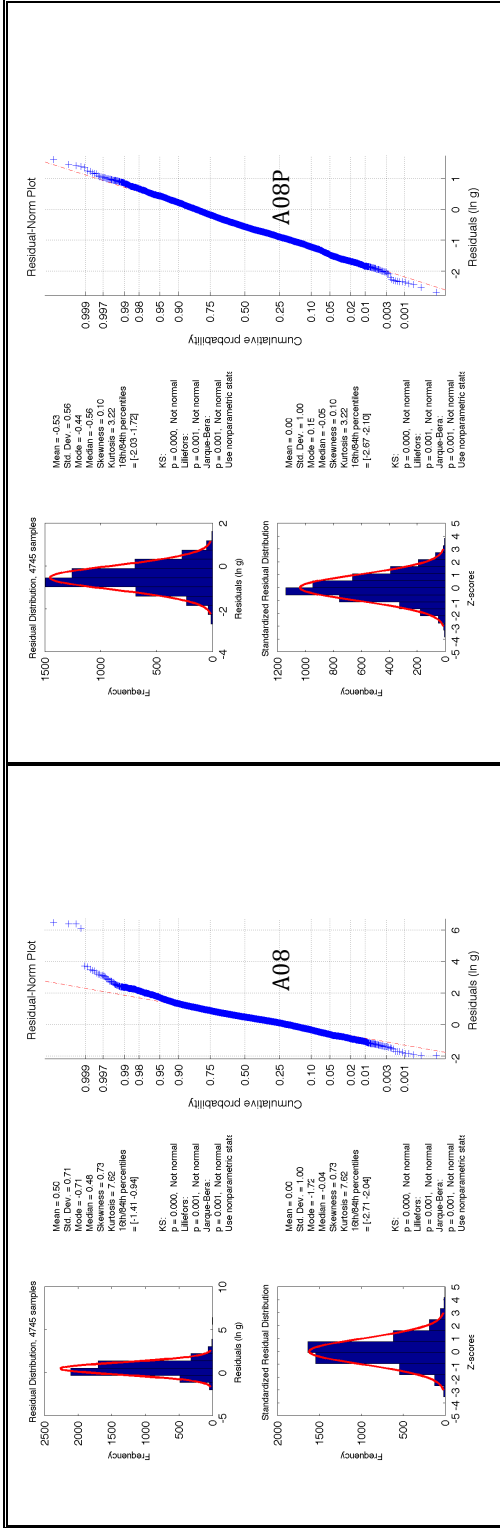
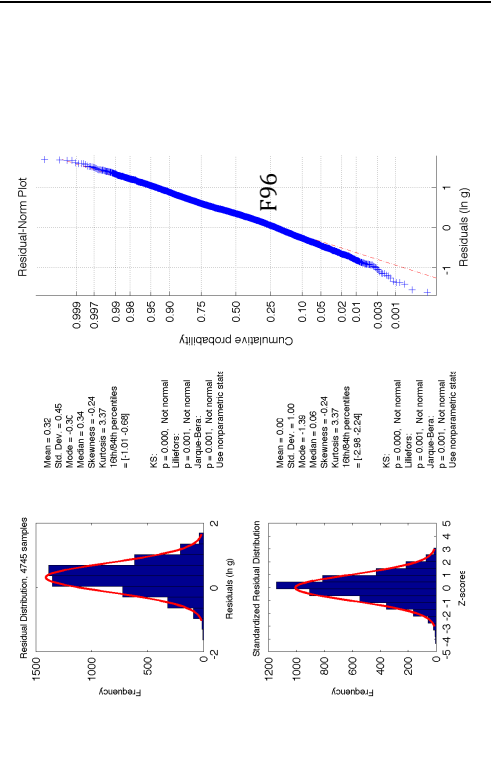
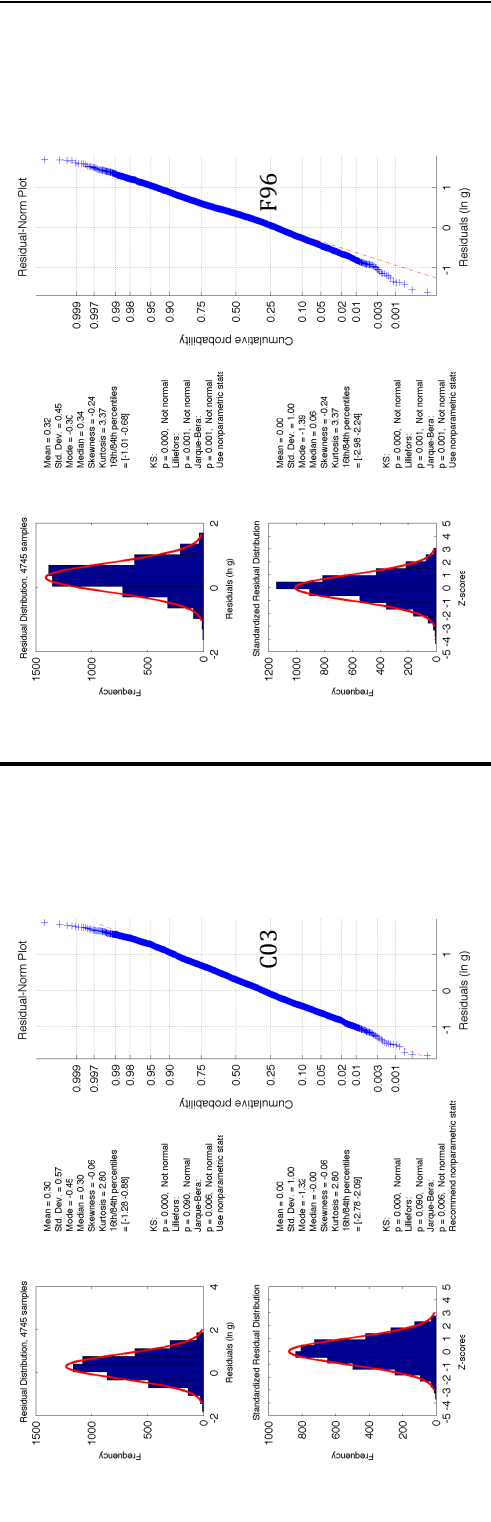
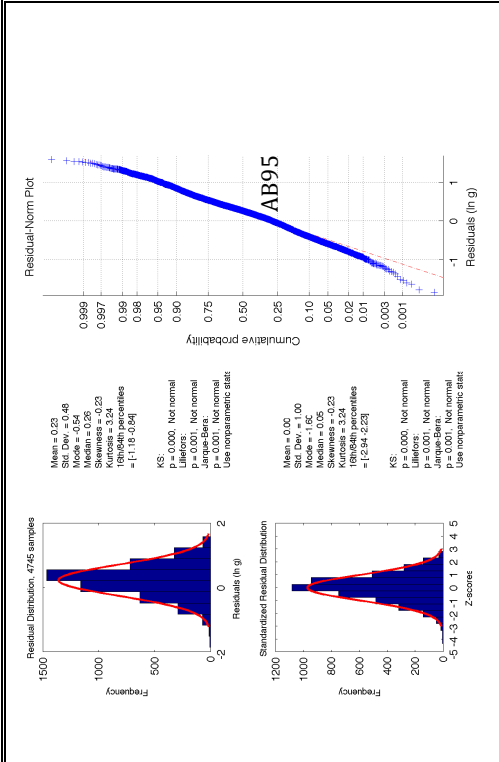
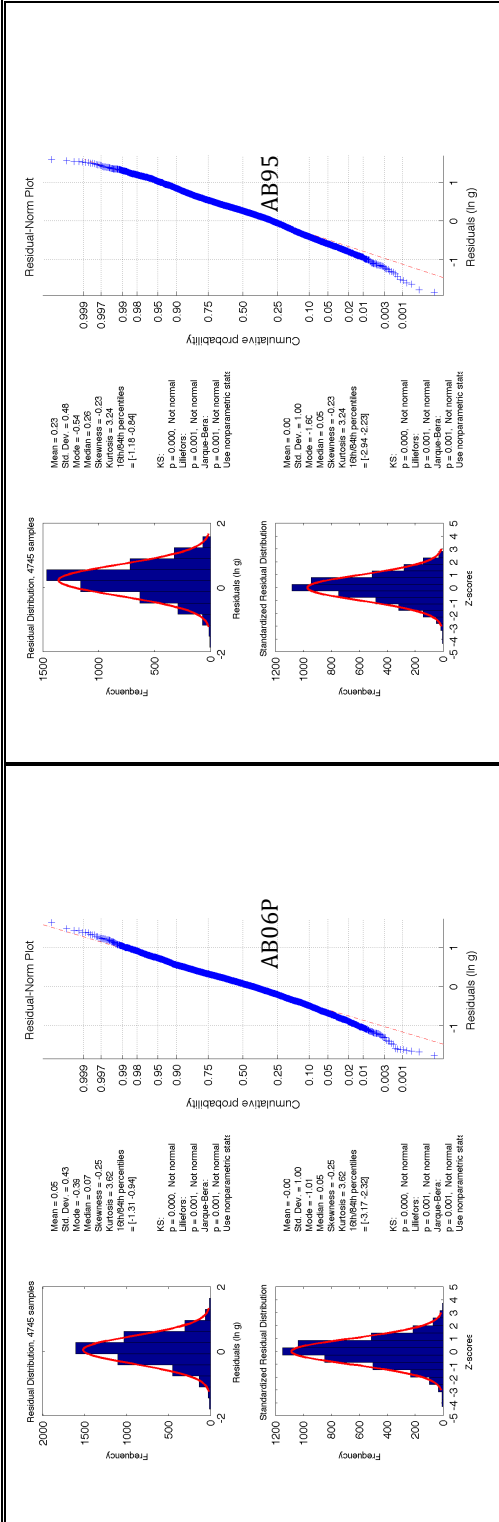
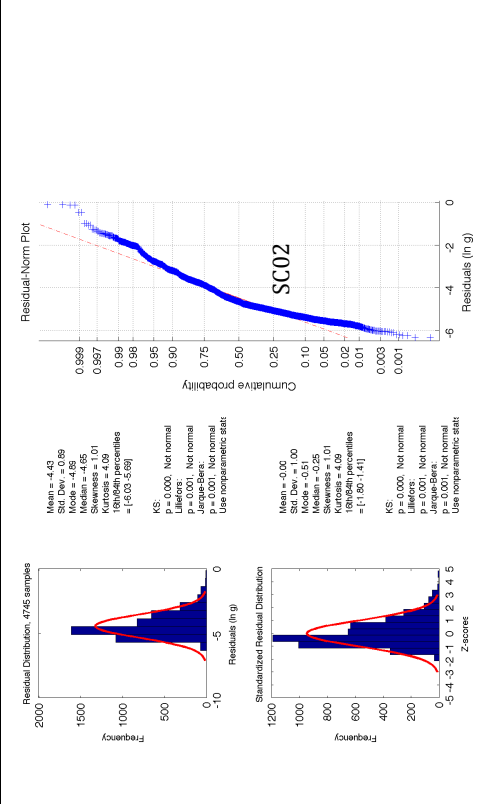
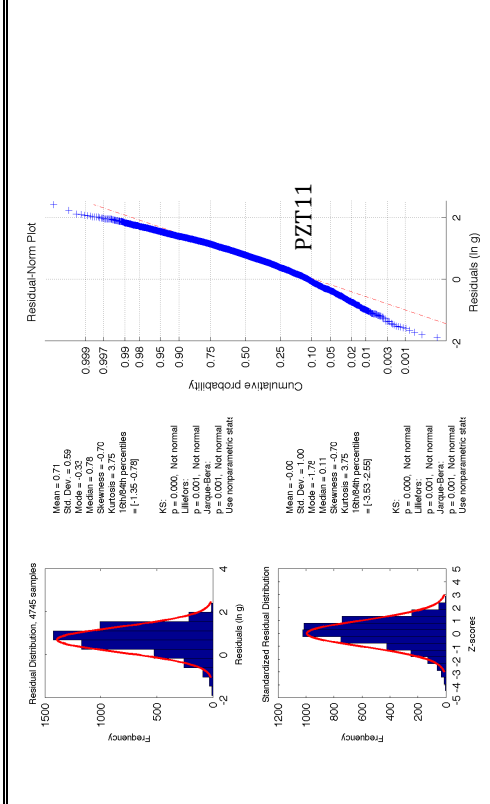
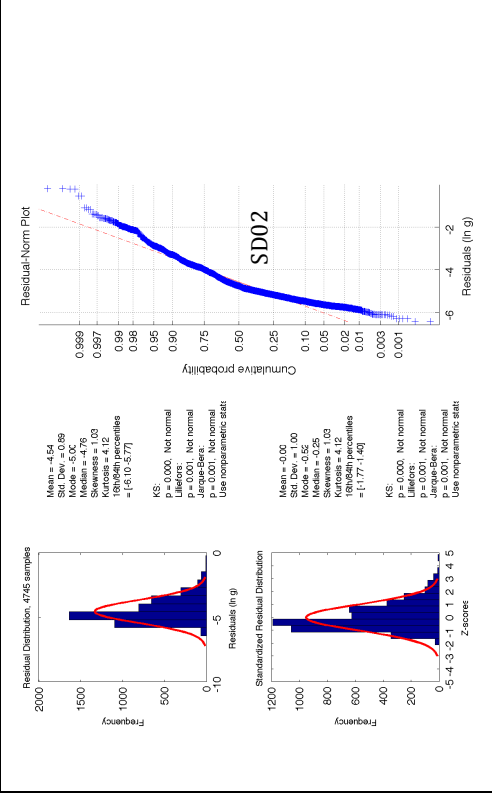
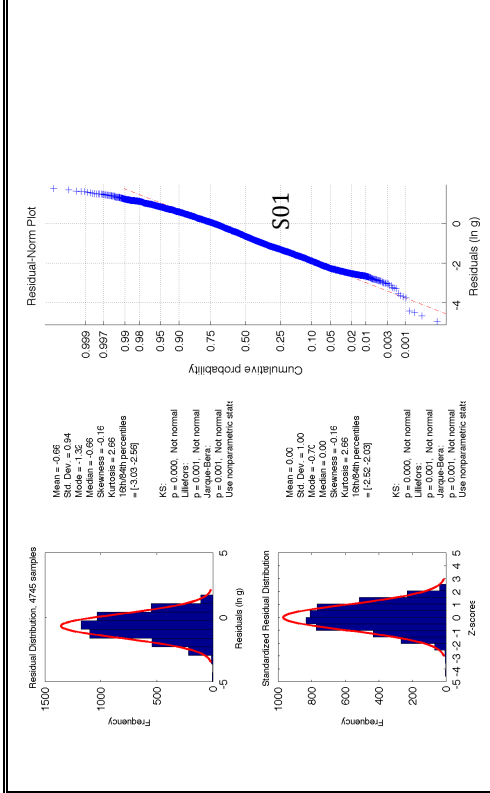
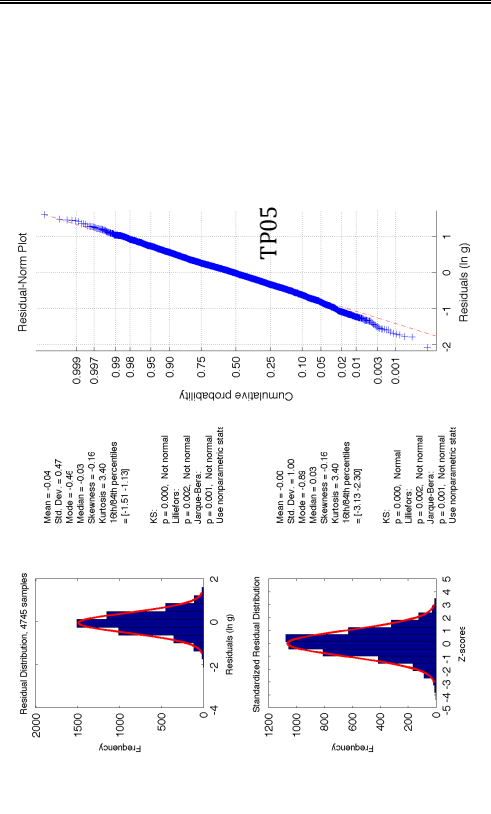
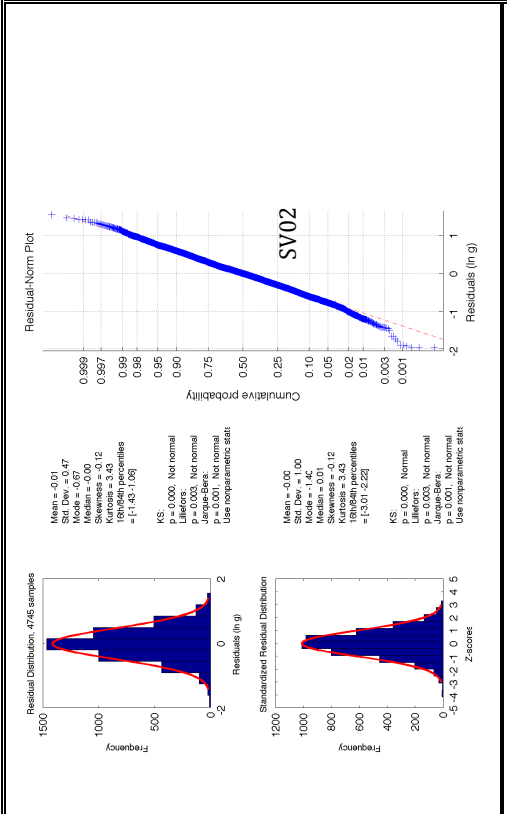
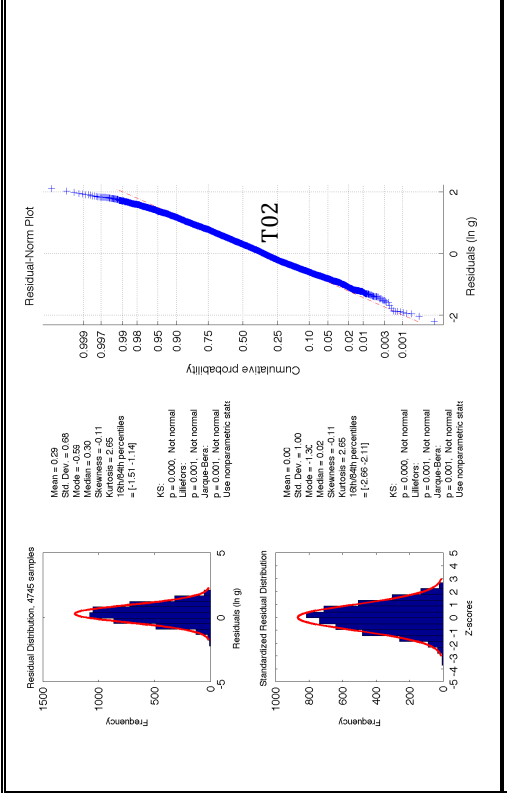


Figure 15: Plot for the 0.3s spectral Acceleration









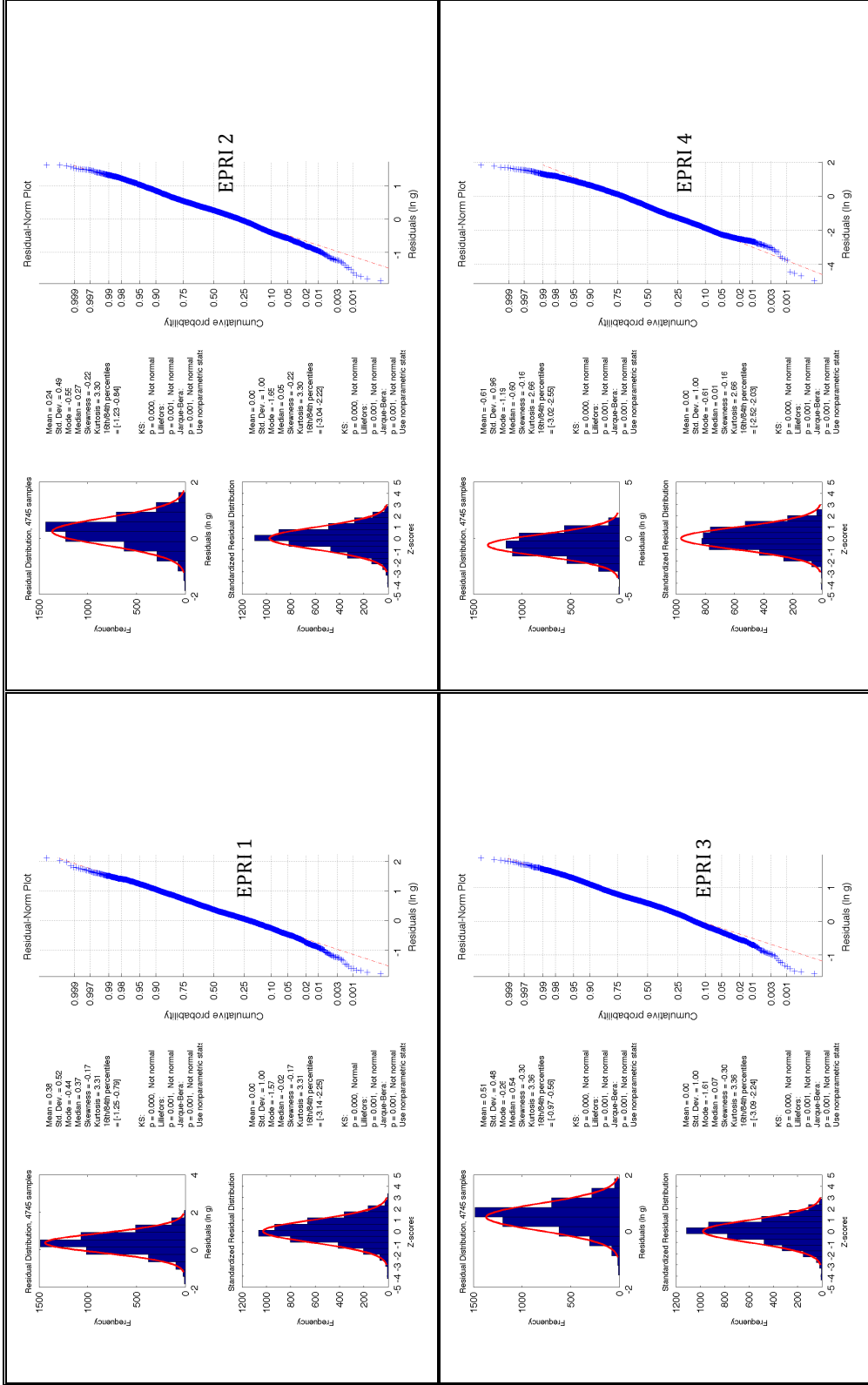
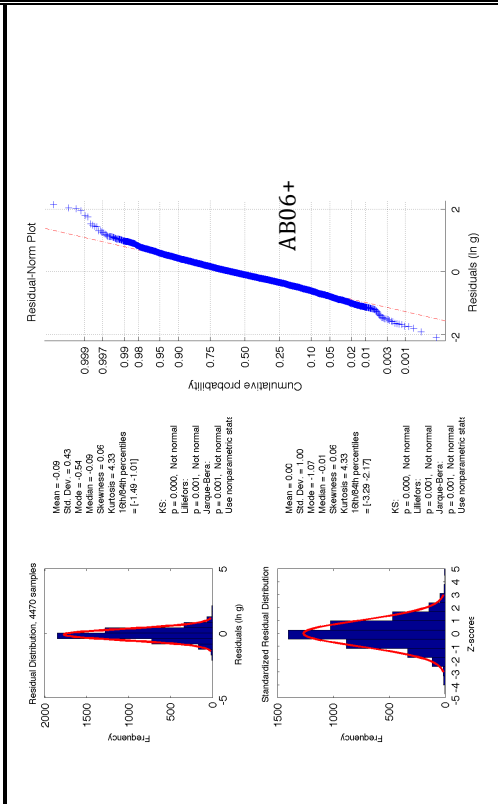
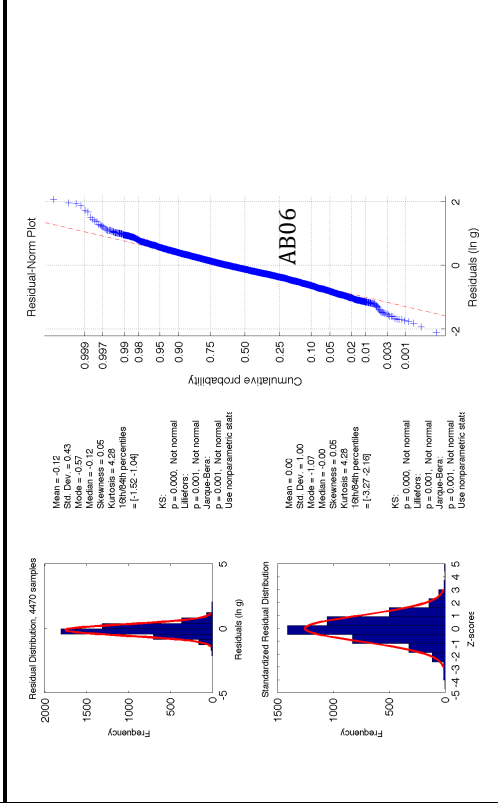
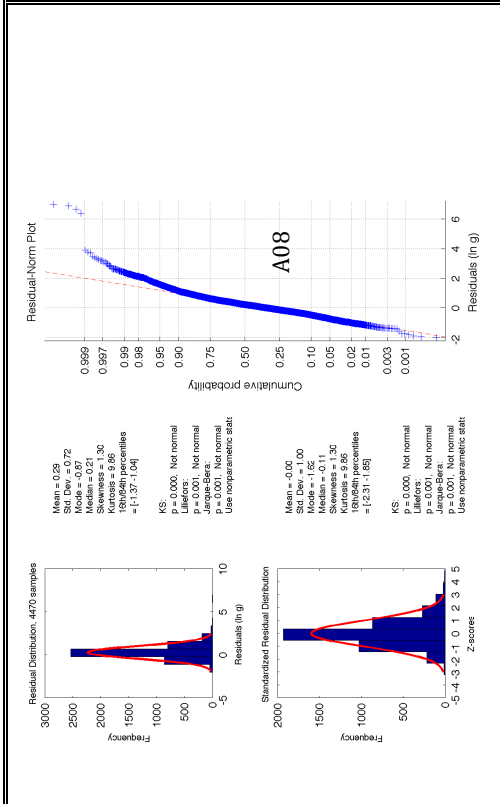
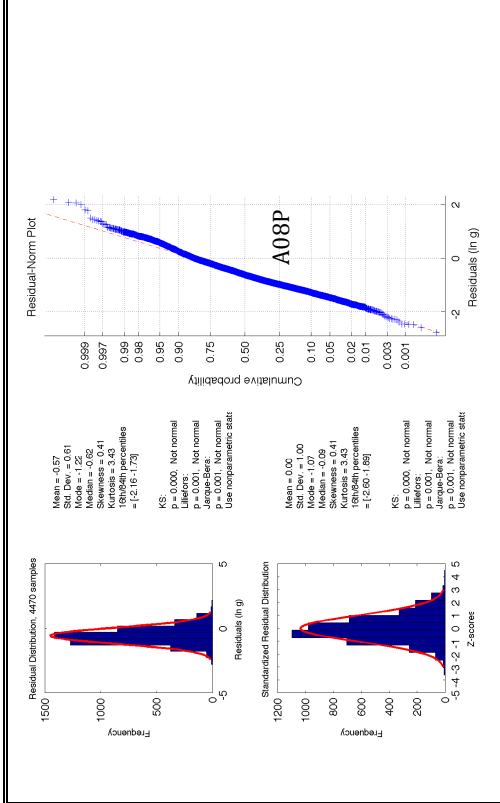
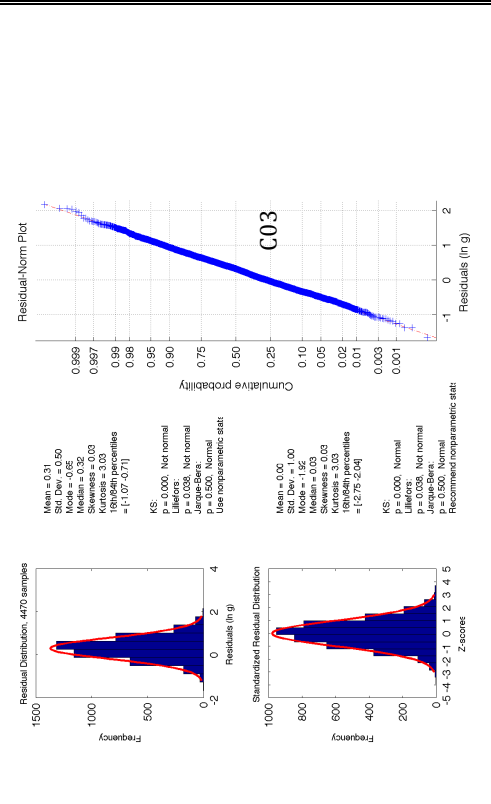
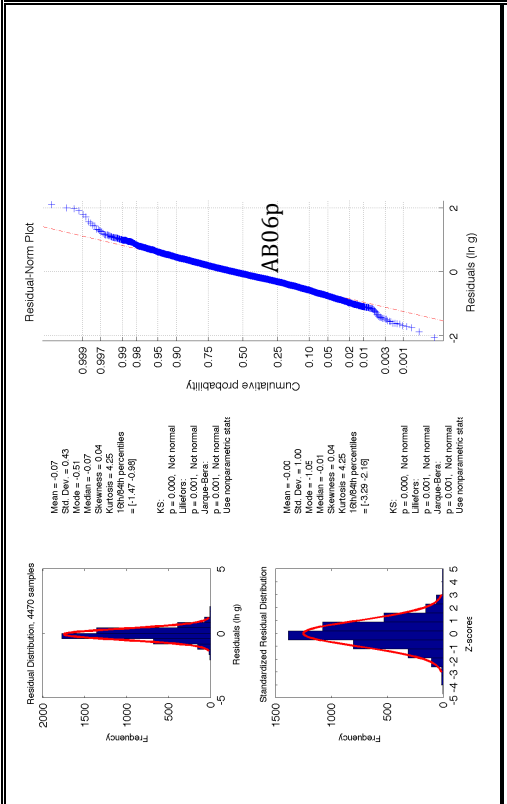
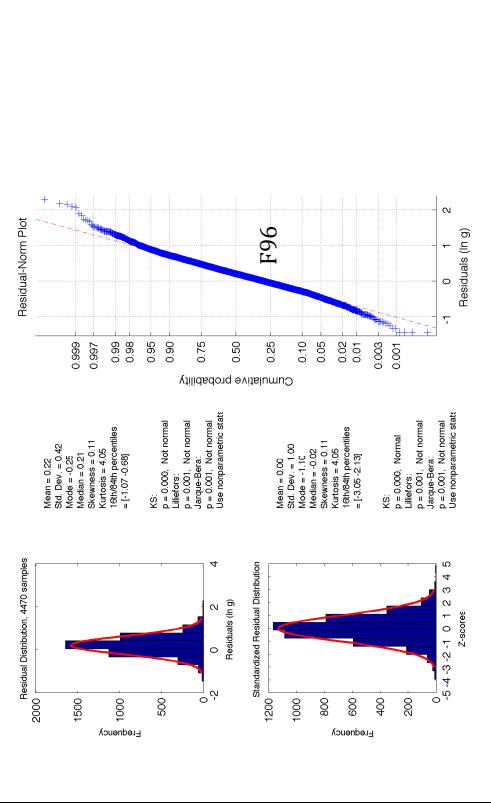
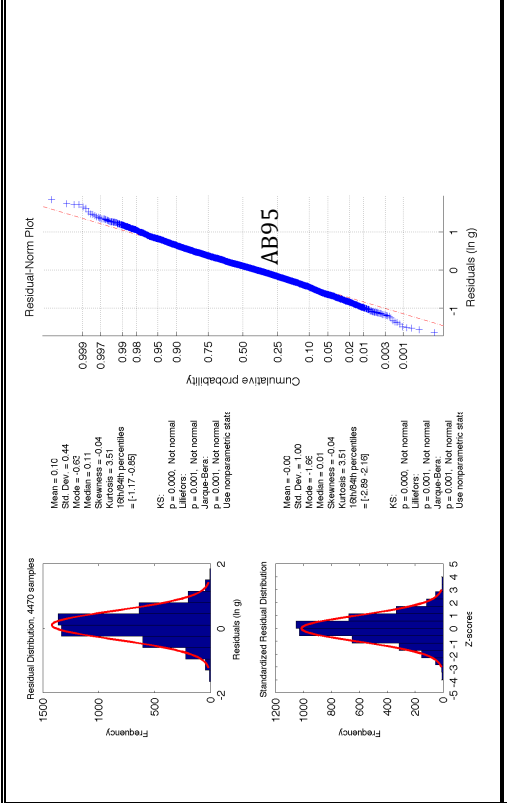
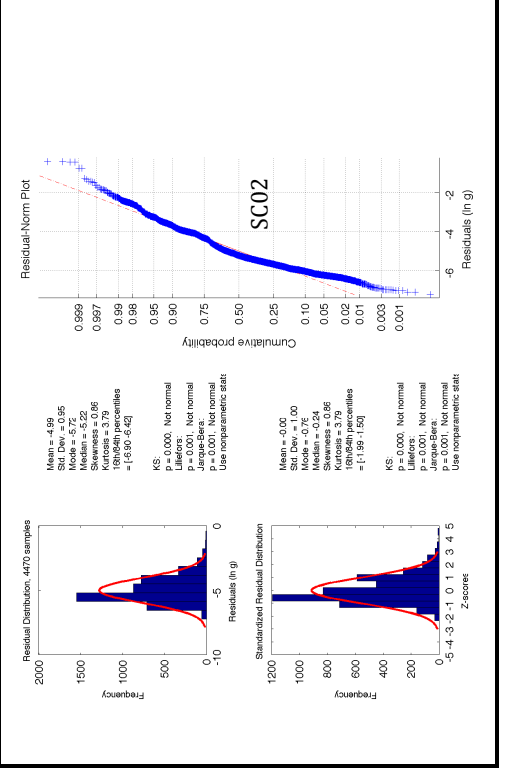
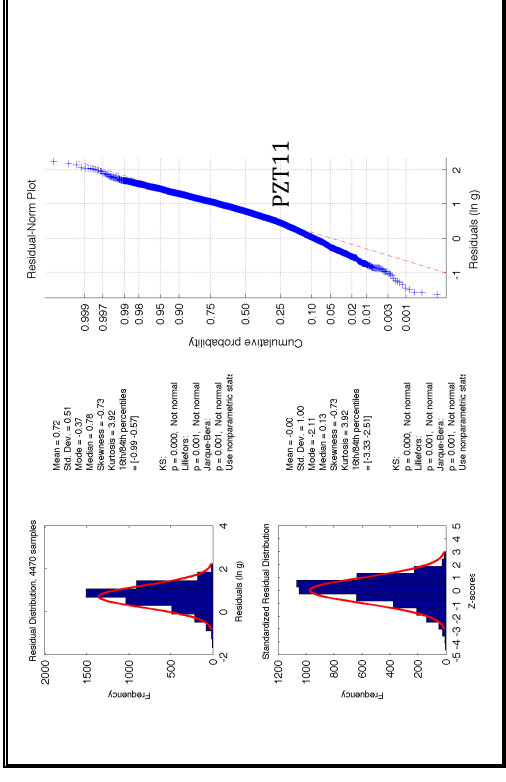
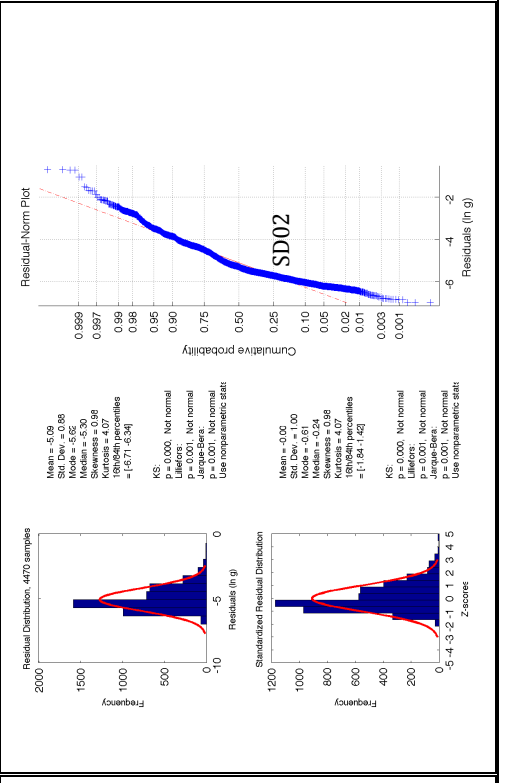
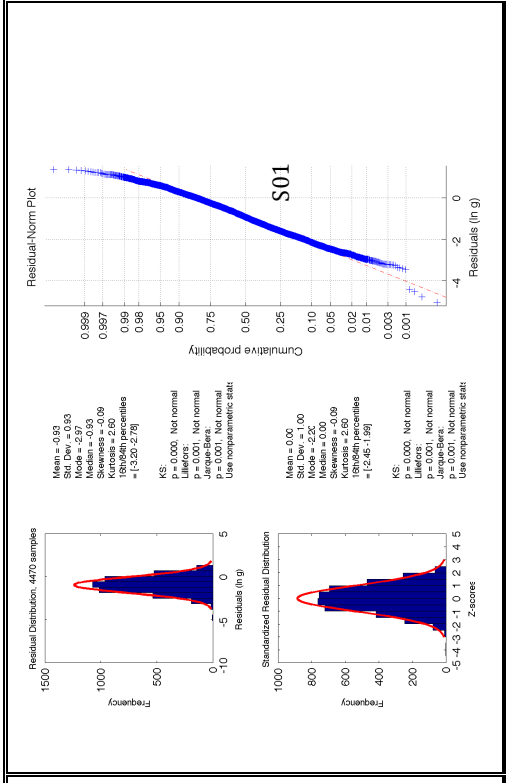
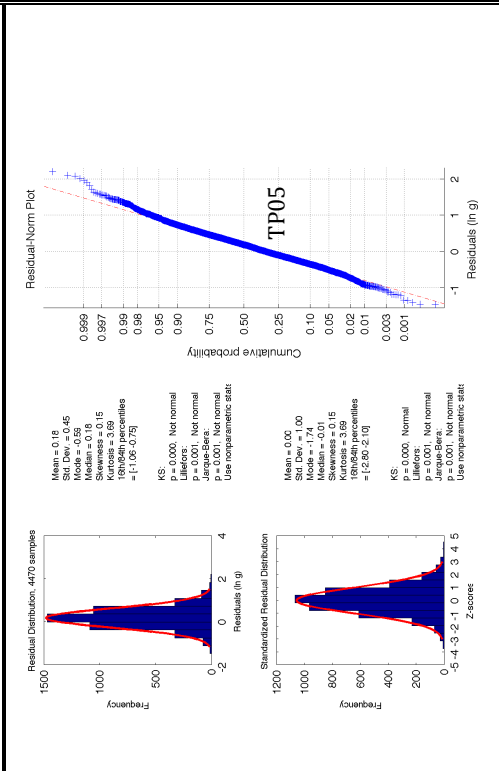
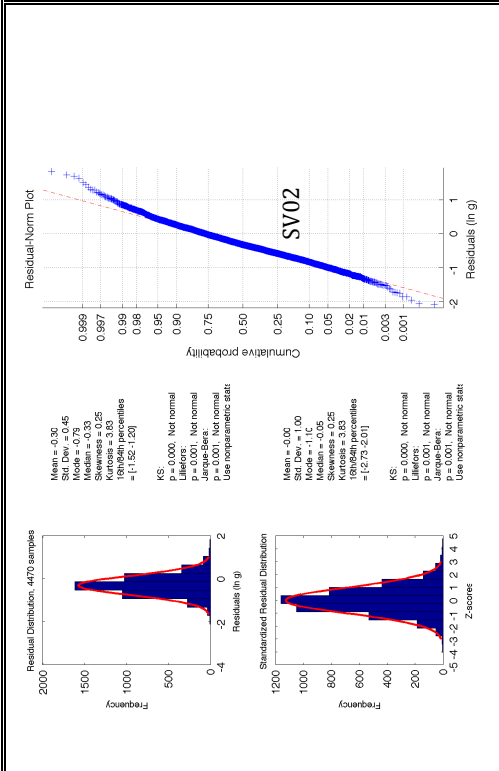
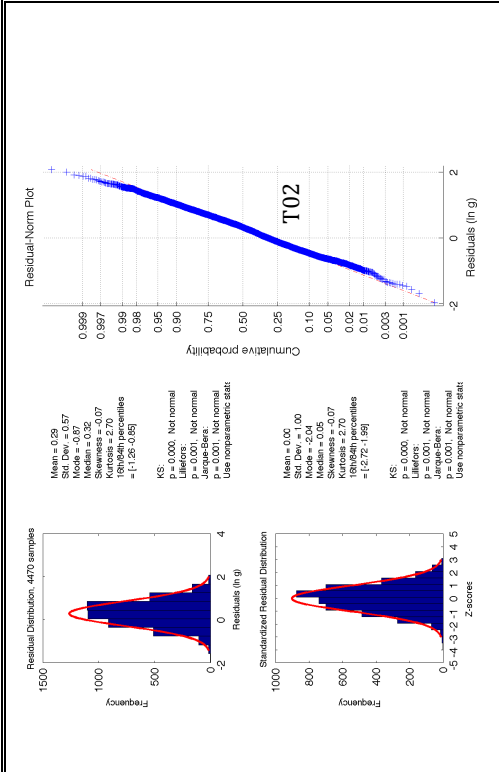


Figure 16: Plot for the 0.5s spectral Acceleration









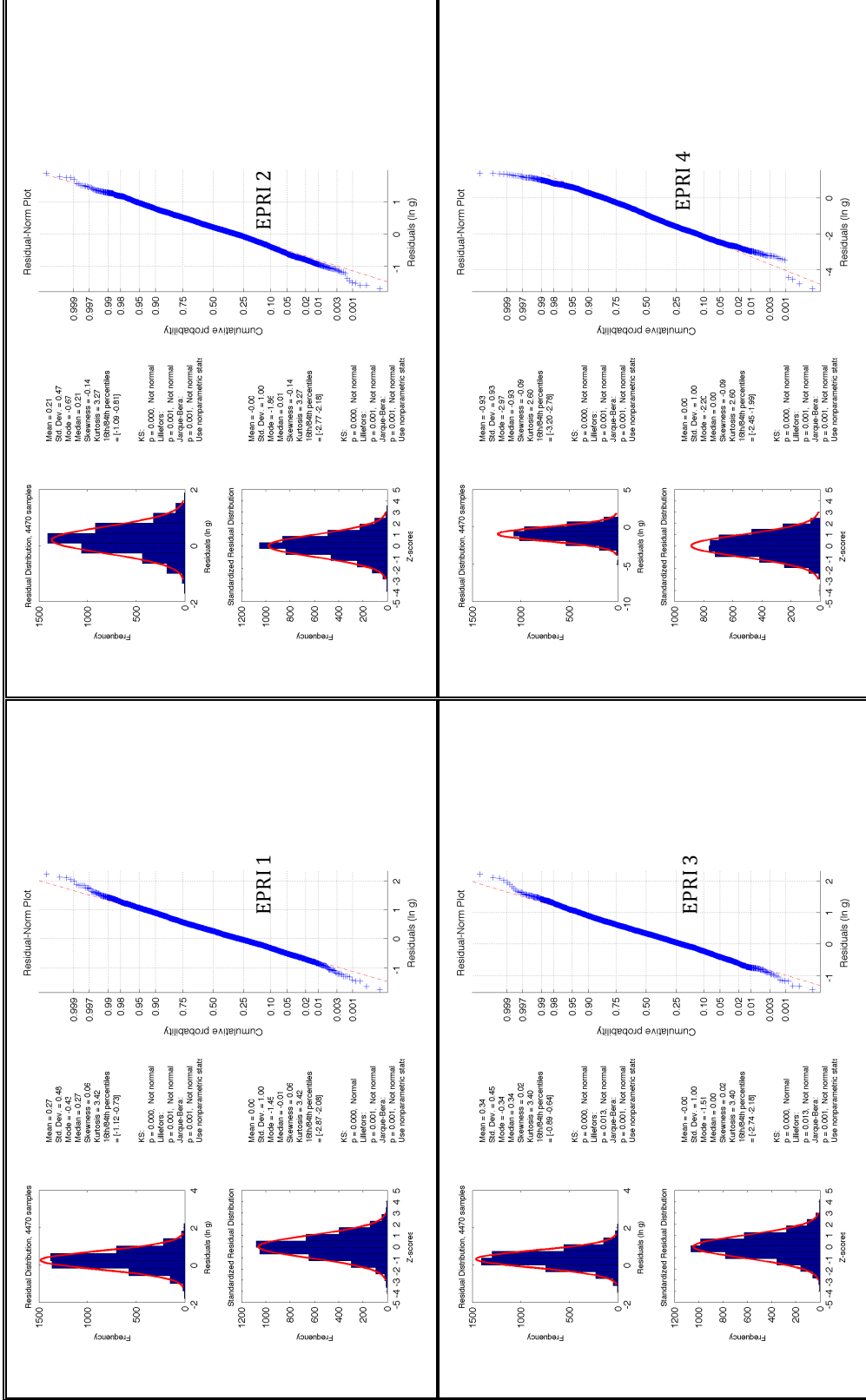
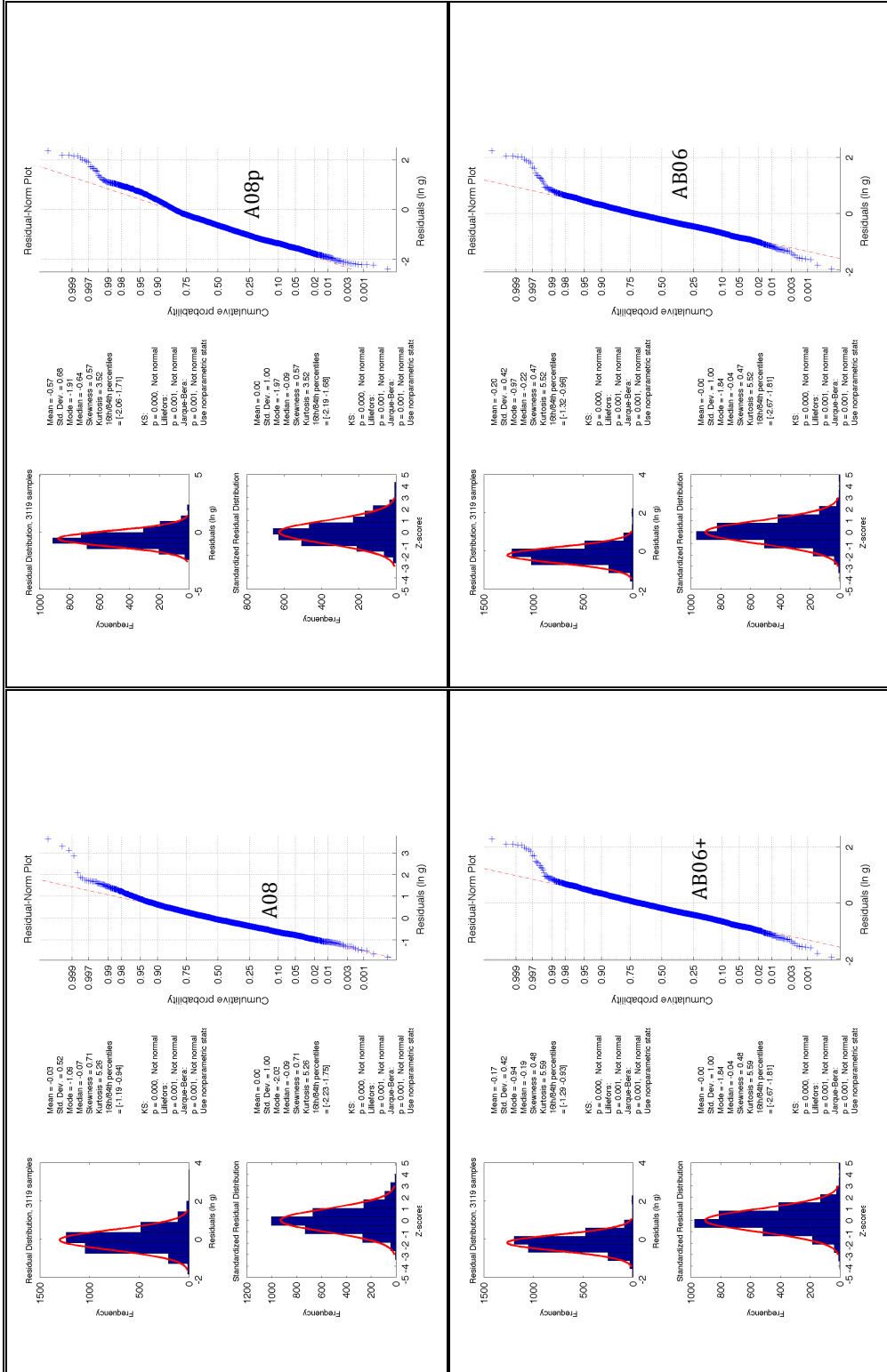
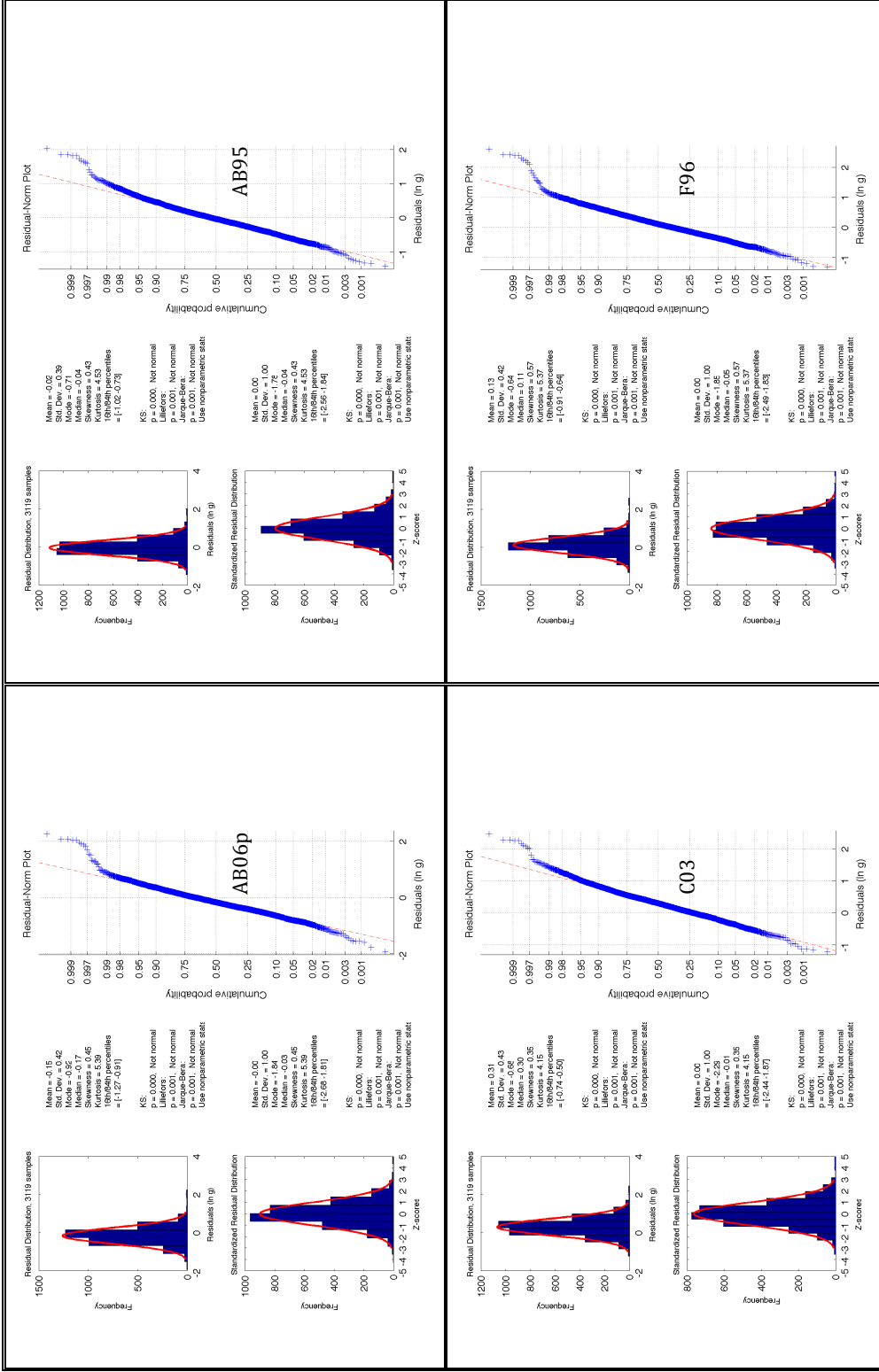
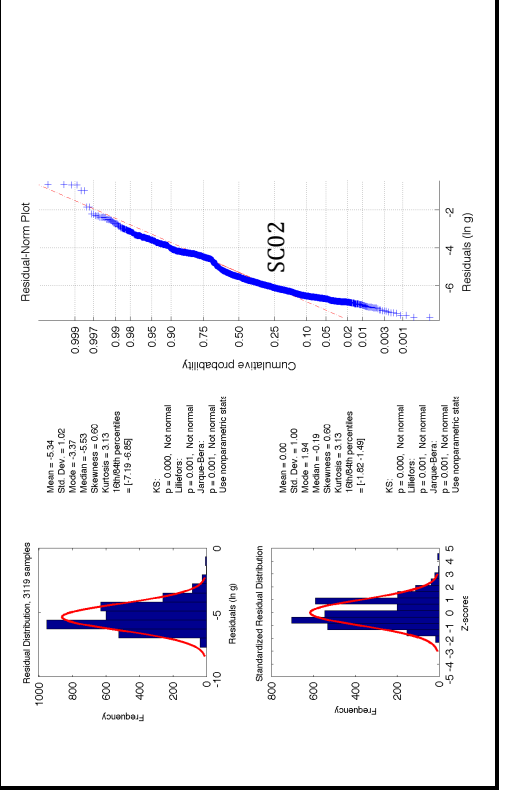
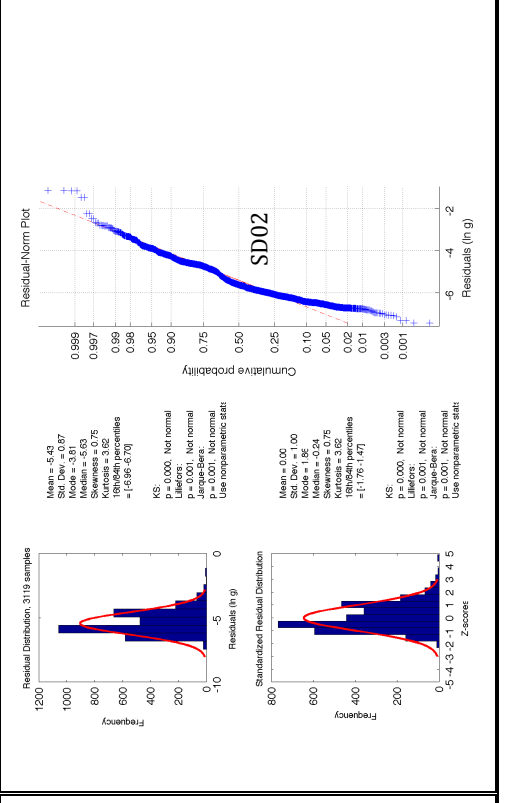
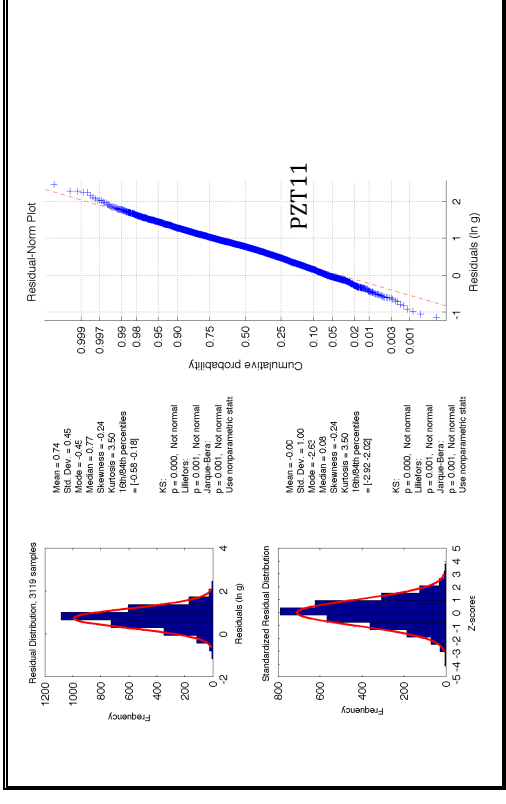
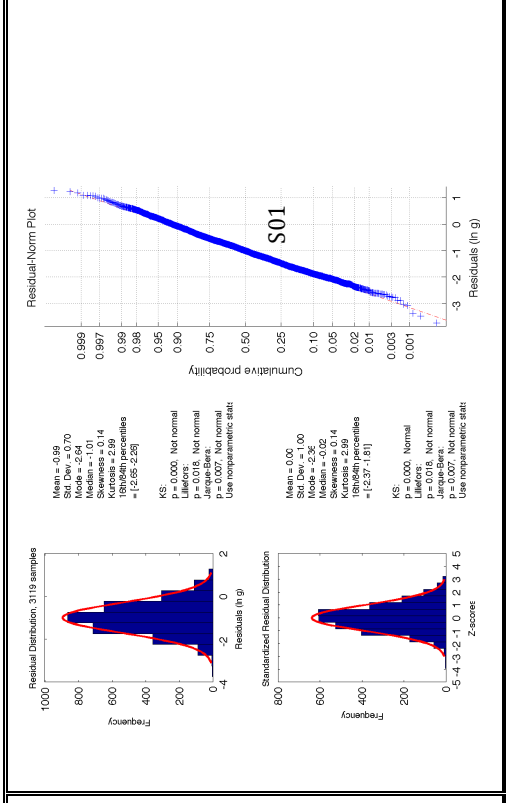
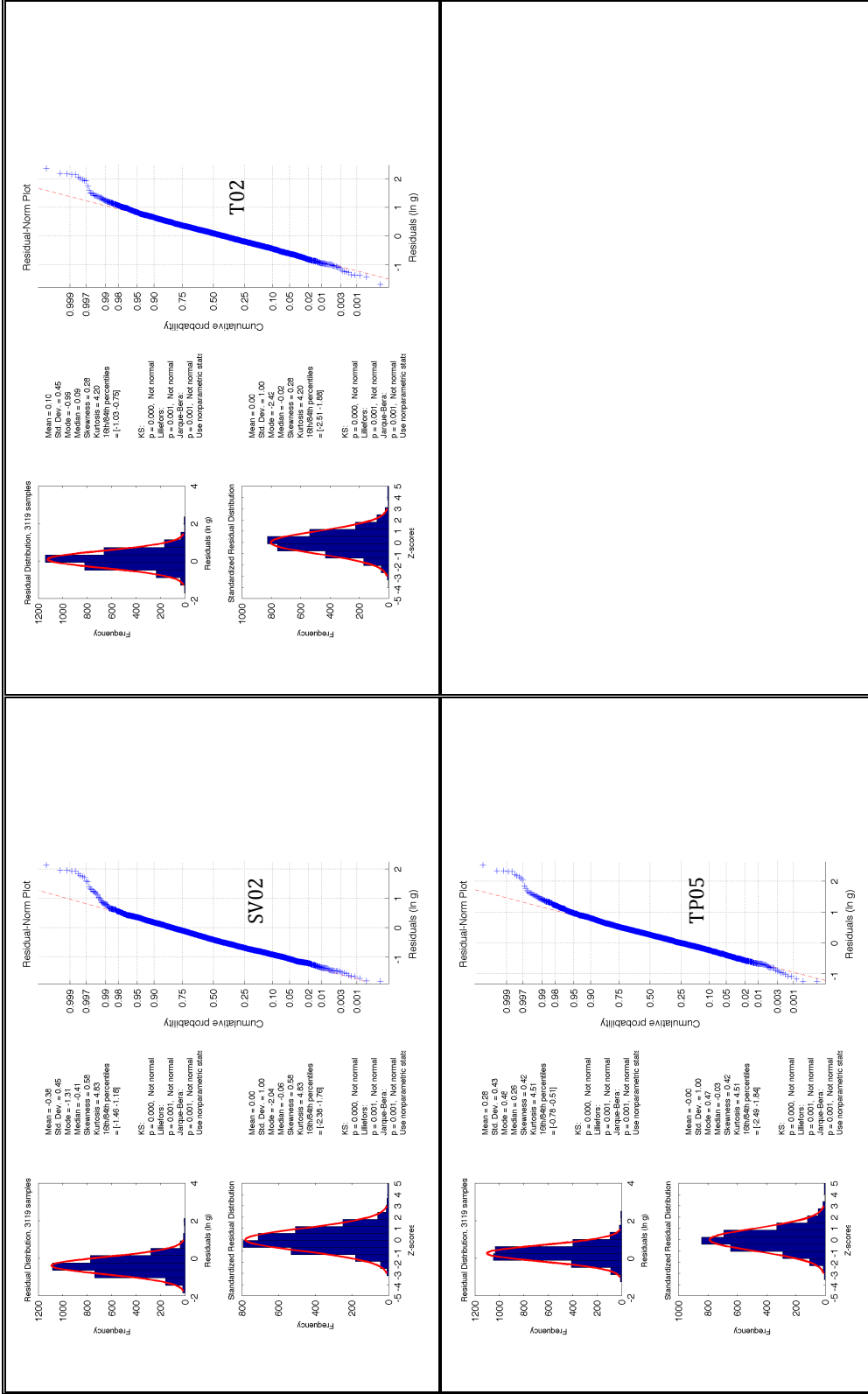


Figure 17: Plot for the 1.0s spectral Acceleration









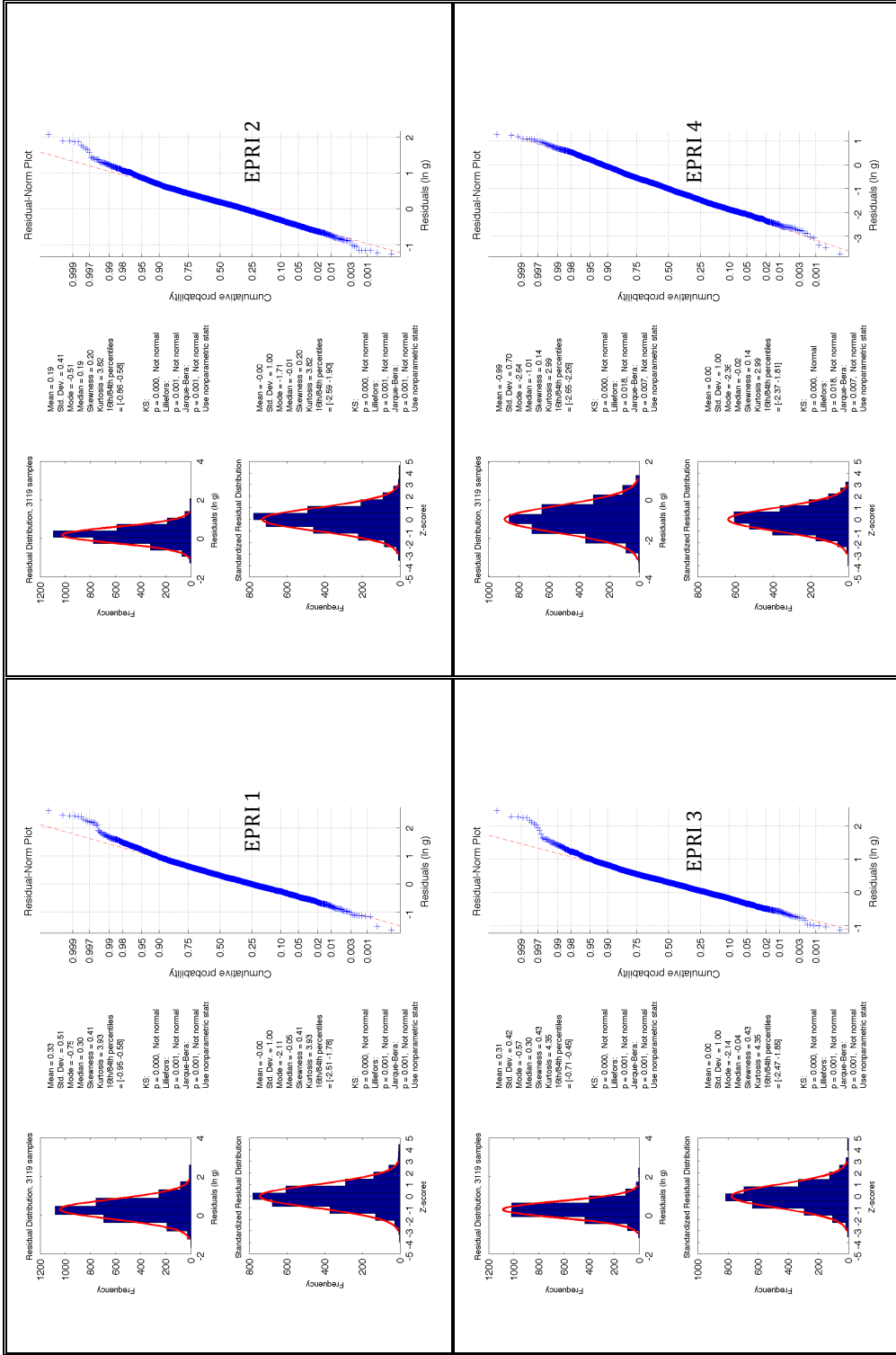


Figure 18: Plot for the 2.0s spectral Acceleration

Appendix 3: Results of LLH

Table 27: Summary Table for LLH results for Soil sites and within 100km

GMPE	pga	0.1s	0.2s	0.3s	0.5s	1.0s	2.0s	Factor	Rank
AB06p	2.556	2.503	2.483	2.462	2.370	2.399	2.318	2.442	1
AB06	2.557	2.504	2.481	2.460	2.374	2.400	2.336	2.445	2
AB06+	2.556	2.503	2.482	2.461	2.372	2.399	2.345	2.445	3
EPRI 3	2.598	2.489	2.485	2.449	2.383	2.441	2.361	2.458	4
AB95	2.593	2.542	2.499	2.448	2.397	2.432	2.332	2.463	5
F96	2.581	2.546	2.499	2.461	2.400	2.424	2.338	2.464	6
PZT11	2.550	2.508	2.494	2.540	2.471	2.416	2.377	2.479	7
TP05	2.574	2.552	2.518	2.503	2.435	2.453	2.362	2.485	8
C03	2.606	2.542	2.537	2.482	2.451	2.476	2.351	2.492	9
EPRI 2	2.713	2.640	2.491	2.445	2.401	2.432	2.345	2.495	10
SV02	2.550	2.545	2.507	2.507	2.445	2.485	2.429	2.496	11
EPRI 1	2.537	2.608	2.501	2.489	2.389	2.504	2.590	2.517	12
SC02	2.597	2.585	2.553	2.544	2.491	2.500	2.451	2.532	13
SD02	2.598	2.585	2.551	2.545	2.490	2.505	2.459	2.533	14
T02	2.628	2.684	2.668	2.570	2.510	2.517	2.382	2.566	15
A08p	3.085	2.818	2.656	2.578	2.462	2.550	2.639	2.684	16
S01	2.820	2.712	2.719	2.705	2.760	2.773	2.627	2.731	17
EPRI 4	2.820	2.712	2.719	2.713	2.778	2.773	2.627	2.735	18
A08	5.423	2.932	2.614	2.669	2.467	2.751	2.650	3.072	19

Table 28: Summary Table for LLH results for Deep Soil sites and within 100km

GMPE	pga	0.1s	0.2s	0.3s	0.5s	1.0s	2.0s	Factor	Rank
AB06p	2.628	2.619	2.599	2.526	2.448	2.379	2.304	2.500	1
AB06+	2.628	2.619	2.600	2.526	2.451	2.380	2.304	2.501	2
AB06	2.629	2.620	2.601	2.527	2.454	2.381	2.304	2.502	3
EPRI 1	2.619	2.627	2.590	2.527	2.449	2.374	2.344	2.504	4
PZT11	2.606	2.589	2.592	2.622	2.488	2.360	2.298	2.508	5
SV02	2.625	2.590	2.590	2.538	2.498	2.425	2.345	2.516	6
EPRI 3	2.654	2.612	2.596	2.539	2.466	2.405	2.342	2.516	7
SC02	2.621	2.587	2.588	2.541	2.502	2.429	2.350	2.517	8
SD02	2.622	2.588	2.587	2.539	2.502	2.435	2.367	2.520	9
F96	2.654	2.637	2.623	2.559	2.468	2.399	2.318	2.523	10
AB95	2.664	2.642	2.619	2.556	2.479	2.404	2.324	2.527	11
TP05	2.640	2.643	2.641	2.613	2.489	2.418	2.350	2.542	12
C03	2.659	2.658	2.662	2.589	2.516	2.430	2.346	2.551	13
EPRI 2	2.782	2.745	2.623	2.559	2.479	2.409	2.330	2.561	14
T02	2.663	2.799	2.777	2.655	2.549	2.470	2.355	2.610	15
A08p	3.266	2.910	2.723	2.585	2.481	2.430	2.413	2.687	16
A08	3.622	2.951	2.694	2.751	2.509	2.483	2.317	2.761	17
S01	2.924	2.854	2.859	2.810	2.783	2.770	2.560	2.794	18
EPRI 4	2.924	2.854	2.859	2.816	2.798	2.770	2.560	2.797	19

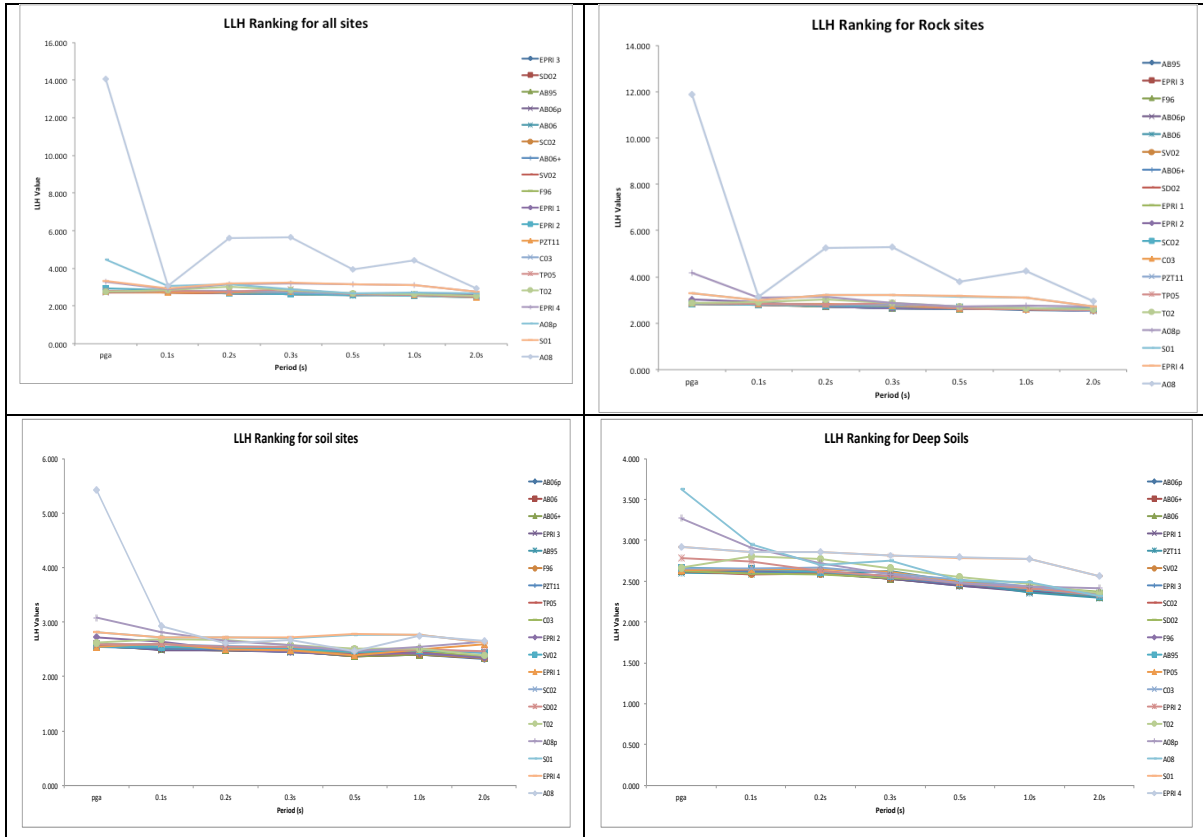


Figure 19: LLH Values versus Spectral periods calculated for the GMPEs under study

Appendix 4: Results for EDR Methodology

Table 29: Summary Table for MDE results for Soil sites and within 100km

GMPE	PGA	0.1s	0.2s	0.3s	0.5s	1.0s	2.0s	Factor	Rankk
TP05	1.411	1.377	1.395	1.436	1.250	1.241	1.407	1.359	1
AB06+	1.445	1.408	1.438	1.462	1.250	1.215	1.377	1.371	2
SD02	1.510	1.461	1.486	1.492	1.256	1.225	1.357	1.398	3
EPRI 2	1.850	1.566	1.566	1.529	1.345	1.211	1.257	1.475	4
T02	1.550	1.461	1.384	1.709	1.495	1.553	1.730	1.554	5
SV02	1.662	1.510	1.750	1.782	1.587	1.297	1.337	1.561	6
A08	1.936	1.662	1.601	1.644	1.477	1.355	1.424	1.585	7
AB06p	2.085	1.714	1.724	1.737	1.543	1.323	1.250	1.625	8
AB06	1.895	1.680	1.723	1.818	1.638	1.319	1.322	1.628	9
F96	1.908	1.777	2.122	2.062	1.762	1.406	1.342	1.768	10
PZT11	2.138	2.061	2.003	1.986	1.665	1.366	1.310	1.790	11
EPRI 1	2.313	1.994	1.898	1.941	1.765	1.541	1.674	1.875	12
EPRI 3	1.912	1.799	2.127	2.549	1.570	1.556	1.680	1.885	13
EPRI 4	2.272	2.213	2.212	2.228	1.849	1.433	1.313	1.931	14
SC02	2.596	2.434	2.391	2.307	1.914	1.431	1.353	2.061	15
A08p	2.538	2.431	2.454	2.507	2.079	1.720	1.616	2.192	16
C03	2.608	2.514	2.801	2.662	2.352	1.995	1.529	2.352	17
AB95	4.828	3.993	4.563	5.090	6.071	7.420	9.103	5.867	18
S01	4.623	3.866	4.571	5.226	6.316	7.623	9.150	5.911	19

Table 30: Summary Table for Kappa results for Soil sites and within 100km

GMPE	PGA	0.1s	0.2s	0.3s	0.5s	1.0s	2.0s	Factor	Rankk
AB06+	1.122	1.146	1.124	1.111	1.069	1.113	1.166	1.121	1
TP05	1.114	1.139	1.115	1.108	1.073	1.130	1.183	1.123	2
SD02	1.150	1.170	1.143	1.123	1.075	1.126	1.164	1.136	3
EPRI 2	1.247	1.143	1.162	1.153	1.180	1.101	1.063	1.150	4
AB06	1.390	1.295	1.306	1.341	1.347	1.202	1.094	1.282	5
A08	1.347	1.287	1.253	1.273	1.287	1.284	1.264	1.285	6
T02	1.189	1.246	1.200	1.366	1.328	1.363	1.411	1.300	7
EPRI 3	1.274	1.274	1.450	1.595	1.207	1.289	1.362	1.350	8
SV02	1.455	1.400	1.506	1.465	1.427	1.275	1.216	1.392	9
PZT11	1.466	1.500	1.459	1.445	1.404	1.292	1.204	1.396	10
SC02	1.623	1.588	1.529	1.475	1.397	1.201	1.067	1.412	11
AB06p	1.594	1.419	1.465	1.459	1.524	1.359	1.213	1.433	12
EPRI 4	1.561	1.610	1.561	1.528	1.415	1.277	1.150	1.443	13
F96	1.573	1.538	1.673	1.574	1.506	1.340	1.236	1.492	14
EPRI 1	1.762	1.660	1.520	1.505	1.497	1.440	1.438	1.546	15
A08p	1.717	1.784	1.731	1.730	1.602	1.487	1.382	1.633	16
C03	1.831	1.831	1.953	1.834	1.769	1.635	1.268	1.732	17
AB95	1.858	1.733	1.825	1.912	1.973	2.051	2.182	1.934	18
S01	1.831	1.701	1.810	1.919	2.032	2.189	2.404	1.984	19

Table 31: Summary Table for EDR results for Soil sites and within 100km

GMPE	PGA	0.1s	0.2s	0.3s	0.5s	1.0s	2.0s	Factor	Rank
TP05	1.571	1.568	1.556	1.590	1.341	1.402	1.665	1.528	1
AB06+	1.621	1.614	1.616	1.624	1.336	1.353	1.605	1.538	2
SD02	1.737	1.709	1.699	1.676	1.350	1.380	1.580	1.590	3
EPRI 2	2.307	1.791	1.819	1.762	1.587	1.334	1.336	1.705	4
T02	1.842	1.820	1.660	2.334	1.985	2.116	2.441	2.028	5
A08	2.606	2.139	2.005	2.093	1.902	1.740	1.800	2.041	6
AB06	2.632	2.175	2.250	2.439	2.206	1.586	1.446	2.105	7
SV02	2.417	2.114	2.634	2.611	2.266	1.653	1.625	2.189	8
AB06p	3.324	2.433	2.525	2.535	2.352	1.798	1.516	2.355	9
PZT11	3.135	3.092	2.922	2.870	2.338	1.766	1.577	2.529	10
EPRI 3	2.436	2.293	3.083	4.066	1.896	2.005	2.289	2.581	11
F96	3.002	2.734	3.550	3.246	2.654	1.884	1.659	2.676	12
EPRI 4	3.547	3.562	3.454	3.406	2.617	1.830	1.510	2.847	13
EPRI 1	4.075	3.310	2.885	2.921	2.644	2.219	2.407	2.923	14
SC02	4.215	3.866	3.655	3.404	2.674	1.719	1.444	2.997	15
A08p	4.357	4.336	4.249	4.338	3.330	2.557	2.233	3.628	16
C03	4.775	4.602	5.470	4.884	4.161	3.261	1.940	4.156	17
AB95	8.971	6.921	8.328	9.730	11.977	15.220	19.864	11.573	18
S01	8.462	6.576	8.274	10.027	12.834	16.687	21.994	12.122	19

Table 32: Summary Table for MDE results for Deep Soil sites and within 100km

GMPE	PGA	0.1s	0.2s	0.3s	0.5s	1.0s	2.0s	Factor	Rank
TP05	1.411	1.377	1.395	1.436	1.250	1.241	1.407	1.359	1
AB06+	1.445	1.408	1.438	1.462	1.250	1.215	1.377	1.371	2
SD02	1.510	1.461	1.486	1.492	1.256	1.225	1.357	1.398	3
EPRI 2	1.850	1.566	1.566	1.529	1.345	1.211	1.257	1.475	4
T02	1.550	1.461	1.384	1.709	1.495	1.553	1.730	1.554	5
SV02	1.662	1.510	1.750	1.782	1.587	1.297	1.337	1.561	6
A08	1.936	1.662	1.601	1.644	1.477	1.355	1.424	1.585	7
AB06p	2.085	1.714	1.724	1.737	1.543	1.323	1.250	1.625	8
AB06	1.895	1.680	1.723	1.818	1.638	1.319	1.322	1.628	9
F96	1.908	1.777	2.122	2.062	1.762	1.406	1.342	1.768	10
PZT11	2.138	2.061	2.003	1.986	1.665	1.366	1.310	1.790	11
EPRI 1	2.313	1.994	1.898	1.941	1.765	1.541	1.674	1.875	12
EPRI 3	1.912	1.799	2.127	2.549	1.570	1.556	1.680	1.885	13
EPRI 4	2.272	2.213	2.212	2.228	1.849	1.433	1.313	1.931	14
SC02	2.596	2.434	2.391	2.307	1.914	1.431	1.353	2.061	15
A08p	2.538	2.431	2.454	2.507	2.079	1.720	1.616	2.192	16
C03	2.608	2.514	2.801	2.662	2.352	1.995	1.529	2.352	17
AB95	4.828	3.993	4.563	5.090	6.071	7.420	9.103	5.867	18
S01	4.623	3.866	4.571	5.226	6.316	7.623	9.150	5.911	19

Table 33: Summary Table for Kappa results for Deep Soil sites and within 100km

GMPE	PGA	0.1s	0.2s	0.3s	0.5s	1.0s	2.0s	Factor	Rankk
AB06+	1.122	1.146	1.124	1.111	1.069	1.113	1.166	1.121	1
TP05	1.114	1.139	1.115	1.108	1.073	1.130	1.183	1.123	2
SD02	1.150	1.170	1.143	1.123	1.075	1.126	1.164	1.136	3
EPRI 2	1.247	1.143	1.162	1.153	1.180	1.101	1.063	1.150	4
AB06	1.390	1.295	1.306	1.341	1.347	1.202	1.094	1.282	5
A08	1.347	1.287	1.253	1.273	1.287	1.284	1.264	1.285	6
T02	1.189	1.246	1.200	1.366	1.328	1.363	1.411	1.300	7
EPRI 3	1.274	1.274	1.450	1.595	1.207	1.289	1.362	1.350	8
SV02	1.455	1.400	1.506	1.465	1.427	1.275	1.216	1.392	9
PZT11	1.466	1.500	1.459	1.445	1.404	1.292	1.204	1.396	10
SC02	1.623	1.588	1.529	1.475	1.397	1.201	1.067	1.412	11
AB06p	1.594	1.419	1.465	1.459	1.524	1.359	1.213	1.433	12
EPRI 4	1.561	1.610	1.561	1.528	1.415	1.277	1.150	1.443	13
F96	1.573	1.538	1.673	1.574	1.506	1.340	1.236	1.492	14
EPRI 1	1.762	1.660	1.520	1.505	1.497	1.440	1.438	1.546	15
A08p	1.717	1.784	1.731	1.730	1.602	1.487	1.382	1.633	16
C03	1.831	1.831	1.953	1.834	1.769	1.635	1.268	1.732	17
AB95	1.858	1.733	1.825	1.912	1.973	2.051	2.182	1.934	18
S01	1.831	1.701	1.810	1.919	2.032	2.189	2.404	1.984	19

Table 34: Summary Table for EDR results for Deep Soil sites and within 100km

GMPE	PGA	0.1s	0.2s	0.3s	0.5s	1.0s	2.0s	Factor	Rank
TP05	1.571	1.568	1.556	1.590	1.341	1.402	1.665	1.528	1
AB06+	1.621	1.614	1.616	1.624	1.336	1.353	1.605	1.538	2
SD02	1.737	1.709	1.699	1.676	1.350	1.380	1.580	1.590	3
EPRI 2	2.307	1.791	1.819	1.762	1.587	1.334	1.336	1.705	4
T02	1.842	1.820	1.660	2.334	1.985	2.116	2.441	2.028	5
A08	2.606	2.139	2.005	2.093	1.902	1.740	1.800	2.041	6
AB06	2.632	2.175	2.250	2.439	2.206	1.586	1.446	2.105	7
SV02	2.417	2.114	2.634	2.611	2.266	1.653	1.625	2.189	8
AB06p	3.324	2.433	2.525	2.535	2.352	1.798	1.516	2.355	9
PZT11	3.135	3.092	2.922	2.870	2.338	1.766	1.577	2.529	10
EPRI 3	2.436	2.293	3.083	4.066	1.896	2.005	2.289	2.581	11
F96	3.002	2.734	3.550	3.246	2.654	1.884	1.659	2.676	12
EPRI 4	3.547	3.562	3.454	3.406	2.617	1.830	1.510	2.847	13
EPRI 1	4.075	3.310	2.885	2.921	2.644	2.219	2.407	2.923	14
SC02	4.215	3.866	3.655	3.404	2.674	1.719	1.444	2.997	15
A08p	4.357	4.336	4.249	4.338	3.330	2.557	2.233	3.628	16
C03	4.775	4.602	5.470	4.884	4.161	3.261	1.940	4.156	17
AB95	8.971	6.921	8.328	9.730	11.977	15.220	19.864	11.573	18
S01	8.462	6.576	8.274	10.027	12.834	16.687	21.994	12.122	19